Deletion of the FAT10 Gene Alters Energy Homeostasis in Mice

By:

Jason DeFuria

A Dissertation Submitted to the
Friedman School of Nutrition Science and Policy at Tufts University
In Partial Fulfillment of the
Requirements for the Degree of
Doctor of Philosophy

Thesis Committee:

Martin S. Obin

Andrew S. Greenberg

Sang-Woon Choi

Xiang-Dong Wang

TABLE OF CONTENTS

ACKNOWLEDGEMENTS

I would like to thank first and foremost my thesis advisor Dr. Martin S. Obin. Marty's fervor for science compelled me to join his group and his unyielding and insightful mentorship helped propel myself through this very challenging and rewarding project. I would like to thank the members of my thesis committee Dr. Andrew S. Greenberg, Dr. Sang Woon Choi and Dr. Xiang-Dong Wang for their insightful advice that helped shape my thesis into the interesting story presented in this text. I would like to thank my academic advisor Dr. Sarah Booth for her guidance as I tackled the challenging courses that accompanied my dissertation work. I would particularly like to thank Dr. Katherine J. Strissel for her expertise in all aspects of laboratory science.

I would like to thank all the members of the Obesity and Metabolism Lab both past and present: Drs. James W. Perfield, Grace Bennett, Nicole Rogers, Yun Lee, Eugene Chang, Qing-Wu Yan, Victoria Viera-Potter, Brook Hasson, Christine E. Graham, Thomas Bowman, Sajid Hussain as well as Vladimir Kustanovich, Chen Xie, Ayla Mansur. I would like to thank Dr. Donald Smith and the entire Comparative Biology Unit for their care and attention regarding all of my animal projects.

I would like to thank all of my friends at the Friedman School that I was so fortunate to have made during my time here. I consider myself lucky to meet such intelligent and fun people all in one place. I would also like to thank the greatest roommates of 188 Willow Ave who all taught me there is some sort of balance between graduate school and life. You will all be missed.

I would like to thank all of my friends who reminded me constantly that I was in my late twenties and still in school. Your inspirational words and encouragement helped get me through the tough times.

Last, but in no way least, I would like to thank my mother, Donna, and father, Stephen, who have supported and encouraged me in every way possible during my graduate work. I don't think I would have survived this experience without such a strong support system.

ABSTRACT

Chronic increased caloric intake without concomitant increases in energy metabolism result in obesity. The rise in obesity in the US can be attributed to over-nutrition and a sedentary lifestyle. Understanding nutritional and genetic factors that promote energy metabolism are critical for combating obesity and associated disorders and maintain overall health. Muscle, adipose tissue (AT), liver and the pancreas respond to nutrient intake and establish inter-tissue communication via release of circulating signaling factors including hormones (e.g. insulin from the pancreas) and fatty acids (from AT). These processes promote balanced energy storage and use, known collectively as energy homeostasis. Over-nutrition and/or poor diet can disturb normal energy homeostasis promoting obesity and associated complications such as insulin resistance.

The Human Leukocyte Antigen (HLA) F-adjacent transcript 10 (FAT10) is an emerging player in regulation of energy homeostasis. FAT10 has been implicated in chronic diseases such as Type I Diabetes, cancer and genetic lipodystrophies. In these pathologies, energy homeostasis has been altered due to genetic mutations. Fat10 is expressed in a variety of insulin sensitive tissues including liver, muscle, adipose as well as the pancreas. We hypothesize that ablation of the FAT10 gene will alter systemic energy metabolism. This thesis work demonstrates the major finding that genetic deletion of the FAT10 gene in mice alters energy homeostasis and significantly decreases adipose mass through increases in AT and muscle catabolism. In mice fed a normal diet, we demonstrate that FAT10 is expressed during normal AT growth. FAT10 KO mice have reduced adiposity and burn more calories (enhanced energy expenditure) compared to WT mice without decreasing caloric intake or increasing exercise. Using indirect calorimetry, we demonstrate that FAT10 KO mice preferentially burn lipid. Skeletal muscle exhibits increased expression of lipid burning genes. This response appears to be due to increased circulating fatty acids derived from AT release (lipolysis). FAT10 KO mice have constitutively low circulating insulin that may be permissive for the observed enhanced adipose tissue lipolysis. This model suggests that increases in lipolysis are due to decreases in available circulating insulin. The enhanced lipid burning in muscle is in response to the fatty acid load in the blood from AT lipolysis. When FAT10 KO and WT mice were fed a high fat diet, the KO mice retained mildly enhanced energy expenditure and became obese at a slower rate compared to WT mice fed the same diet. Interestingly, FAT10 KO mice on a HFD remained insulin sensitive. Altering lipid content of the diet to primarily saturated fat diminishes the hypermetabolic phenotype.

This thesis work indicates that FAT10 is a novel gene involved in the regulation of systemic energy metabolism that may be dependent on the fatty acid composition of the diet. Because the FAT10 gene was absent from all tissues, it is not possible to identify the tissue influencing the increased energy metabolism. This point warrants further dissection by tissue specific ablation of the FAT10 gene to identify how FAT10 affects systemic energy metabolism. Additionally, since FAT10 is associated with increased risk for chronic disease (diabetes, cancer, HIV associated nephropathy) and is interactive with key cellular regulators (p53 and NFκB), this research opens new avenues for further investigation of the tissue-specific biological function of FAT10.

LIST OF FIGURES

LIST OF TABLES

CHAPTER I

REVIEW OF THE LITERATURE

1.1. Adipocyte and Adipose Tissue Metabolism

1.1.1. Hormonal Regulation of Adipocyte Metabolism

The balance of adipocyte energy metabolism is dictated by nutrient availability that directly modulates concentrations of circulating hormones such as insulin, glucagon and catecholamines (1). Insulin coordinates the post-prandial, anabolic response promoting nutrient uptake and storage. Conversely, in the presence of low insulin concentrations, catecholamines and glucagon direct the fasting catabolic response resulting in breakdown of energy stores and counter-regulate insulin action (i.e. lipolysis in adipose tissue and glycogenolysis in muscle and liver) (2).

Adipocyte energy storage is orchestrated by insulin. After a meal, the rapid rise in nutrients, particularly blood glucose, stimulates pancreatic release of insulin. Insulin (described mechanistically in the following section) promotes fatty acid and glucose uptake in adipocytes. Fatty acids and glucose metabolites (via de novo lipogenesis pathway) are synthesized to triacylglycerol (TAG) and stored in specialized storage compartments known as lipid droplets. The net result of insulin action on adipocytes is to store energy as neutral lipid while opposing breakdown of lipid stores (See Sections below for mechanistic descriptions).

Opposing adipocyte energy storage, fasting induces release of catecholamines that promote lipid droplets to release neutral lipid that are subsequently broken down by a series of glyceride-specific lipases. Catecholamines (specifically) bind to cell surface β3-adrenergic receptors inducing an intracellular signaling cascade that elevates the

concentration of cAMP resulting in PKA activation and phosphorylation of perilipin, the major lipid droplet protein and master regulator of lipolysis (3-6). Following perilipin phosphorylation, adipocyte lipases and accessory proteins are recruited to the lipid droplet to mediate breakdown of triglycerides into one molecule of glycerol and three fatty acids (7). The glycerol can be used for re-esterification of fatty acids or released from the adipocyte (8). The fatty acids can be released for local or systemic uptake and β-oxidation for ATP production.

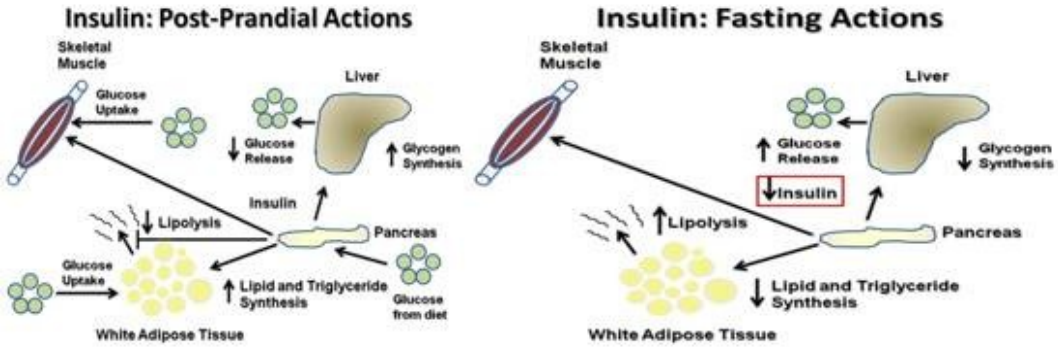

Figure 1-1. Post-prandial and fasting actions of insulin

Hormonal regulation of adipocyte metabolism is tightly coupled with increases and decreases nutrient intake. In times of caloric excess, insulin promotes energy storage (Figure 1-1) while fasting decreases insulin concentrations and increases catecholamines to mediate breakdown of metabolic substrates for the body. Disturbing this counter-regulatory system can produce both adverse and beneficial metabolic effects in adipocytes.

1.1.2. Insulin Signaling in Adipocytes

Insulin is a major anabolic hormone in the body that coordinates systemic growth with peripheral and central nutrient sensing and lifespan (9, 10). At the adipocyte cell surface, as with other insulin sensitive cells, insulin binds to the insulin receptor (IR). Ligand binding initiates an intracellular signaling cascade via a protein and lipid phospho-relay system that results in proteolytic and transcriptional changes that promotes cellular anabolism and energy storage (11).

Upon insulin binding, the insulin receptor autophosphorylates tyrosine (pY) residues that produces docking sites for adaptor and signaling proteins. Insulin receptor substrate proteins (IRS1-4) dock at pY recognition sequences and become phosphorylated. This culminates in a phospho-relay system resulting in phosphorylation of AKT proteins, the main signaling hub in the insulin cascade (12). In adipocytes, AKT amplifies upstream signals to downstream effector proteins that regulate many aspects of insulin stimulated anabolic metabolism and growth (13). Adipocyte AKT acitivity promotes synthesis and activation of lipogenic enzymes while opposing the lipolytic pathway (14).

1.1.3. Adipocyte Nutrient Uptake and Storage

The biological role of AT is to store excess calories as neutral triglyceride in subcellular compartments known as lipid droplets and to inform the body of stored nutrient status via adipokines (described in section below) (15). Insulin promotes lipid and glucose uptake and storage. Substrate for triglyceride biosynthesis can derive from either dietary fatty acids or from the glucose metabolite acetyl-CoA via de novo lipogenesis. These anabolic processes are promoted by insulin. Glycogen is stored in adipocytes; however, glycogen contributes minimally to adipocyte energy stores (16).

Fatty acid uptake involves lipoprotein metabolism, membrane translocation, intracellular fatty acid binding and lipid trafficking (17). Lipoprotein lipase at the cell membrane participates in lipoprotein metabolism to liberate fatty acids for cellular uptake. The CD36 scavenger receptor participates in fatty acid uptake. Intracellular fatty acids are sequestered by a family of fatty acid binding proteins that determine the subcellular localization of the fatty acid (18). Fatty acids destined for long term energy stores are re-esterified to a glycerol backbone are stored in lipid droplets.

Glucose uptake involves trafficking of insulin-responsive Glut4 transporter containing vesicles to the adipocyte membrane. The insulin-responsive Glut4 containing vesicles are kept tethered in cytoplasmic bodies known as the Glut4 storage compartment (GSC) by a series of proteins, most notably AS160 (19, 20). AKT phosphorylation of AS160 represses tethering activity and allows translocation of Glut4 vesicles (21). The insulin-responsive amino peptidase (IRAP) is an identifying feature of insulin-sensitive Glut4 vesicles (22). Increasing the expression of Glut4 in transgenic mice up-regulates IRAP positive vesicles and enhances Glut4 membrane trafficking and receptor density effectively reducing blood glucose levels and enhancing not only adipocyte lipogenesis but also adipocyte proliferation that produces enlarged adipose depots with small, metabolically healthy adipocytes (23, 24).

Insulin signaling promotes energy storage in adipocytes by facilitating fatty acid uptake, TAG biosynthesis and storage as well as glucose uptake for de novo fatty acid biosynthesis. These events are mediated by the insulin signaling cascade and the effectors of AKT activation. Conditions that interfere with the insulin signaling cascade via increased cytokine production (obesity, lipodystrophy, other inflammatory diseases) or

inability to produce sufficient insulin (Type I diabetes) will perturb homeostatic nutrient storage and handling in adipocytes.

1.1.4. Adipocyte Lipolysis

During times of increased energy demands such as fasting, calorie restriction and prolonged exercise, circulating insulin concentrations drop and stored triglyceride in lipid droplets is hydrolyzed to fatty acids (FA) and glycerol (24). FAs are released into systemic circulation for peripheral tissue uptake for β-oxidation and generation of ATP. Also, fatty acids and glycerol can be used as substrates for ketogenesis and gluconeogenesis in the liver, respectively (8).

Lipolysis is regulated by increased catecholamine and decreased insulin concentrations (Figure 1-2 (25)). Catecholamine signaling (described in previous section) culminates in release of fatty acids from lipid droplets. Lipid droplets are composed of repertoire of proteins that regulate lipid trafficking into and out of the lipid droplet (26). The most abundant protein at the lipid droplet surface is perilipin (3). Upon β-adrenergic stimulation, perilipin contains consensus sequences that become phosphorylated by PKA. This phosphorylation induces localization of the lipolytic machinery, release of TAG from the lipid droplet core and subsequent hydrolysis of stored TAG into three fatty acids and one molecule of glycerol.

Lipolytic enzymes recruited to the phosphorylated perilipin protein hydrolyze TAG in a sequential manner. The major lipases in adipocytes are ATGL, HSL and MGL which hydrolyze TAGs, DAGs and MAGs, respectively (6, 27). ATGL is the rate limiting enzyme in adipocyte lipolysis and requires an accessory protein, CGI-58, for full lipolytic activity (28, 29). Interestingly, adipocyte specific over- expression of ATGL

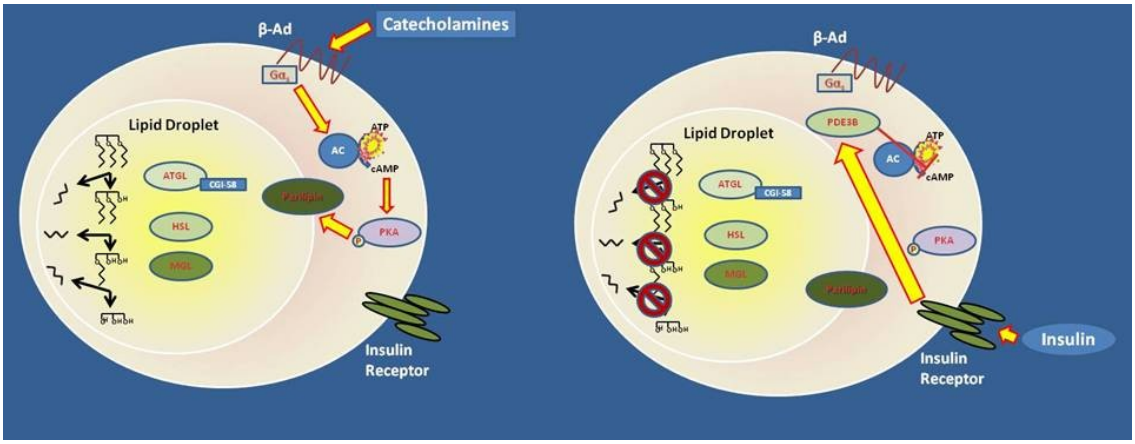

Figure 1-2. Adipocyte lipolysis in (Left) fasted and (Right) fed state. Adapted from (6).

results in enhanced adipocyte beta-oxidation with increased re-esterification and renders mice resistant to diet induced obesity.

Adipocyte lipolysis is positively regulated by glucocorticoids and negatively regulated by insulin. Forkhead box O1 (FOXO1) transcription factor is a central regulator of transcription of the lipolytic machinery (30). Under high glucocorticoid, low-insulin concentrations, FOXO1 resides in the nucleus and participates in transcription of genes important for lipolysis. Insulin induces FOXO1 phosphorylation and exclusion from the nucleus thereby down-regulating the expression of ATGL, the rate limiting lipolytic enzyme (31).

1.1.5. Adipose Tissue as an Endocrine Organ

Adipose tissue (AT), composed of adipocytes and a diverse population of non-adipocyte stromal-vascular cells (SVCs), is an important regulator of whole body lipid and energy metabolism (32). Traditionally thought to be an inert long term energy store, adipose tissue can directly influence systemic insulin sensitivity and inflammation via release of soluble factors such as fatty acids and adipocyte hormones known as

adipokines (33-35). Increases in non-esterified free fatty acid (NEFAs) release from adipocytes can result in ectopic lipid deposition and insulin resistance in skeletal muscle and liver (36). Insulin resistance increases blood glucose levels via inhibition of muscle glucose uptake and enhancement of hepatic glucose output.

Released from adipose tissue, adipokines act in an autocrine, paracrine, and/or endocrine fashion to promote metabolic homeostasis. These adipocyte peptide hormones integrate AT, liver, muscle, and CNS physiology by impacting lipid metabolism, glucose homeostasis, inflammation, angiogenesis and food intake. Because of the plethora of biological processes affected, regulation of adipokine secretion is critical to maintain systemic metabolic homeostasis.

In non-obese, lean individuals normally have small adipocytes that secrete the adipokines adiponectin and leptin which promote a healthy systemic metabolic profile (37-41). Alterations in adipocyte mass either through hypertrophy, as with obesity, or lipoatrophy, as with lipodystrophy, produces characteristic changes in AT metabolism and adipokine secretion that are associated with the development of insulin resistance and associated metabolic complications. These adipose tissue pathologies alter the adipocyte's response to normal hormonal regulation. Both such pathologies are associated with increased levels of local and systemic pro-inflammatory cytokine productions (42) . Elevated levels of TNF, IL-6, IL-1 released locally by adipocytes and immune cells as well as from distal systemic sites directly increase FA release from adipocytes as well as decreases anti-inflammatory and insulin sensitizing adipokines (adiponectin) (43-47). This sequence of altered peptide hormones and fatty acid release

directly contributes to systemic insulin resistance and subsequent metabolic complications in both obesity and lipodystrophy.

1.2. Dysregulation of Adipose Tissue Metabolism

Dysregulation of adipose tissue mass through excessive expansion (obesity) or loss (lipodystrophy) is characterized by infiltration of peripheral immune cells, inflammation, cell death and insulin resistance (42). Excessive adipose tissue mass and/or cell size is a hallmark of obesity and a major risk factor for type II diabetes, cardiovascular disease, hypertension and certain forms of cancer. Conversely, complete or partial loss of adipose tissue mass, as with genetic lipodystrophies, promotes metabolic abnormalities such as insulin resistance, hypertriglyceridemia, and hepatic steatosis. Therefore, understanding the molecular mechanisms that disrupt adipocyte and adipose tissue homeostasis is critical for developing therapies for adipose tissue pathologies.

1.3. Skeletal Muscle

1.3.1. Metabolism

Skeletal muscle is the major glucose disposing organ in the body and contributes significantly to fatty acid oxidation after a meal and during high intensity exercise. In order to maintain homeostasis, the body needs to keep blood glucose levels within a narrow optimal range of about 5 mM. When blood glucose levels rise, as occurs after a meal, insulin is released by the pancreas (described below), allowing the periphery, including muscle, liver, and adipose tissue, to clear the plasma and take up glucose for utilization or storage.

Muscle is critical to whole body glucose homeostasis, as this tissue is responsible for >70% of whole body insulin stimulated glucose uptake (48). The cellular action of

insulin was described in the previous section. Insulin resistance occurs when peripheral tissues (e.g. muscle) fail to take up glucose appropriately in response to insulin. This can occur when signaling is disrupted at any point in the cascade. Initially, the pancreas produces more insulin to overcome the peripheral resistance and maintain glucose homeostasis, resulting in compensatory hyperinsulinemia (49). However, eventually the pancreas can no longer compensate for the peripheral resistance, resulting in type 2 diabetes (T2D). Maintaining peripheral insulin sensitivity is thus critical to preventing T2D.

There are insulin-dependent and insulin-independent pathways for regulating glucose uptake in skeletal muscle. The insulin-independent pathways involve the protein energy sensor AMPK (50). AMPK is a protein kinase that becomes phosphorylated (activated) by AMP as intracellular ATP levels become depleted. Activated AMPK phosphorylates the protein TBC1D1/4. TBCD1/4, also known as AS160, negatively regulates GLUT4 trafficking to the plasma membrane by help tethering GLUT4 sensitive vesicles in the cytosol (51). This mechanism thereby feeds into the insulin signaling pathway (independent of PI3K and AKT), and increases GLUT4 translocation from cytosol storage to the plasma membrane.

Additionally, metabolism of lipid species in muscle can activate the PPARα pathway. PPARα regulates a specific set of genes that are involved in peroxisomal and mitochondrial oxidation of fatty acids (52). Enhanced activation of PPARα up-regulates genes such as ACOX that promote a feed forward loop promoting fatty acid oxidation in both peroxisomal and mitochondrial pathways. The PPAR co-activator PGC1α is also known to participate in the actions of PPARα promoting oxidation of fatty acids (53).

Therefore, fatty acids themselves can promote PPARα and PGC1α gene expression and activity resulting in fatty acid oxidation in muscle.

AMPK promotes FA oxidation by directly phosphorylating and thereby inactivating acetyl-CoA carboxylase (ACC), an enzyme responsible for producing malonyl CoA in the first and rate limiting step of FA synthesis (54). Malonyl CoA inhibits carnitine palmitoyltransferase-1 (CPT-1), the rate-limiting enzyme for FAs to enter the mitochondria for oxidation (55). Thus, by inactivating ACC, AMPK relieves inhibition on CPT-1 and promotes FA entry to the mitochondrion and oxidation.

Exercise or exercise mimetics increase expression of transcription factors including peroxisome proliferator-activated receptors (PPARδ) and forkhead box transcription factors (FoxOl) (56) in skeletal muscle. PPARδ promotes fatty acid oxidation in part by increasing transcription of genes including UCP-2 and PDK-4, the latter being a kinase responsible for phosphorylating and inactivating the pyruvate dehydrogenase complex, thereby shifting substrate oxidation towards lipid and away from glucose (57). Another downstream target of PPARδ, FoxOl, also modulates lipid metabolism in skeletal muscle. Similar to PPARδ, FoxOl has also been shown to inactivate the pyruvate dehydrogenase complex (58). Therefore, muscle is an important contributor to glucose disposal and fatty acid oxidation.

1.4. Nuclear Factor κ B (NFκB)

1.4.1. NFκB Signaling

The canonical NFκB signaling pathway orchestrates gene expression important for the regulation of immune and inflammatory responses (cytokines and chemokines) and also controls the expression of proteins with anti-apoptotic, pro-proliferative and

antioxidant activities (59). In a non-stimulated state, the IκB family of inhibitory proteins keep NFκB dimers inactive (60). Induction of NFκB signaling induces upstream kinases to phosphorylate and dissociate inhibitory proteins, which are proteolytically processed by the proteasome (see below), from NFκB dimers allowing NFκB nuclear important, DNA binding and transcription factor activity.

1.4.2. NFκB signaling and Energy Metabolism

The NFκB signaling pathway has an established role in the regulation of energy metabolism and inflammation in models obesity-mediated insulin resistance (61-65). Ablation of upstream activators of the NFκB pathway has linked this pathway to the regulation of energy metabolism and insulin sensitivity (63). IKKβ has been linked to obesity-induced insulin resistance while IKKε has been shown to regulate energy balance (64, 65). Therefore, modulating NFκB activity through specific upstream activators affects energy metabolism and insulin sensitivity.

1.5. The Pancreatic Islet: β-cell Nutrient Sensing and Insulin Release

The pancreatic islet is responsible for secreting peptide hormones such as insulin, glucagon, amylin and somatostatin in response to nutrients. The pancreatic β-cell is the site of insulin synthesis and release in response to glucose and to a lesser extent amino acids and lipid.

Insulin is synthesized in pancreatic β-cells as preproinsulin, stored in vesicles, matured by a series of proteolytic cleavage steps and released upon nutrient stimulation (66). In mature adult islets, insulin secretion occurs quickly after an acute bolus of glucose. This secretion has been observed to occur in a biphasic nature in which the primary response exhibits rapid kinetics followed by a second phase shows slower

kinetics of insulin release. These kinetics reflect two signaling pathways in the β-cell; the first phase is K_{ATP} channel dependent while the second phase is K_{ATP}-independent (67). These two pathways affect different pools of insulin. The first phase faciliates release of the immediate early insulin pool while the second phase releases a slower release pool from the pancreatic β-cells.

Chronically elevated circulating concentrations of nutrients such as glucose, amino acids, lipids or a mixture of these adversely affects β-cell number and function. The β-cell does not limit nutrient uptake and therefore is very sensitive to the damaging effects of excessive mitochondrial respiration.

NFkB is a newly appreciated regulator of glucose-stimulated insulin release. Work has demonstrated that inhibition of NFkB does not affect β-cell development but inhibits glucose-stimulated insulin secretion (68). This occurs in the absence of pathological inflammation demonstrating the role of NFkB in homeostatic cell function. Therefore, inhibiting NFkB function can result in dysregulation of β-cell insulin exocytosis in response to nutrient stimulants.

1.6. Ubiquitin and FAT10 Biology

1.6.1. *The Ubiquitin System and Ubiquitin-like Molecules*

Ubiquitin serves as a post-translational modification that determines the function, cellular localization and the ultimate fate of proteins (69). Ubiquitin is a 76-residue protein that forms iso-peptide bonds with its free C-terminal glycine to the ε-amino group of lysines on target proteins. Ubiquitin is conjugated to substrate proteins through a triad of proteins known as ubiquitin conjugating enzymes designated E1, E2 and E3. The E3

enzyme is responsible for the final step in covalent modification of the ubiquitin substrate protein.

Over recent years the ubiquitin family has grown to include many ubiquitin-like proteins, falling into two classes. The ubiquitin-binding proteins (UBPs), HDAC6 for an example, contain ubiquitin binding domains and interact non-covalently with ubiquitin-modified proteins (69). The second class of proteins comprises ubiquitin-like molecules (ULMs) which include LC3, SUMO(1-3), ISG15, NEDD8 and FAT10. Actions of ULMs modulate such processes as cellular signaling, histone function, transcription factor activity, vesicle transport, autophagy, and protein-protein interactions (70).

1.6.2. *Ubiquitin System, Insulin Signaling and Metabolic Homeostasis*

As mentioned, insulin is an anabolic hormone that affects a wide array of metabolic pathways including protein synthesis, glycogen synthesis, cell division and survival as well as translocation of intracellular glucose transporters to the plasma membrane. Ubiquitin and ULMs regulate proteins responsible for systemic insulin homeostasis and insulin receptor signaling (71). Insulin promotes anabolic action by blocking protein breakdown and promoting synthesis. This is believed to be accomplished by dissociating a protein known as the insulin degrading enzyme (IDE) from the proteasome and selectively inhibiting proteolysis. As a negative feedback mechanism to extinguish insulin signaling, IR endocytosis as well as IRS 1 and 2 degradation via the E3 ligases c-Cbl and SOCS 1/3, respectively, is an ubiquitin-mediated process (72-74). FOXO proteins, which promote catabolic functions such as glycogenolysis and lipolysis are negatively regulated by insulin, are ubiquitylated and degraded (75). Concerning glucose transporter trafficking, GLUT4 degradation and

targeting to the insulin responsive GLUT4 storage compartment in muscle and adipocyte cells is regulated by the ULM SUMO (76). Therefore, a highly regulated system involving ubiquitin and ULMs coordinates the anabolic actions of insulin while safeguarding against over-active signaling. Pancreatic β-cell function and glucose-stimulated insulin secretion are also regulated by UMLs. SUMO1 impairs glucose-stimulated secretion by blunting the β-cell excitotoxic response to calcium (77). In summary, ubiquitin and UMLs have diverse functions in keeping fine control of insulin receptor signaling as well as systemic insulin levels via regulating insulin receptor signaling as well as insulin exocytosis from pancreatic β-cells.

1.6.3. Ubiquitin and NFκB

Ubiquitin governs the NFκB signaling pathway in both proteolytic and non-proteolytic capacities (78). Signals that activate the NFκB pathway, such as cytokines, result in ubiquitin-dependent proteasomal processing of the IκB kinase which releases its inhibitory hold on NFκB (described above) allowing full NFκB activity. Additionally, ubiquitin chains that do not result in protein degradation coordinate protein-protein signaling interactions upstream of NFκB promoting the signaling cascade. Therefore, ubiquitin plays an important role in NFκB signaling in various cell types.

1.6.4. *FAT10: Gene structure and localization*

The human leukocyte antigen (HLA) F-adjacent transcript 10 (FAT10) was discovered in a 280 Kb yeast artificial chromosome screen of the human HLA-F locus (79). FAT10 is located adjacent to the major histocompatability complex (MHC) class I locus on human chromosome 6 and mouse chromosome 17. Examination of the FAT10 gene promoter reveals binding sites for interferon regulatory factors (IRF), AP-1, nuclear

factor kappa b (NFkB) (Figure 1-3 (80)). [These features suggest FAT10 may play a role in immune cell function and inflammation. Subsequent work demonstrates that FAT10 is constitutively expressed in B-cells and mature dendritic cells, supporting evidence for a role in immunity (81). However, the role FAT10 plays in cell biology has yet to be accurately identified.]

Consistent with these promoter elements FAT10 is highly up-regulated by the inflammatory cytokines TNFα and IFNγ (82). Additional work has demonstrated that FAT10 is a cell cycle regulated gene, is transcriptionally repressed by p53 and post-translationally modifies p53 promoting transcriptional activity (83-85). These data suggest FAT10 may play a role in cell fate decisions when faced with factors that dysregulate cell cycle events and cellular homeostasis (viral infection, cancer progression, genomic damage).

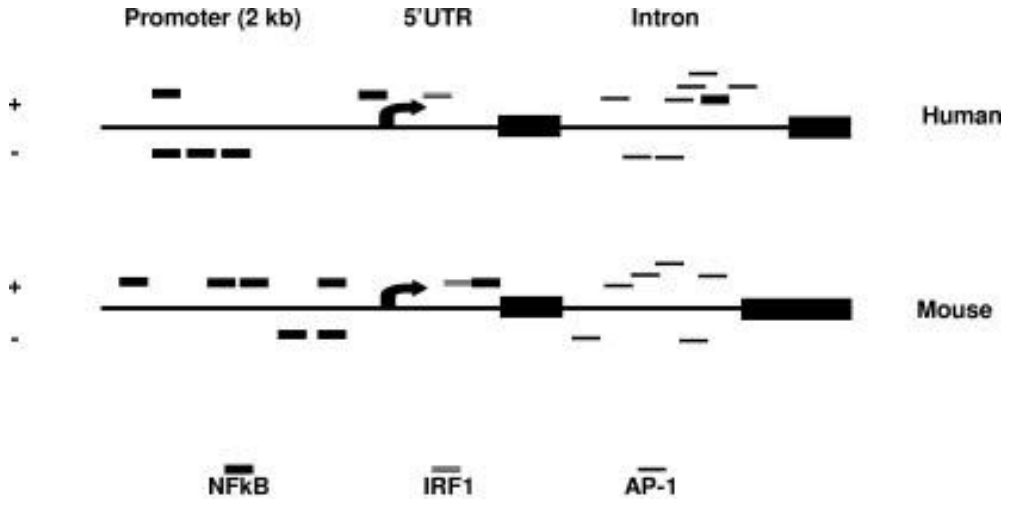

Figure 1-3. FAT10 promoter region (80).

1.6.5. *FAT10: Biological Role*

The role FAT10 plays in cell biology has yet to be accurately identified. Studies suggest that FAT10 can act as a non-covalent protein chaperone, a covalent enhancer of transcriptional activity and a signal for protein degradation (83, 86, 87). Until recently, ubiquitin has been the sole post-translational modification directing proteins to proteasome degradation. Now it is known that FAT10 is a second signal for protein degradation, challenging a well established paradigm of protein degradation. Early work has suggested a role for FAT10 in B-cell and dendritic cell maturation, therefore a putative immuno-modulatory protein (81). However, FAT10 is now known to be expressed in most cells of the body and significantly up-regulated when exposed to inflammatory cytokines TNFα and IFNγ. Outside of a role in protein degradation, FAT10 modifies p53 and promotes its transcriptional activity. Because FAT10 is up-regulated in inflammatory cancers and negatively regulated by p53, FAT10 may influence the balance of cell fate decisions via modulating p53 activity.

1.6.6. Fat10 and NFκB

Recently, FAT10 has been suggested to modulate NFκB activation (88) by an as-yet undetermined mechanism. Specifically, FAT10 KO mice exhibit an impaired response to TNFα challenge manifest by a decreased production of inflammatory cytokines from the liver and kidneys (88). It was demonstrated that knock down of FAT10 in renal cells impaired processing of IκBα accompanied by a decrease in NFκB nuclear translocation and transcriptional activity. Exposure of peritoneal macrophages did not inhibit nuclear translocation of NFκB. The precise mechanism of how FAT10

regulates this process was not elucidated in this study; however, this work suggests FAT10 plays a role in NFκB activation in a cell specific manner.

1.7. Summary

Energy storage and homeostasis is profoundly influenced by adipose tissue metabolism. Once believed to be an inert storage site for neutral lipid, adipose tissue has emerged to be a potent regulator of systemic metabolism and insulin sensitivity through modulating the release of FAs and adipokines. A dynamic interplay of signaling pathways coordinates the adipocyte's response to insulin. Post-prandial increases in insulin promote energy storage while fasting decreases in insulin concentrations results in lipid breakdown and release for energy in peripheral metabolic tissues. Nutrient intake modulates the release of insulin from pancreatic β-cells thus initiating the resulting physiological outcomes of insulin action. Both impairment of insulin release from β-cells or resistance to insulin signaling post-receptor binding will result in enhanced catabolic activity in adipocytes. This can directly affect the body's ability to respond to nutrient flux from adipocytes. Healthy peripheral tissues have the ability to handle an increased flux of FAs from adipose tissue by increasing metabolism of these substrates. However, in insulin resistance tissues, these actions are impaired. Understanding the genetic factors that affects insulin release and action are important for therapies in individuals that have genetic mutations in components of these pathways.

Chapter II

RESEARCH DESIGN AND METHODS

Mice

All experiments were performed in accordance with the Institutional Animal Care and Use Committee of the National Institutes of Health guidelines for the care and use of laboratory animals. FAT10 KO mice were obtained from Allon Canaan (Yale University, New Haven, CT) and re-derived at the Tufts Medical Center Core Transgenics Facility (Tufts University, Boston, MA). After re-derivation, mice were re-located to the Comparative Biology Unit at the JM USDA HNRCA at Tufts University. WT and KO lines were generated from mating heterozygous mice from the F0 generation. WT and KO offspring (F1) from this generation were back-crossed at least 7 generations. Generation of the FAT10 KO mouse has been previously described.

FAT10 KO and WT mice were weaned at 17 days of age and maintained on standard chow diet (Harlan-Teklad 2016S) for the extent of the study. All animals were housed in an AAALAC-approved animal facility with 12-h light/dark cycles and given free access to water and food. Mice were checked daily and body weight and body composition were monitored weekly to track adiposity. At twelve weeks of age, sub-sets of wild type mice and FAT10 KO mice were taken for physiological testing (Insulin tolerance test (ITT) and glucose tolerance test (GTT)), metabolic chamber analysis for assessment of energy expenditure and MRI analysis for final body composition. After a recovery period of at least two days (determined by return to body weight prior to physiological testing assessed by weighing and MRI), mice were sacrificed for blood and tissue collection. Epididymal white adipose tissue (eWAT), quadriceps, liver, pancreas and brown adipose

tissue were taken at harvest. Tissues were snap frozen in liquid nitrogen or fixed for histological analysis.

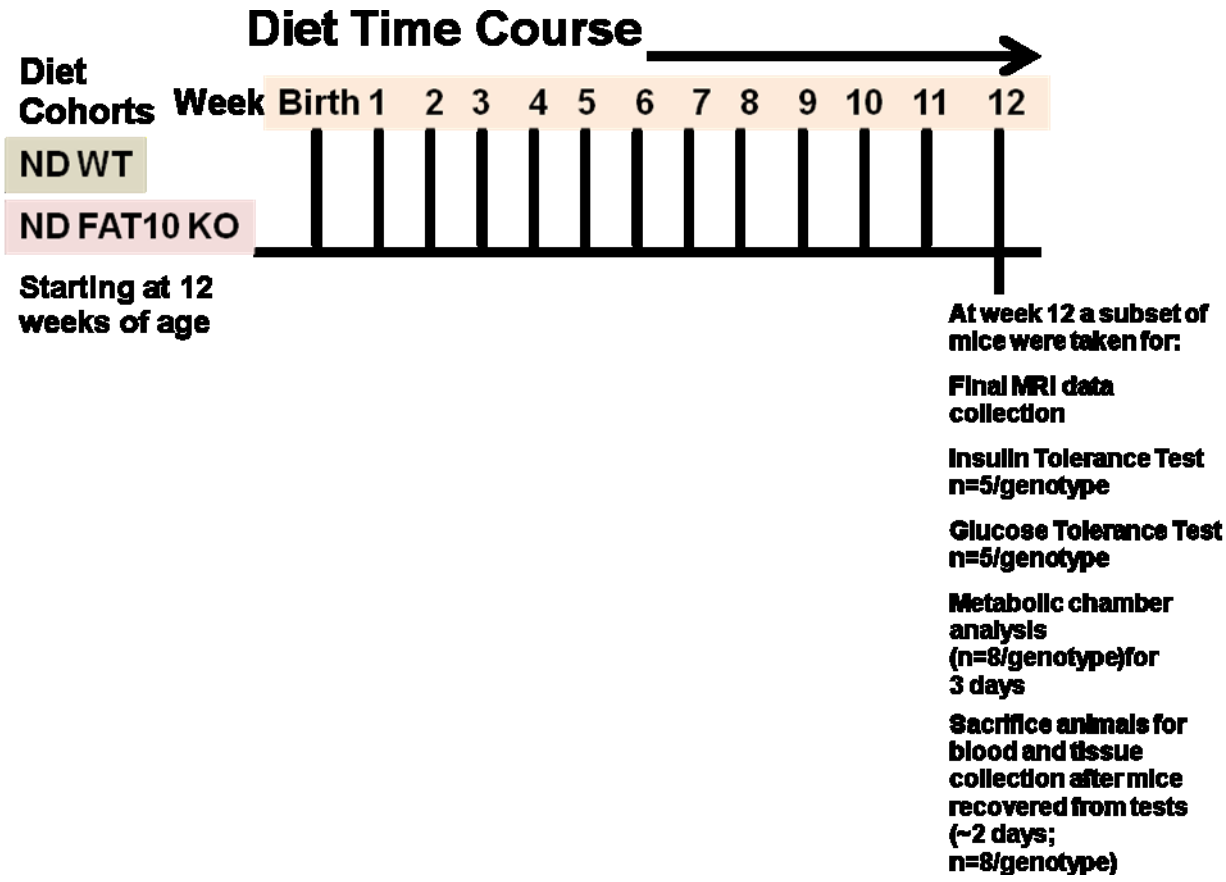

Figure 2-1. Study Design for Study #1.

For Study #2, mice were put on high fat diet (Research Diets) at 12 weeks of age for 12-16 weeks. A subset of FAT10 KO mice were kept on study in order to determine if KO mice would gain as much fat mass as WT mice (These WT mice will be kept on diet only for 12 weeks; therefore, FAT10 KO mice will be evaluated for additional fat gain as to match the total fat of WT mice at 12 weeks of age). Mice from both genotypes were sacrificed for blood and tissue collection at 12 weeks (except for the additional FAT10

mice kept on diet). Epididymal white adipose tissue (eWAT), quadriceps, liver, pancreas and brown adipose tissue were taken at harvest. Tissues were snap frozen in liquid nitrogen or fixed for histological analysis.

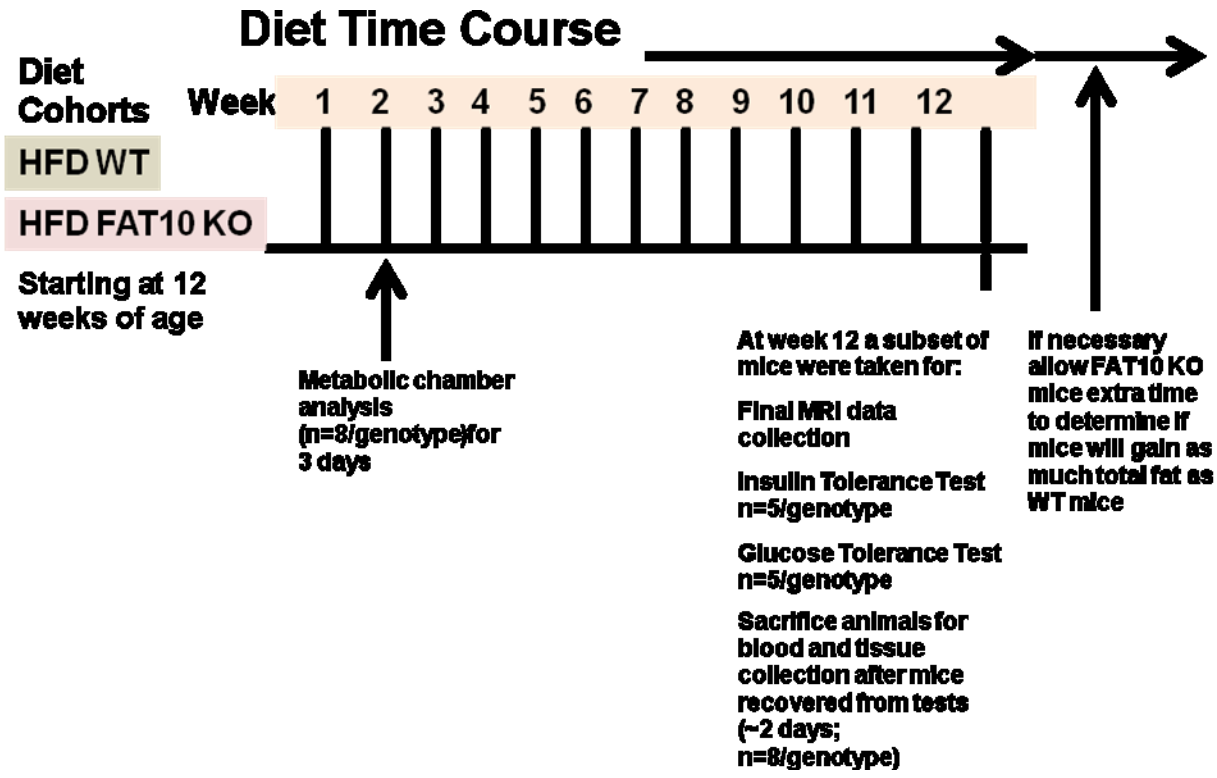

Figure 2-2. Study Design for Study #2. High fat feeding of WT and FAT10 KO mice.

Real Time PCR studies (Study #1 and #2)

All tissues were dissected, snap-frozen in liquid nitrogen, and stored at −80°C. Total RNA was extracted with RNeasy Lipid Mini Kit (Qiagen, Valencia, CA) and quantified (Nanodrop, Thermo Scientific, Wilmington, DE). One microgram of RNA was used as a template for reverse transcription for cDNA synthesis (Promega, Madison, WI). The cDNA product was diluted 1:5 and analyzed by SYBR Green real-time PCR on an Applied Biosystems 7300 Real-time PCR system. Fold expression relative to an

endogenous control gene (cyclophilin A, cyclophilin B and/or 18S) was calculated as $2^{-\Delta\Delta Ct}$ using mice fed the chow diet as the "comparer." All primer sequences are listed in the appendix.

Adipocyte sizing (Study #1 and #2)

Mice were killed by cervical dislocation following CO2 narcosis. Epididymal AT (eAT) were dissected, fixed, embedded in paraffin, and sectioned. Digital images were acquired with an Olympus DX51 light microscope. For each mouse, morphometric data were obtained from digitized tracings of ≥500 adipocytes from 3 or more sections cut at least 50 um apart. Adipocyte size was calculated as described. Adipocytes were binned into size classes by calculating total cells counted and dividing that into the number of adipocytes present in each size class to generate a percentage of cells per size class.

Intraperitoneal insulin and glucose tolerance tests (Study #1 and #2)

Insulin tolerance tests (ITTs) were performed on food-deprived (6 h), nonanesthetized mice. Glucose measures were obtained from whole tail vein blood using an automated glucometer at baseline and at 30, 45, 60, and 90 min following intraperitoneal injection of human insulin (either 0.75 or 1.0 mU/kg). Glucose tolerance tests (GTTs) were performed on food-deprived (12 h), non-anesthetized mice. Glucose measures were obtained similar to the ITT with the following changes. Blood glucose was measured at baseline, 3, 7, 15, 30, 60, 90 and 120 min following intraperitoneal injection of 2 mg/kg glucose bolus. Whole tail vein blood (30 uL) was sampled at baseline, 3, 7, 15 and 30 min in order to measure insulin in a subset of mice from the GTT.

Insulin Signaling Experiments (Study #1)

For assessment of insulin signaling in adipose, liver, and muscle tissues, mice were fasted in the morning for 6 h followed by and IP injection of either saline or insulin (1.0 U/kg). Mice were sacrificed by CO2 narcosis followed by cervical dislocation 10 m post injection and tissues were harvested and immediately snap-frozen in liquid nitrogen. Tissues were homogenized in the appropriate lysis buffer and 15-20 ug of lysate protein was analyzed by SDS-PAGE analysis.

Antibodies (Study #1)

Rabbit polyclonal antibodies anti-AKT (9272), anti-pAKT (9271), anti-ACC (3662), anti-pACC were purchased from Cell Signaling Technologies (Danvers, MA). Goat polyclonal anti-Glut4 was purchased from Santa Cruz Biotechnology (Santa Cruz, CA). Perilipin was made in house. Phospho-perilipin was made (S522) was made at Vala Sciences by request.

Metabolic Studies (Study #1 and #2)

Studies were performed on mice at 12 weeks of age on a chow diet and housed in TSE metabolic chambers (TSE Instruments; See study design above). The TSE system simultaneously and continuously monitored food intake, oxygen consumption, and CO2 production. Data were collected for 72 h, during which time mice had free access to food and water. The first 24 h were considered an acclimation period and excluded from analyses. Data were sampled every ten minutes over the data collection time course. For each animal in Study #1, six values were averaged and these data are representative of 24 h metabolic rate clearly divided into night and day cycles. Energy balance was calculated by taking absolute energy expenditure (kcal) and subtracting total calories

consumed (kcal). Positive energy balance promotes weight gain while negative energy balance promotes weight loss.

Isolation of Pancreatic Insulin Content (Study #1)

Total pancreatic insulin content was recovered from pancreata of mice fed for 4 h. Entire mouse pancreas (~ 0.90-1.30 g) was placed into 5 mL of Acid-Ethanol solution (1.5% HCl in 70% EtOH) followed by an overnight incubation at -20C. Tissue was homogenized in Polytron homogenizer and then placed back at -20C overnight. The following day lysates were centrifuged at 2000 rpm for 15 m at 4C (Beckman GS-6R). 100 uL of the Acid-Ethanol solution was neutralized with 100 uL of 1M Tris-HCl pH 7.5. Samples were then further diluted 1:100 and analyzed with an mouse insulin ELISA (CrystalChem, Downers Grove, IL). Total pancreatic insulin was normalized to total pancreas weight.

Isolation of total liver and muscle glycogen (Study #1)

Total liver and muscle glycogen was extracted and quantified using the EnzyChrom Glycogen Assay Kit from Bioassay Systems (Hayward, CA). Briefly, frozen liver samples (~20 mg) were homogenized in PBS with 10mM EDTA. The sample was placed in 1 mL of buffer and then sonicated. Liver lysate was diluted 1:10 prior to spectrophotometric assay. Total glycogen was normalized to tissue weight.

Isolation of total liver and muscle triglyceride (Study #1 and #2). Total triglyceride was extracted as follows. From liver and muscle, ~20 mg of sample into 1 mL PBS-10 mM EDTA buffer. Samples were then sonicated 15-30s each. Protein concentration was determined by the BCA assay. A total of 3 µl of samples (in triplicate) were used for protein determination. Following the protein determination, calculate amount of

homogenate volume equivalent for 25 ug of protein. All tubes are rinsed with heptane the previous day and allow to evaporate in a fume hood. Sample was added in volume equal to 25 ug of protein in a total volume of 200 uL of PBS-10 mM EDTA, pH 7.4. Each sample was then mixed by vortexing. The 200 uL volume was then added to 2 ml of isopropanol-hexane-water (IHW- 80:20:2 v/v/v). Tubes were then covered with aluminum foil and were allowed to incubate for 30 minutes at room temperature. To the 2.2 mL volume add 500 ul of hexane-diethyl ether (1:1) to each tube and mix by vortexing followed by a 10 minute incubation at room temperature covering the tubes with aluminum foil. Following, 1 ml of water was added to separate phases and samples were mixed by vortexing. Samples were covered with aluminum foil and were allowed to incubate for ~20 minutes at room temperature. From the top of the organic phase pipette ~900 uL into the corresponding 4 mL glass vial with screw on top. The organic phase was evaporated with nitrogen at 100-kPa/14.0 p.s.i. At < 100 degrees C. Triglyceride content was determined spectrophotometrically using a commercially purchased kit from Wako.

Adipocyte lipolysis (Study #1)

Mice between 10-12 weeks of age were used for lipolysis experiments. Mice were sacrificed in the fed state at 9 am the morning of the experiment. Approximately 2 g of adipose tissue was isolated from KO and WT mice and placed in 5 mL of KHB buffer supplemented with 4% BSA, glucose and adenosine. Tissue was minced into approximately 10-20 mg pieces and Type II Collagenase (Worthington) was added for a final concentration of 1 mg/mL (255 U/mg). Tissue was incubated with shaking in a 37C water bath for up to 1 h. Digested tissue was poured into a cut-off 10 mL syringe and

filtered through 255 uM sterile nylon mesh. Cells were washed 3x's with fresh KHB buffer by centrifugation (500 g for 1 m). Cells were re-suspended in 10 mL of KHB. While swirling, 500 uL of cell suspension were aliquoted to treatment tubes containing 2.5 mL of KHB supplemented with PIA, ADA, ISO and/or insulin in duplicate. Additional 500 uL of cell suspension was set aside for total lipid isolation as well as cell sizing. Treatment tubes were incubated for 2 h at 37C in a shaking water bath. The lipolysis reaction was extinguished by placing the cells on ice for 5 minutes after the 2 h incubation. A volume of 500 uL from each replicate of each treatment was removed and saved for the glycerol assay. Glycerol was measured spectrophotometrically using Glycerol reagent (Sigma, St. Louis, MO).

CHAPTER III

RESULTS

3.1. Deletion of the FAT10 Gene Alters Energy Homeostasis in Mice

In Preparation for Submission to Endocrinology

Jason DeFuria[1], Grace Bennett[1], Katherine J. Strissel[1], Allon Canaan[2], Sherman Weissman[2], Andrew S. Greenberg[1], Martin S. Obin[1]

1. Obesity and Metabolism Laboratory, Jean Mayer USDA Human Nutrition Research Center on Aging at Tufts University, Boston, MA, USA 02111
2. Department of Genetics, Internal Medicine, Boyer Center for Molecular Medicine, Yale University School of Medicine, New Haven, CT 06511

Corresponding author: Martin S. Obin, PhD, 711 Washington St Room 607 Boston MA 02111. Phone (617) 556-3049 Fax (617) 556-3344, martin.obin@tufts.edu

Abstract

The human leukocyte antigen (HLA) F-adjacent transcript 10 (FAT10), diubiquitin, class I gene is recognized as an inflammation inducible transcript in human cancers and inflammatory diseases. Here we demonstrate a surprising role for FAT10 in the regulation of energy metabolism, fuel partitioning and insulinotrophic axis. In mice fed a normal diet, we demonstrate that FAT10 is expressed during normal AT growth. FAT10 KO mice have reduced adiposity and burn more calories (enhanced energy expenditure) compared to WT mice without decreasing caloric intake or increasing exercise. Using indirect calorimetry, we demonstrate that FAT10 KO mice preferentially burn lipid. Skeletal muscle exhibits increased expression of lipid burning genes. This response appears to be due to increased circulating fatty acids derived from AT release (lipolysis). FAT10 KO mice have constitutively low circulating insulin that may be permissive for the observed enhanced adipose tissue lipolysis. This model suggests that increases in lipolysis are due to decreases in available circulating insulin. The enhanced lipid burning in muscle is in response to the fatty acid load in the blood from AT lipolysis. We propose that FAT10 is a novel gene that influences systemic energy metabolism. Since FAT10 is associated with increased risk for chronic disease (diabetes, cancer, HIV associated nephropathy) and is interactive with key cellular regulators (p53 and NFκB), this work opens new avenues for further investigation of the tissue-specific biological function of FAT10.

Introduction

Adipose tissue (AT) an important regulator of whole body lipid and energy metabolism directly influencing systemic insulin sensitivity and inflammation via release of adipokines and fatty acids (FA) (35). Adipose tissue metabolism can be influenced by both dietary and genetic factors. Excess dietary caloric intake increases adipose mass, inflammation and obesity-associated pathologies while genetic lipodystrophies deceases adipose tissue mass and increases inflammation. Inflammatory mediators (TNFα, IL6, IL1β) and their effector signaling pathways such as c-Jun N-terminal Kinase (JNK) and Nuclear Factor κ B (NFκB) play important roles in the development of adipose tissue dysfunction and insulin resistance in both obesity and genetic lipodystrophies (61, 89-93). However, a role for these mediators and pathways in non-pathological, homeostatic regulation of AT is now becoming more evident as ablation of cytokines or pathway components of inflammatory signaling can either promote or inhibit adipose tissue growth in the absence of diet-induced obesity (64, 94-96).

FAT10 is a MHC Class I-associated gene that is dramatically up-regulated in response to inflammatory cytokines (TNFα and IFNγ) in both immune and non-immune cell types (81, 97). Recently, deletion of the FAT10 gene in mice has demonstrated an impaired response to TNFα stimulation and *in vitro* gene knock-down was shown to attenuate cell-specific NFκB activation (88). In other studies, gene array profiling has revealed dramatic up-regulation of FAT10 expression in AT of a mouse model of lipodystrophy and down-regulation of expression in AT of calorically restricted animals (92, 98). Therefore, the FAT10 gene is expressed in AT of mice and responds to changes in AT inflammation, metabolism and mass.

Currently, the role of FAT10 in physiological adipose tissue growth and metabolism has not been investigated. We took advantage of FAT10 KO mice to investigate the role of FAT10 in the regulation of body composition and adipose tissue mass. Increases in FAT10 expression is correlated with adipose tissue growth in WT, normal-diet fed mice. FAT10 KO mice revealed a substantial decrease in adiposity due in part to smaller adipocytes with concomitant increases in energy expenditure. FAT10 KO mice have a preference for burning fatty acids during the light phase and this is supported by increases in circulating FAs as well as in basal and stimulated *in vitro* lipolysis. Fat10 KO mice have constitutively lower circulating insulin concentrations during fasting and fed states indicating that the enhanced energy expenditure and catabolic state of the KO mice may be secondary to decreased insulin concentrations. Deletion of the FAT10 gene in mice results in dramatic changes in energy homeostasis.

Materials and Methods

Mice

FAT10 KO, fixed on a C57bl/6 background were obtained from Yale University (New Haven, CT) and re-derived at the Tufts Medical Center Core Transgenics Facility (Tufts University, Boston, MA). After re-derivation, heterozygotes re-located to the Comparative Biology Unit at the JM USDA HNRCA at Tufts University. WT and KO founders were generated from 12 heterozygous mating pairs. These *founders* were used to generate WT and KO lines. Generation of the FAT10 KO mouse has been previously described (80).

Intraperitoneal insulin and glucose tolerance tests

Insulin tolerance tests (ITTs) were performed on food-deprived (6 h), nonanesthetized mice. Glucose measures were obtained from whole tail vein blood using an automated glucometer at baseline and at 30, 45, 60, and 90 min following intraperitoneal injection of human insulin (either 0.75 or 1.0 mU/kg). Glucose tolerance tests (GTTs) were performed on food-deprived (12 h), non-anesthetized mice. Glucose measures were obtained similar to the ITT with the following changes. Blood glucose was measured at baseline, 3, 7, 15, 30, 60, 90 and 120 min following intraperitoneal injection of 2 mg/kg glucose bolus. Whole tail vein blood (30 uL) was sampled at baseline, 3, 7, 15 and 30 min in order to measure insulin in a subset of mice from the GTT.

Insulin Signaling Experiments

For assessment of insulin signaling in adipose, liver, and muscle tissues, mice were fasted in the morning for 6 h followed by and IP injection of either saline or insulin (1.0 U/kg). Mice were sacrificed by CO2 narcosis followed by cervical dislocation 10 m post injection and tissues were harvested and immediately snap-frozen in liquid nitrogen. Tissues were homogenized in the appropriate lysis buffer and 15-20 ug of lysate protein was analyzed by SDS-PAGE analysis.

Antibodies

Rabbit polyclonal antibodies anti-AKT, anti-pAKT and anti-IRβ were purchased from Cell Signaling Technologies (Danvers, MA). Goat polyclonal anti-Glut4 was purchased from Santa Cruz Biotechnology (Santa Cruz, CA).

Metabolic Studies

Indirect calorimetry was performed as previously described (99).

Body Composition

Body weights were measured weekly and body composition was determined weekly using nuclear magnetic resonance technology (EchoMRI-100; Echo Medical Systems, Houston, TX).

Real Time PCR

All tissues were dissected, snap-frozen in liquid nitrogen, and stored at −80°C. Gene expression analysis was performed as previously described (99). All primer sequences are listed in the data supplement.

Pancreatic Insulin Content

Total pancreatic insulin content was recovered from pancreata of mice fed for 4 h. Entire mouse pancreas (~ 0.90-1.30 g) was placed into 5 mL of Acid-Ethanol solution (1.5% HCl in 70% EtOH) followed by an overnight incubation at -20C. Tissue was homogenized in Polytron homogenizer and then placed back at -20C overnight. The following day lysates were centrifuged at 2000 rpm for 15 m at 4C (Beckman GS-6R). 100 uL of the Acid-Ethanol solution was neutralized with 100 uL of 1M Tris-HCl pH 7.5. Samples were then further diluted 1:100 and analyzed with a mouse insulin ELISA (CrystalChem, Downers Grove, IL). Total pancreatic insulin was normalized to total pancreas weight.

Liver and muscle metabolites

Total liver and muscle triglyceride were extracted and quantified as previously described (100) and glycogen was extracted and quantified with the Enzychrom Glycogen Kit per manufacturer's instructions (Bioassay Systems).

Adipocyte lipolysis

Adipocyte lipolysis was performed as previously described (101). Glycerol was measured spectrophotometrically using Glycerol reagent (Sigma, St. Louis, MO).

Statistical Analysis

Data are presented as mean ± SE. Data were determined to have a normal distribution with equal variance, and statistical differences were determined by PROC TTEST or PROC GLM using the Tukey least significant differences test with SAS v9.2 (Cary, NC). Significant differences were determined between groups at $p<0.05$.

Results

FAT10 is expressed in visceral AT and is up-regulated with normal AT growth in C57Bl/6 mice

FAT10 gene expression [is highly up-regulated in mouse models of AT lipodystrophy and down-regulated during calorie restriction (92, 98), we wanted to determine if expression was modulated by non-pathological, normal AT growth.] Between 6-18 weeks of age, as mice accrue epididymal adipose tissue mass there is a significantly correlated increase in FAT10 expression (Figure 3-1A-C). Because of the heterogenous composition of AT, we wanted to identify the cellular source of FAT10 is expressed in T-cells, dendritic cells, macrophages and B-cells (81, 87), we therefore determined if the source of FAT10 expression in adipose tissue was due to presence of immune cells. Separation of adipocytes from SVCs followed by real time PCR indicates that both adipocytes and stromal vascular cells both express FAT10, but adipocytes adipocytes express ~1.8 fold higher expression than the SVC fraction (Figure 3-1D). To more closely examine FAT10 expression in adipocytes, we used 3T3-L1 cell line. Consistent with these data, FAT10 expression increased during differentiation of 3T3-L1

cells. Additionally, when compared to other metabolic tissues, FAT10 expression was highest in white adipose tissue (Figure 3-1E).

FAT10 KO mice have reduced adiposity

To investigate the role of FAT10 *in vivo*, we obtained FAT10 KO mice and examined their AT. We acquired FAT10 KO mice and determined body weight as well as lean and fat mass by MRI of 12 week old, male KO and WT mice (Figure 3-2). There was no difference in total lean mass; however, total body weight was reduced by ~1 g in KO mice due to the reduction of 50% loss of body fat (Figure 3-2A). Therefore, the difference in body weight was can be accounted for by the decreased fat mass of the KO mice. Histological examination of epididymal adipose tissue revealed a reduction in adipocyte size (Figure 3-2B). The distribution of cell size revealed a greater proportion on adipocytes in smaller size classes (0-3000 μm^2) while virtually absent from larger size classes (3000-5000 μm^2). However, there was no difference in cell number between genotypes (data not shown). Therefore, reduced adiposity in FAT10 KO mice is due in part to decreased adipocyte size.

Previous studies have demonstrated that alterations in adipocyte size have been correlated with adipocyte specific gene expression patterns of adipokines. Consistent with reduced adipocyte size, epididymal adipose tissue gene expression of leptin was decreased while adiponectin was increased (Figure3- 2C).

Increased energy intake and expenditure in FAT10 KO mice

Surprisingly, reduced adiposity was associated with higher energy intake in the FAT10 KO mice. Assessment of energy intake revealed that FAT10 KO mice consume equal amount of calories as WT mice; moreover, when normalized to body weight

FAT10 KO mice consume 10% more calories than WT mice (Figure 3-3A). Because FAT10 KO mice have reduced adiposity despite equivalent or slightly higher energy intake, we hypothesized that FAT10 mice would have increased energy expenditure. Indirect calorimetry revealed that FAT10 KO expend more energy (increased VO2 and VCO2) in both night and day cycles (Figure 3-3B). Moreover, enhanced energy expenditure is not due to increased locomotor activity, as KO mice have slightly reduced activity during the day (Figure 3-3D).

Since, FAT10 KO mice do not consume more calories and have increased energy expenditure, one would predict that FAT10 mice have alterations in energy balance, the difference between energy intake and energy expenditure. FAT10 KO mice are in more negative energy balance during the light phase (Figure 3-3C). These data suggest that the lean phenotype of the FAT10 mice reflects a greater negative energy balance during the light phase.

Normally during the light phase, decreased food intake reduces the respiratory energy ratio, an indices of carbohydrate (RQ = 1.0) and fat (RQ = 0.7) utilization, indicating a preferential use of fat during the light phase. FAT10 KO mice have a significantly lower RQ during the light phase compared to WT mice ($p = 0.05$) thus indicating increased fatty acid utilization (Figure 3-3G).

Increased in the KO mice could reflect an increased thermogenic demand. To assess the potential of adaptive thermogenesis we housed FAT10 KO and WT mice at thermoneutrality (30^{o}C) for 5 weeks and assessed body weight and fat gain. Both KO and WT mice gained both weight and fat at thermoneutrality; however, KO mice gained less of each (Supplementary Figure 3-1S) indicating that the increased energy expenditure in

KO mice is not due to adaptive thermogenesis. Consistent with these results, body temperature of KO and WT mice were not significantly different **(**data not shown**).**

FAT10 KO mice have an enhanced adipocyte lipolytic program

Decreased adiposity reflects the relative contribution of lipid synthesis (anabolism) or an enhancement of lipolysis (catabolism) in AT. The RQ suggested that the decrease in adiposity reflected an enhanced catabolism of adipocyte triglyceride. Therefore, we performed functional *ex vivo* lipolysis assays on isolated adipocytes. Lipolysis assay results indicate that FAT10 KO mice have increased basal as well as stimulated lipolysis compared to WT mice (Figure 3-4A). This data is supported *in vivo* evidence by an increase in perilipin phosphorylation during fasting, a metabolic state that promotes lipolysis (Figure 3-4A). performed gene expression analysis in order to determine if genetic pathways involved in adipocyte lipid metabolism were altered in KO mice. Genes encoding Lipe (HSL) and PNPLA2 (ATGL) were up-regulated in adipose tissue of 12 h fasted KO mice supporting an enhanced lipolytic tone (Figure 3-4B).

Lipolysis is associated with triglyceride cycling (re-esterification) and β-oxidation within adipocytes (102, 103). Consistent with enhanced adipocyte hypothesis (above), genes involved in both triglyceride biosynthesis and β-oxidation were up-regulated in AT (Figure 3-4C). To further investigate a possible role for β-oxidation, we measured total and phosphorylated ACC1 protein levels. There was a 48% increase in phosphorylated ACC1 suggesting an increase in lipid partitioning to the mitochondria (Figure 3-4C). These data together support that enhanced lipolysis is accompanied by increases in adipocyte β-oxidation.

Decreased skeletal muscle TAG and increased oxidative metabolic gene expression in quadriceps of FAT10 KO mice

As it appears, FAT10 KO mice prefer the use of FA as a metabolic substrate; therefore, we examined expression of markers of β-oxidation in quadriceps of FAT10 KO and WT mice. Figure 3-5A shows that FAT10 KO mice have significant increases in genes involved in fatty acid catabolism (ACOX, ACOT1, ACOT3, PPARα) as well as up-regulation in genes involved in energy uncoupling (UCP2 and UCP3) (Figure 3-5A). Interesting, genes involved in fatty acid synthesis are also up-regulated. These data taken together suggest that the skeletal muscle in FAT10 KO mice have the increased capacity for fatty acid use. Additionally, it appears that increases in fatty acid synthesis may parallel the need for increased substrate that may be directly partitioned for oxidative metabolism.

Increased lipolysis may result in accumulation of ectopic lipid in peripheral metabolic tissues. Triglyceride measurements in liver revealed no difference in total lipid between genotypes (Figure 3-5B). However, in skeletal muscle there was decreased lipid in KO mice (Figure 3-5B). These data show that the increased lipolysis exhibited by KO AT does not result in accumulation of lipid in peripheral tissue; moreover, the decrease in skeletal muscle lipid suggests this tissue contributes to fatty acid utilization.

Hypo-insulinemia and insulin sensitivity in FAT10 KO mice

Triglyceride storage reflects the net balance of lipolytic inputs and anti-lipolytic inputs. Insulin inhibits lipolysis and promotes fat storage in adipocytes. Accordingly we investigated insulin secretion and insulin action in FAT10 KO mice. We measured insulin in the fasted and fed state and observed a 50% reduction in insulin (Figure 3-6A).

Yet despite this blood glucose was maintained at a lower concentration (Figure 3-6A). We therefore investigated insulin sensitivity in these mice.

KO mice were more insulin sensitive evidenced by enhanced glucose clearance during an IPITT when adjusted for baseline glucose concentrations (Figure 3-6B). Insulin signaling in AT, liver and quadriceps revealed enhanced AKT phosphorylation in the KO mouse (Figure 3-6C) supporting the IPITT data.

Enhanced glucose tolerance, decreased pancreatic insulin secretion and altered pancreatic Islets in FAT10 KO mice

To assess sensitivity to endogenous insulin levels, IPGTT tests were performed in 12 h fasted mice. KO mice maintained significantly lower glucose levels throughout the entire GTT as assessed by AUC analysis (Figure 3-7A). Insulin levels were significantly reduced in the KO mice at baseline and throughout the first 30 m of the GTT (Figure 3-7A).

Decreased circulating insulin in the fed state can be a result of a defect in pancreatic β-cell number, insulin synthesis and/or insulin vesicle exocytosis. Examination of total pancreatic insulin content revealed KO mice have significantly, although slightly decreased pancreatic insulin levels when adjusted to total pancreatic weight. Histological examination of Islets revealed no abnormal morphology. However, average Islet area was decreased by 27% in the KO mouse pancreas (Figure 3-7B). Therefore, the constitutively low circulating insulin may result from decreases in total Islet area.

Discussion

In this study, we demonstrate that FAT10 gene expression increases with normal adipose tissue growth. AT is known to be composed of a highly heterogeneous

population of cells that include adipocytes and SVCs. Because the expression of FAT10 was originally described in hematopoietic immune cells (81, 108), the increase in AT FAT10 expression could be due in part to increased expression in immune cells. Interestingly, FAT10 gene expression was ~3-fold higher in adipocytes compared to the SVCs suggesting that the increase in FAT10 expression is contributed by the adipocytes rather than immune cells. These findings prompted our group to investigate the potential role FAT10 plays in AT tissue growth and metabolism as well as body composition by metabolically phenotyping FAT10 KO mice.

Work first describing the FAT10 KO phenotype did not evaluate body composition or energy metabolism (80). This current study demonstrates that in the absence of FAT10, mice on a normal diet exhibit changes in body composition, whole body energy expenditure and adipose tissue metabolism. At 12 weeks of age, KO mice had ~50% decreased adipose tissue mass compared to WT mice and this difference was due in part to a smaller proportion of adipocytes. Several knockout mouse models that exhibit decreased adiposity also had substantial increases in energy expenditure and food intake (95, 109-111). The reduced fat mass in FAT10 KO mice were associated with increases in energy expenditure; however, food intake adjusted for body weight showed a modest 10% increase. Furthermore, KO mice did not exhibit increased locomotor activity indicating that enhanced energy expenditure is due to an intrinsic mechanism of substrate utilization.

During the day cycle FAT10 KO mice have significantly lower RQ values indicating a preference for metabolizing fatty acids. This can be achieved by increasing adipocyte lipolysis and burning fatty acids within the adipose tissue or in peripheral

metabolic tissues such as muscle and liver (102). Both basal and stimulated lipolysis was increased in KO mice suggesting enhanced lipid flux. Additionally, fasting circulating NEFA concentrations were slightly elevated supporting a role for increased lipid release from adipocytes. Adipocytes from KO mice up-regulated genes involved in β-oxidation and had an increased proportion of phosphorylated ACC1 suggesting a proportion of the lipid released from lipolysis was being oxidized within adipocytes. With reduced adipose tissue, FA can be shunted to peripheral metabolic tissues and stored as ectopic lipid interfering with insulin sensitivity (112). Inspection of skeletal muscle and liver triglyceride reveal no signs of ectopic lipid deposition and moreover suggest that muscle may also be involved in fatty acid utilization in this model.

In respect to insulin sensitivity, KO mice exhibited enhanced insulin sensitivity. Glucose tolerance was improved in KO mice. Paradoxically, insulin concentrations during the first and second phase insulin release during the GTT indicate that KO mice clear glucose with significantly lower insulin. To test insulin release under physiological conditions, mice were re-fed for 4 hours and circulating insulin concentrations were measured. Re-fed KO mice exhibited lower insulin concentrations as well as decreased blood glucose. These data suggest that KO mice maintain glycaemia with reduced insulin. The GLUT4 transgenic (113) mice both exhibit improved glycemic control, decreased insulin concentrations and increased lipolysis resulting in high circulating fatty acids during fasting. Therefore, other KO models provide evidence where low insulin concentrations result in increased lipolysis.

Due to constitutively low insulin levels, we investigated whether islets from KO mice were altered. We began by measuring total pancreatic insulin concentrations

demonstrating that KO pancreata had slight but significant decreases in insulin. We next examined pancreatic Islet area and discovered that KO mice have 27% reduced total islet area. Islet number between genotypes was not different. These data suggests that KO mice are able to maintain reduced blood glucose levels in the presence of markedly reduced insulin levels, an observation made in several other mouse knockout models (104-107).

As FAT10 is an ubiquitin-like molecule, it is of great importance to determine substrates that FAT10 covalently modifies. Recent work has demonstrated FAT10 modifies p53 and increases its transcriptional activity (83). P53 is known to affect energy sensing and cell growth pathways and is a viable target to investigate the biochemical function of FAT10. Additional work has demonstrated FAT10 is involved upstream of NFκB activation; however, no substrates were identified in this study (88). NFκB has been demonstrated to be necessary for glucose-stimulated insulin secretion from β-cells. Therefore, the primary site of FAT10 activity in normal, physiological processes may facilitate normal β-cell insulin release via promoting activation of the NFκB pathway.

In conclusion, genetic deletion of the FAT10 gene results in mice that have reduced adiposity and enhanced energy expenditure. Adipocytes from KO mice exhibit increased lipolysis, prefer FAs during the day as a metabolic substrate, up-regulate genes involved in β-oxidation and have increased phospho-ACC1 protein in AT. Taken together these data suggest that FAs released from lipolysis are oxidized within AT and possibly skeletal muscle. Decreased Islet area in KO mice in conjunction with slightly reduced total pancreatic insulin may result in constitutively low circulating insulin concentrations. This low circulating insulin may be the primary cause of enhanced lipolysis while

peripheral metabolic tissues adapt by increases substrate utilization. Since FAT10 is associated with increased risk for chronic disease (diabetes, cancer, HIV associated nephropathy) and is interactive with key cellular regulators (p53 and NFκB), this molecule may orchestrate aspects of glucose and fatty acid metabolism in the diseased state.

Figure 3-1

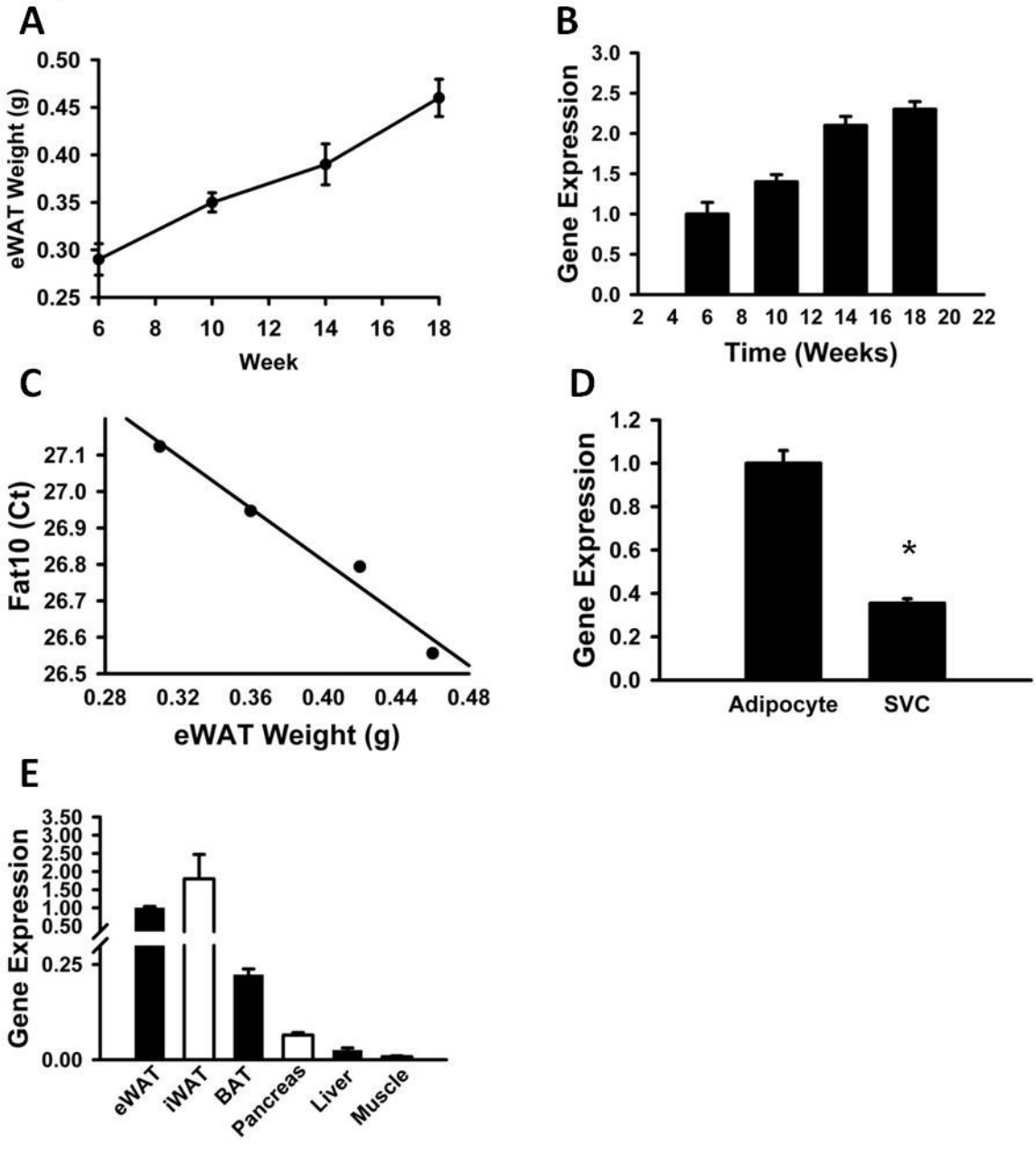
A
eWAT Weight (g)
0.50
0.45
0.40
0.35
0.30
0.25
6 8 10 12 14 16 18
Week
B
Gene Expression
3.0
2.5
2.0
1.5
1.0
0.5
0.0
2 4 6 8 10 12 14 16 18 20 22
Time (Weeks)
C
Fat10 (Ct)
27.1
27.0
26.9
26.8
26.7
26.6
26.5
0.28 0.32 0.36 0.40 0.44 0.48
eWAT Weight (g)
D
Gene Expression
1.2
1.0
0.8
0.6
0.4
0.2
0.0
*
Adipocyte
SVC
E
Gene Expression
3.50
3.00
2.50
2.00
1.50
1.00
0.50
0.25
0.00
eWAT
iWAT
BAT
Pancreas
Liver
Muscle

Figure 3-1. FAT10 gene expression is associated with adipose tissue growth in mice. A) eat weight of WT mice over 12 weeks on normal diet. B) FAT10 gene expression in eWAT from WT mice at indicated time points. C) FAT10 gene expression is associated with adipose tissue growth. D) FAT10 gene expression in isolated adipocytes and SVCs. E) FAT10 gene expression in eWAT, iWAT, BAT, pancreas, liver and muscle. Data are expressed as mean ± SEM (n=6-8 mice/genotype). *, $P < 0.05$.

Figure 3-2

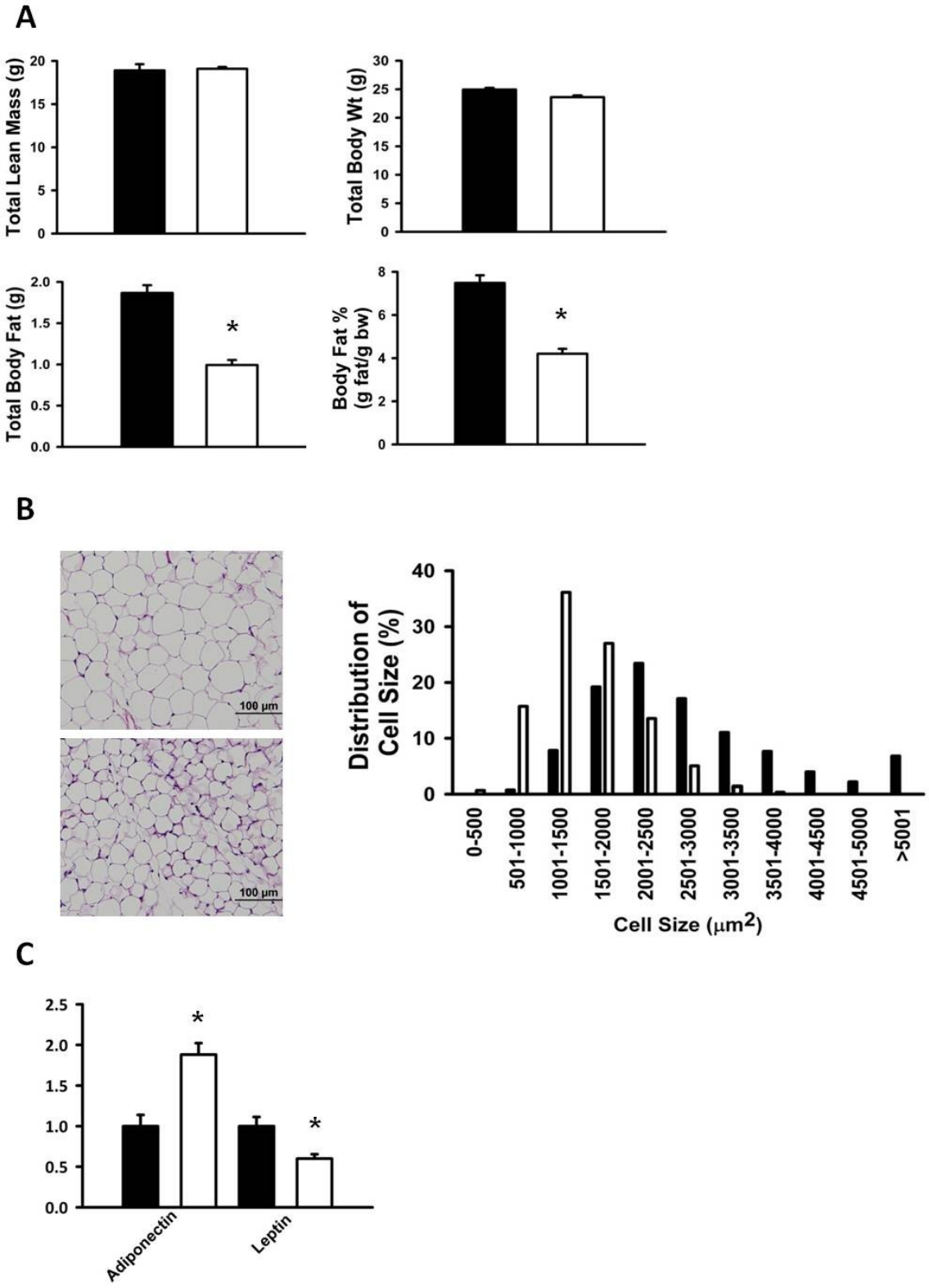
A
Total Lean Mass (g)
Total Body Wt (g)
Total Body Fat (g)
Body Fat % (g fat/g bw)
*
*
B
100 µm
100 µm
Distribution of Cell Size (%)
0-500
501-1000
1001-1500
1501-2000
2001-2500
2501-3000
3001-3500
3501-4000
4001-4500
4501-5000
>5001
Cell Size (µm2)
C
*
*
Adiponectin
Leptin

Figure 3-2. Body composition of WT and FAT10 KO mice. A) *Top*, Total lean mass and body weight of WT (black bars) and FAT10 KO (white bars) mice at 12 weeks of age. A. *Bottom*, Total body fat and adiposity of WT and KO mice. B) Histology of epidydimal adipose tissue and cell size distribution. C) Gene expression. Data are expressed as mean ± SEM (n=6-8 mice/genotype). *, $P < 0.05$.

Figure 3-3

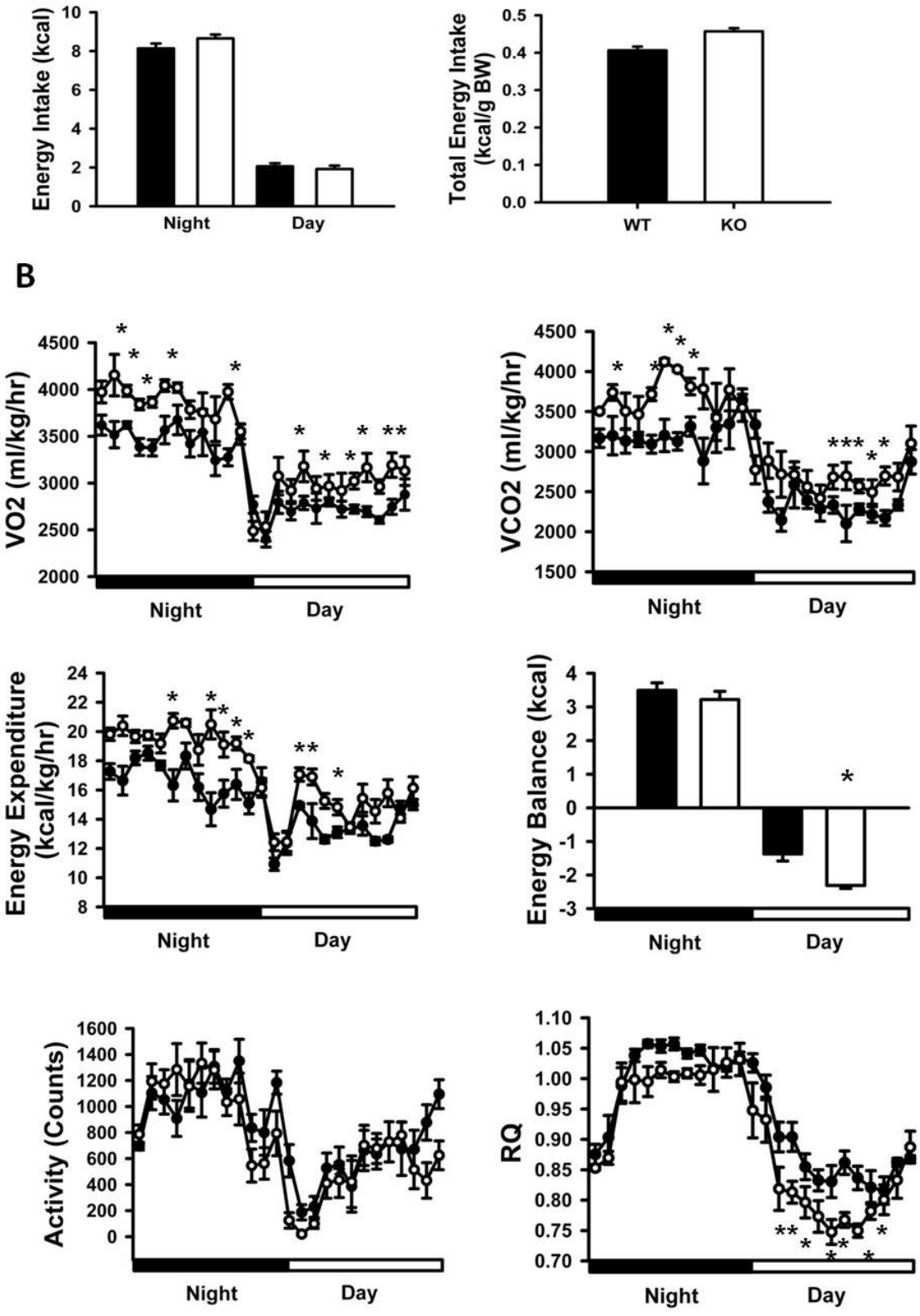
A
Energy Intake (kcal)
Night
Day
Total Energy Intake (kcal/g BW)
WT
KO
B
VO2 (ml/kg/hr)
VCO2 (ml/kg/hr)
Energy Expenditure (kcal/kg/hr)
Energy Balance (kcal)
Activity (Counts)
RQ

Figure 3-3. Energy expenditure analysis. A) Total and body weight-adjusted energy intake in night and day cycles. B) Oxygen consumption, C_{O2} release, energy expenditure, energy balance, activity and RQ over 24 hours of WT (closed circles) and KO (open circles). Data are expressed as mean ± SEM (n=8 mice/genotype). *, $P < 0.05$.

Figure 3-4

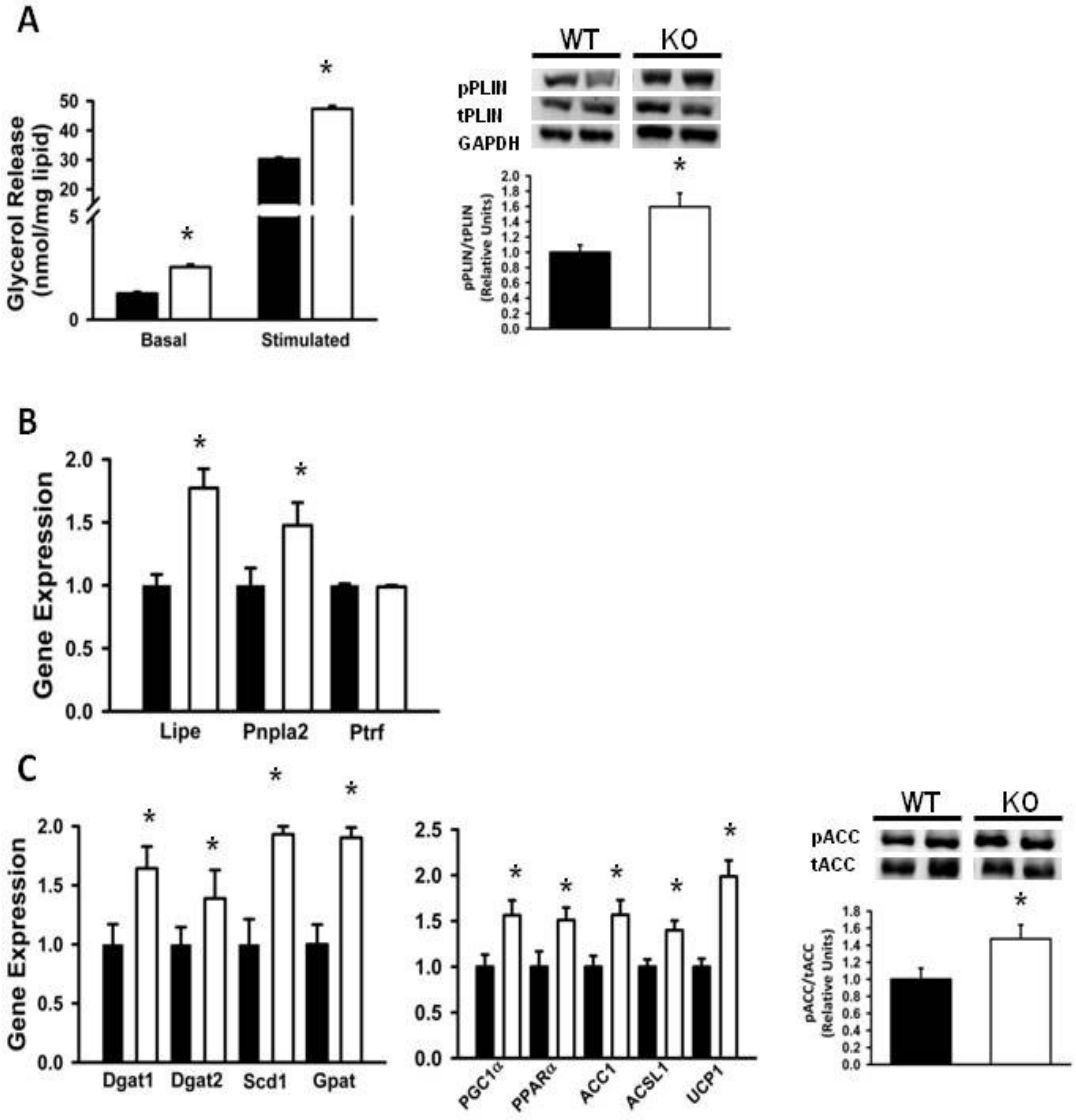
A
Glycerol Release (nmol/mg lipid)
Basal
Stimulated
WT
KO
pPLIN
tPLIN
GAPDH
pPLIN/tPLIN (Relative Units)
B
Gene Expression
Lipe
Pnpla2
Ptrf
C
Gene Expression
Dgat1
Dgat2
Scd1
Gpat
PGC1α
PPARα
ACC1
ACSL1
UCP1
WT
KO
pACC
tACC
pACC/tACC (Relative Units)

Figure 3-4. FAT10 KO mice exhibit enhanced AT lipolysis. A) *Left,* Basal and stimulated lipolysis from isolated adipocytes and *Right,* Phosphorylated and total perilipin protein. B) Gene expression of lipolytic mediators. C) *Left,* Genes involved in TAG biosynthesis. *Middle,* Genes involved in β-oxidation and uncoupling. *Right,* Phosphorylated and total ACC protein. Data are expressed as mean ± SEM (n=5-8 mice/genotype). *, $P < 0.05$.

Figure 3-5

A

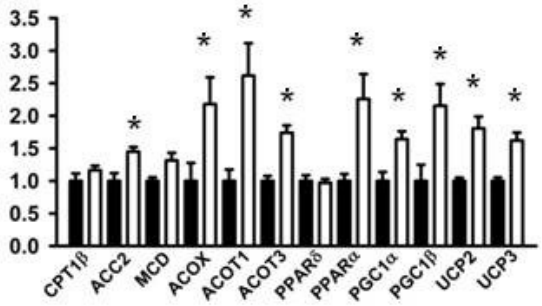
3.5
3.0
2.5
2.0
1.5
1.0
0.5
0.0
CPT1β
ACC2
MCD
ACOX
ACOT1
ACOT3
PPARδ
PPARα
PGC1α
PGC1β
UCP2
UCP3

B

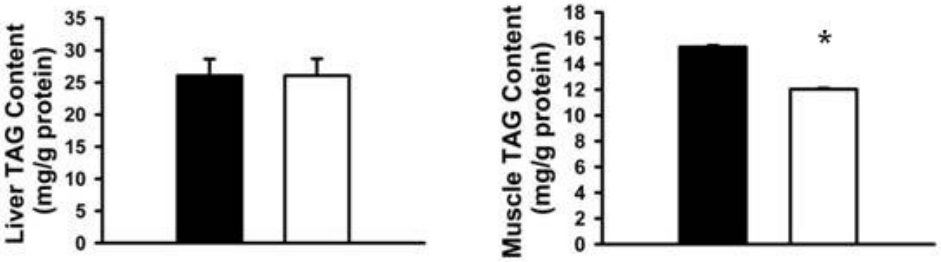
Liver TAG Content (mg/g protein)
35
30
25
20
15
10
5
0
Muscle TAG Content (mg/g protein)
18
16
14
12
10
8
6
4
2
0

Figure 3-5. FAT10 KO mice have decreased skeletal muscle TAG content with increases in lipid oxidative genes. A) Gene expression analysis of lipid metabolizing and oxidative gene expression. B) *Left,* Total liver triglyceride content and *Right*, Total muscle triglyceride content. Data are expressed as mean ± SEM (n=5-8 mice/genotype). *, $P < 0.05$.

Figure 3-6

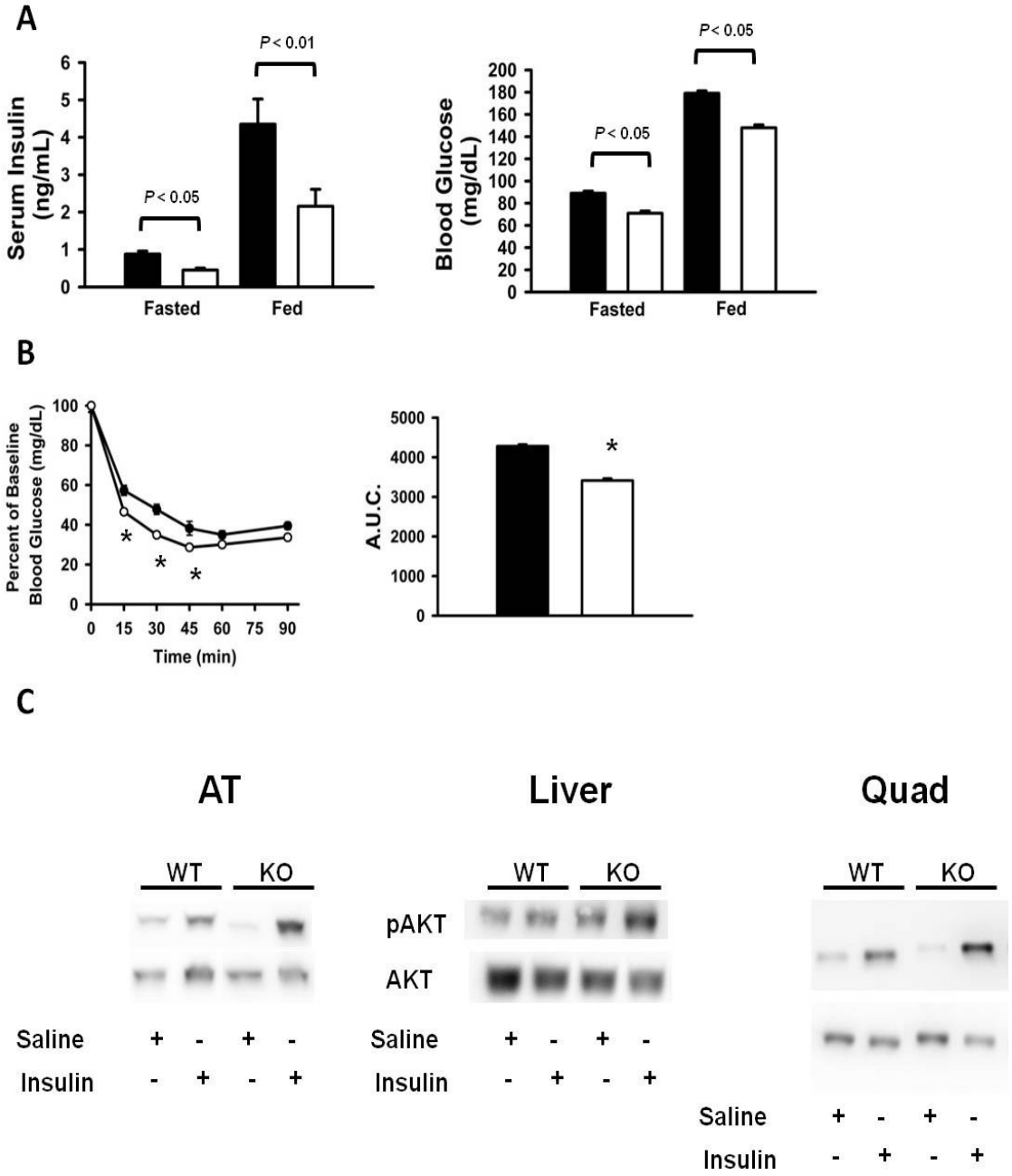
A
Serum Insulin (ng/mL)
P < 0.01
P < 0.05
Fasted
Fed
Blood Glucose (mg/dL)
P < 0.05
P < 0.05
Fasted
Fed
B
Percent of Baseline Blood Glucose (mg/dL)
Time (min)
A.U.C.
C
AT
Liver
Quad
WT
KO
pAKT
AKT
Saline
Insulin

Figure 3-6. FAT10 KO mice exhibit enhanced insulin sensitivity and glucose tolerance. A) Fasting and fed insulin and blood glucose concentrations. B) Insulin tolerance test and A.U.C. C) AKT signaling in AT, liver and quadriceps from mice administered an IP bolus of either insulin (0.75U/kg) or saline. Data are expressed as mean ± SEM (n=5-6 mice/genotype). *, $P < 0.05$.

Figure 3-7

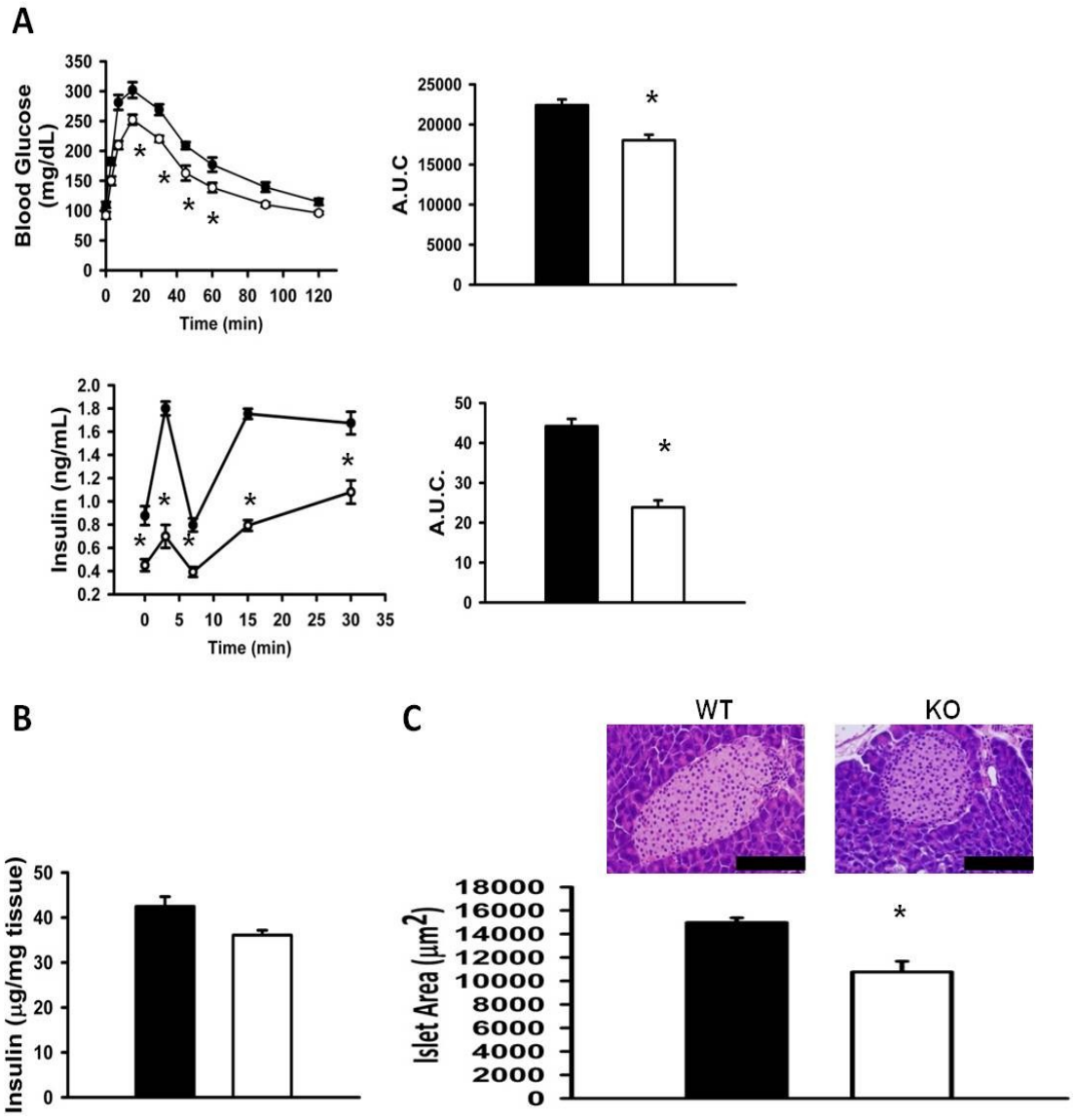
A
Blood Glucose (mg/dL)
Time (min)
A.U.C
Insulin (ng/mL)
Time (min)
A.U.C.
B
Insulin (µg/mg tissue)
C
WT
KO
Islet Area (µm2)

Figure 3-7. FAT10 KO mice have lower insulin concentrations in fasting and fed state and reduced total Islet area. A) *Top,* Intraperitoneal glucose tolerance test (IPGTT) and A.U.C. *Bottom,* Insulin concentrations during the IPGTT and A.U.C. B) Insulin concentrations for total pancreatic extraction. C) Histology of pancreatic Islets and Islet area. Data are expressed as mean ± SEM (n=4-6 mice/genotype). Scale bars represent 100 μm. *, $P < 0.05$.

Figure 3-1s

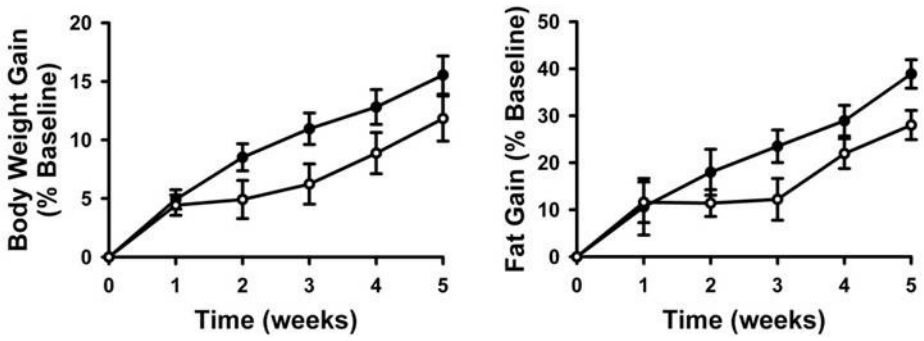

Figure 3-1S. FAT10 KO mice do not exhibit increased fat gain at thermoneutrality.

Left, Body weight gain as a percentage of baseline and *Right*, Fat gain as a percentage of baseline (n=8 mice/genotype).

3.2. FAT10 KO Mice are Protected from Insulin Resistance but not Obesity on a High Fat Diet

In Preparation for Submission to BBRC

Jason DeFuria[1], Grace Bennett[1], Katherine J. Strissel[1], Allon Canaan[2], Sherman Weissman[2], Andrew S. Greenberg[1], Martin S. Obin[1]

1. Obesity and Metabolism Laboratory, Jean Mayer USDA Human Nutrition Research Center on Aging at Tufts University, Boston, MA, USA 02111
2. Department of Genetics, Internal Medicine, Boyer Center for Molecular Medicine, Yale University School of Medicine, New Haven, CT 06511

Corresponding author: Martin S. Obin, PhD, 711 Washington St Room 607 Boston MA 02111. Phone (617) 556-3049 Fax (617) 556-3344, martin.obin@tufts.edu

Abstract

FAT10 is associated with increased risk for chronic disease (diabetes, cancer, HIV associated nephropathy) and is interactive with key cellular regulators of survival and metabolism (p53 and NFκB). Previous work has demonstrated that FAT10 KO mice are hyper-metabolic and lean. We were therefore interested to determine whether FAT10 KO mice are protected from obesity when introduced to a high saturated fat diet. FAT10 KO mice became obese at a slower rate compared to WT mice and had ~15% less total fat after 12 weeks of high fat feeding. Attenuated weight gain in FAT10 KO mice was paralleled by slight but significant increases in energy expenditure with similar energy intake. KO mice exhibited increased insulin sensitivity and a modest protection against glucose intolerance. These data indicate that FAT10 KO mice fed a high saturated FAT10 diet are partially protected from becoming obese while remaining insulin sensitive. Future work is warranted to dissect the molecular mechanism contributing to the retention of insulin sensitivity in the presence of obesity and how this mechanism differs from the insulin sensitivity observed in the lean FAT10 KO mouse.

Introduction

Obesity continues to increase in developing countries, with dramatic impacts on morbidity and mortality. Obesity and being overweight increases the risk of chronic diseases, such as type 2 diabetes, cardiovascular disease, hypertension and stroke, hypercholesterolemia, hypertriglyceridemia, arthritis, asthma, and certain forms of cancer (114). Moreover, recent studies suggest inverse associations between visceral fat deposition and longevity *per se* (115). These observations suggest that elucidating the biological bases by which adipose mass is regulated (and dysregulated in obesity) may provide significant public health benefit.

FAT10 is a MHC Class I-associated gene that is dramatically up-regulated in response to inflammatory cytokines (TNFα and IFNγ) in both immune and non-immune cell types (81, 82, 108, 116). FAT10 is associated with increased risk for chronic disease (diabetes, cancer, HIV associated nephropathy) and is interactive with key cellular regulators of survival and metabolism (p53 and NFκB) (83-85, 88, 117-120). Recently, deletion of the FAT10 gene in mice has demonstrated an impaired response to TNFα stimulation and *in vitro* gene knock-down was shown to attenuate cell-specific NFκB activation (88). In other studies, gene array profiling has revealed dramatic up-regulation of FAT10 expression in AT of a mouse model of lipodystrophy and down-regulation of expression in AT of calorically restricted animals (42, 98). Therefore, the FAT10 gene is expressed in AT of mice and responds to changes in AT inflammation, metabolism and mass.

Previous work from our laboratory has demonstrated that FAT10 KO mice are hyper-metabolic with significant decreases in adipose tissue mass and increases in lipid burning in skeletal muscle. We were therefore interested to see whether FAT10 KO mice were resistant to high-fat diet induced obesity and the onset of insulin resistance. FAT10 KO mice fed a high fat diet maintained lower body weight and adiposity compared to WT mice by 16%; however, when fed for an additional 4 weeks (16 weeks). FAT10 KO mice became as obese as WT mice fed for 12 weeks. FAT10 KO mice examined at 12 weeks on diet (when mice had less total adiposity compared to WT mice), KO mice had increased anti-inflammatory gene expression in adipose tissue. Additionally, KO mice appeared to have higher gene expression for lipolytic and mitochondrial uncoupling.

FAT10 KO mice had increases in energy expenditure with no preference in substrate use. Skeletal muscle analysis indicates that increased uncoupling gene expression along with decreased muscle triglyceride indicate a preference for burning fatty acids in skeletal muscle. These observations are accompanied by substantial increases in insulin sensitivity along with reduced fasting blood glucose and fasting insulin concentrations. Therefore, FAT10 KO mice fed a high fat diet are not protected from obesity but remain insulin sensitive due in part to increases in skeletal muscle lipid oxidation. This phenotype differs from the hyper-metabolic phenotype observed in normal diet fed FAT10 KO mice. This suggests that the composition of dietary fatty acids modulates the ability of the FAT10 mouse to remain hyper-metabolic.

Materials and Methods

Mice and Diet

FAT10 KO mice were obtained from Allon Canaan (Yale University, New Haven, CT) and re-derived at the Tufts Medical Center Core Transgenics Facility (Tufts University, Boston, MA). After re-derivation, mice were re-located to the Comparative Biology Unit at the JM USDA HNRCA at Tufts University. WT and KO lines were generated from mating heterozygous mice from the F0 generation. WT and KO offspring (F1) from this generation were back-crossed at least 7 generations. Generation of the FAT10 KO mouse has been previously described. Mice were placed on high fat diet (Research Diets) at 12 weeks of age and maintained for 12-16 weeks.

Intraperitoneal insulin and glucose tolerance tests

Insulin tolerance tests (ITTs) were performed on food-deprived (6 h), nonanesthetized mice. Glucose measures were obtained from whole tail vein blood using an automated glucometer at baseline and at 30, 45, 60, and 90 min following intraperitoneal injection of human insulin (either 0.75 or 1.0 mU/kg). Glucose tolerance tests (GTTs) were performed on food-deprived (12 h), non-anesthetized mice. Glucose measures were obtained similar to the ITT with the following changes. Blood glucose was measured at baseline, 15, 30, 60, 90 and 120 min following intraperitoneal injection of 2 mg/kg glucose bolus.

Metabolic Studies

Studies were performed as previously described. Mice were assessed for metabolic parameters after between weeks 2 and 3 of HFD feeding.

Body Composition

Body weights and composition was determined weekly using nuclear magnetic resonance technology (EchoMRI-100; Echo Medical Systems, Houston, TX).

Real Time PCR studies

All tissues were dissected, snap-frozen in liquid nitrogen, and stored at −80°C. Gene expression analysis was performed as previously described. All primer sequences are listed in the data supplement.

Isolation of total liver and muscle metabolites

Total liver and muscle triglyceride were extracted and quantified as previously described.

Statistical Analysis

Data are presented as mean ± SE. Data were determined to have a normal distribution with equal variance, and statistical differences were determined by PROC TTEST or PROC GLM using the Tukey least significant differences test with SAS v9.2 (Cary, NC). Significant differences were determined between groups at $p<0.05$.

Results

FAT10 KO mice exhibit attenuated weight gain on a high fat diet

Because FAT10 mice have been shown to exhibit enhanced energy expenditure, we predicted that KO mice would be protected from high fat diet-induced obesity and insulin resistance. KO mice gained body weight and fat mass at an attenuated rate compared to WT mice (Figure 4-1). When assessing total adiposity, KO mice maintain a 16% reduction in body weight at the end of the 12 week feeding time course (Figure 4-1). Moreover, KO mice fed a HFD for an additional four weeks achieved body weight and total adiposity equal to WT mice on HFD for 12 weeks (Figure 4-1A).

At twelve weeks on diet, histological assessment of epidydimal adipocyte cell size indicate a small but significant decrease in average size which is consistent with a reduction in adiposity (Figure 4-1B). Assessing cell death by Crown-like Structure (CLS)

frequency between obese FAT10 KO and WT mice indicates no difference in the proportion of adipocyte death between genotypes (Figure 4-1B). Infiltration of peripheral immune cells is coincident with enhanced adipose tissue inflammation and metabolic derangements. Expression of classic inflammatory genes indicates that there are no differences in pro-inflammatory molecules between genotypes. However, examination of anti-inflammatory genes IL4 and IL13 suggests that KO mice have an increased counter-regulatory system to combat detrimental inflammation. Therefore, KO mice have attenuated weight and fat gain. The increased anti-inflammatory gene expression profile in adipose tissue suggests that FAT10 KO mice respond to inflammation by up-regulating anti-inflammatory molecules. However, FAT10 KO mice are not protected from adipocyte hypertrophy or adipocyte death.

FAT10 KO mice have increases in gene expression of markers for lipolysis, lipid synthesis and uncoupling

FAT10 mice have been demonstrated to have enhanced lipolytic gene expression coincident with increased oxidative gene expression in adipose tissue on a normal diet. This could account for decreased lipid deposition throughout the feeding time course. Examining genes involved in lipolysis, triglyceride recycling and β-oxidation, FAT10 KO mice on a high fat diet had significantly elevated HSL, ATGL, LPL, FAS as well as UCP1 gene expression in adipose tissue (Figure 4-2). Therefore, the attenuated weigh gain may be due in part to increases in increases fatty acid utilization in adipose tissue.

Obese FAT10 KO mice have slight increases in energy expenditure

The attenuated weight gain in FAT10 KO mice may be attributed to slight increases in total energy expenditure or decreases in energy intake. FAT10 KO and WT

mice eat similar amounts of calories during both the night and the day (Figure 4-3). When inspecting total energy expenditure KO mice had slight but significantly increased energy expenditure during the day (Figure 4-3). This increased energy expenditure was not due to increases in activity. Therefore, the maintenance of decreased adiposity over 12 weeks of high fat feeding in FAT10 KO mice can be attributed in part to mild increases in energy expenditure during the day.

Obese FAT10 KO mice have decreased ectopic lipid in skeletal muscle

Metabolic analysis revealed that KO mice had slightly but significantly higher oxygen consumption with no difference in RQ. MRI analysis indicates that KO mice have 16% less fat after 12 weeks if HFD. The lack of effect of FAT10 KO on RQ suggested that there was no difference in fuel selection, suggesting the increased oxygen consumption was secondary to increased thermogenesis. UCP (1-3) gene expression was assessed in quadriceps. There was significant up-regulation of UCP3 gene expression whereas there was no change in UCP1 or 2 expression (Figure 4-4). Coincident with increased UCP3 expression there was decreased total triglyceride in quadriceps suggesting the increased uncoupling promotes FA use. Therefore, KO mice may maintain modest weigh reduction by increased burning of FA in skeletal muscle on a high fat diet.

FAT10 KO mice maintain insulin sensitivity and modest glucose tolerance

Having decreased lipid in skeletal muscle and small increases in energy expenditure, FAT10 KO mice are predicted to exhibit comparable increases in insulin sensitivity. Despite not being completely protected from DIO and adipocyte hypertrophy, KO mice were remarkably insulin sensitivity as assessed by ITT (Figure 4-3). GTT revealed that mice were slightly more glucose tolerant than WT mice (Figure 4-3). KO

mice exhibit decreased fasting insulin concentrations compared to WT animals (Figure 4-3). Therefore, KO mice retain insulin sensitivity and modest glucose tolerance despite not being resistant to obesity or adipocyte hypertrophy. Additionally, KO mice do not achieve the fasting hyperinsulinemia that WT mice exhibit when fed HFD for 12 weeks.

Discussion

Work first describing the FAT10 KO phenotype did not evaluate body composition or energy metabolism (80). Previous work from our lab investigating the lean phenotype of the FAT10 KO mice indicated that FAT10 KO mice are hyper-metabolic with alterations in both adipose tissue and muscle metabolism. This current study demonstrates that in the absence of FAT10, mice on a high fat diet are not completely resistant to obesity; however, mice are metabolically protected against insulin resistance.

As immune cell infiltrate increased, increased pro-inflammatory cytokine production and adipocyte death are associated with the onset of insulin resistance (49, 121). We investigated these criteria by histological analysis and gene expression. Both genotypes exhibited similar frequency of cell death and pro-inflammatory cytokine gene expression. However, to determine if there was similar expression of anti-inflammatory gene markers, FAT10 KO mice were revealed to have increased expression of IL4 and IL3. These cytokines have been demonstrated to be protected against metabolic perturbations associated with obesity. It is interesting to speculate that FAT10 may influence not the production of pro-inflammatory cytokines but the response to balance the pro-inflammatory response in obesity. As FAT10 has been shown to be involved in B

cell, dendritic cell and T cell activation (81, 108), FAT10 may be a candidate gene for modulating the inflammatory response in obese adipose tissue.

After 12 weeks on a high fat diet, FAT10 KO mice had ~16% decreased total adiposity compared to WT mice. This observation is in stark contrast to the 50% difference in adiposity observed in lean FAT10 KO mice. Several knockout mouse models that exhibit decreased adiposity also had substantial increases in energy expenditure and food intake (95, 109-111). The marginally reduced fat mass in FAT10 KO mice from the current study was associated with small but significant increases in energy expenditure. Furthermore, KO mice did not exhibit increased locomotor activity (data not shown) indicating that enhanced energy expenditure is due to an intrinsic mechanism of substrate utilization. Compared to the lean FAT10 KO mouse, the high fat diet fed KO mouse did not retain all the metabolic benefits the lean mouse exhibited.

Most interestingly, the FAT10 KO mouse retained complete insulin sensitivity on a high fat diet. Recently, FAT10 has been shown to interact with p53, enhancing p53's transcriptional activity (83). It is also well known that p53 heterozygous mice fed a high fat diet become obese but remain insulin sensitive (122). Therefore, it is tempting to suggest that FAT10 may exert its affects on insulin sensitivity in the obese state through modulation of p53 activity. However, this was not assessed in this study. Additionally, FAT10 has been shown to be involved in activation of NFκB (88). However, there were no differences in pro-inflammatory gene expression of NFκB dependent genes analyzed in this study. On the other hand, STAT6 dependent genes IL4 and IL13 were significantly up-regulated in obese adipose tissue from FAT10 KO mice. Therefore, FAT10 may exert

its influence in a tissue specific and cell signaling specific manner through modulation of anti-inflammatory mediators.

This work opens up many questions for the biological relevance of FAT10. It will be necessary to test whether FAT10 is mediating its affects primarily through p53, NFκB or an as-of-yet identified target protein. Additionally, tissue specific KO models of FAT10 are needed to determine the specific site of biological actions on insulin sensitivity in the high fat fed model.

Figure 4-1

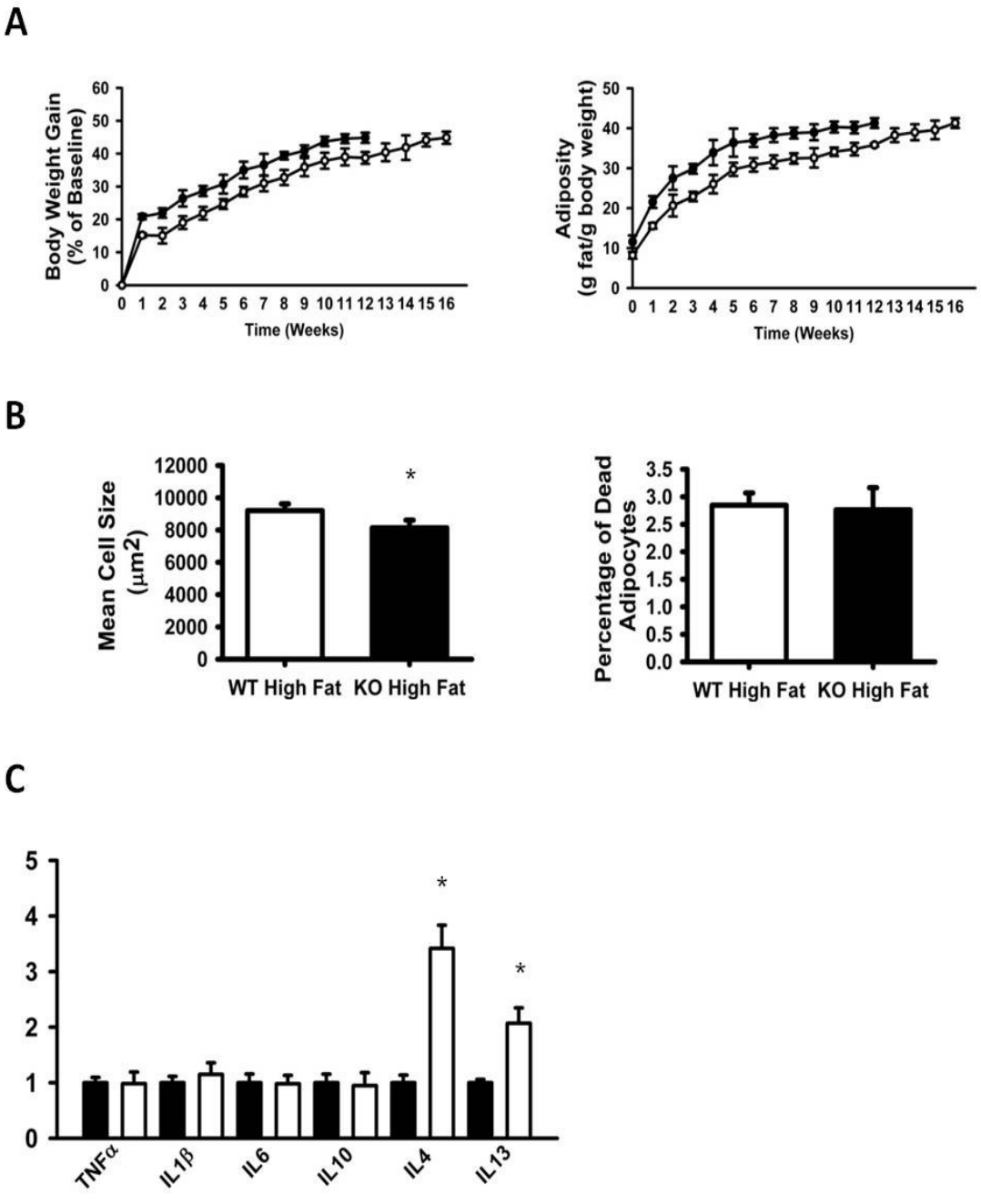
A
Body Weight Gain (% of Baseline)
Time (Weeks)
Adiposity (g fat/g body weight)
Time (Weeks)
B
Mean Cell Size (μm2)
WT High Fat
KO High Fat
Percentage of Dead Adipocytes
WT High Fat
KO High Fat
C
TNFα
IL1β
IL6
IL10
IL4
IL13

Figure 4-1. FAT10 KO mice have attenuated weight gain and smaller mean adipocyte size. A) *Left,* Body weight gain expressed as percent of baseline weight of WT (closed circles) and KO (open circles) mice. FAT10 KO mice were maintained on diet for an additional 4 weeks to determine if they would become equally obese as WT mice. A) *Right*, Change in adiposity over feeding time course. Each time point represents the ratio total fat/body weight. B *Left,* Mean adipocyte cell size. B) *Right,* Percent of dead adipocytes as assessed by CLS. C) Gene expression of pro- and anti-inflammatory makers in epidydimal adipose tissue. In this figure data are represented by mean ± SEM (n=8 mice/genotype). *, $P < 0.05$.

Figure 4-2

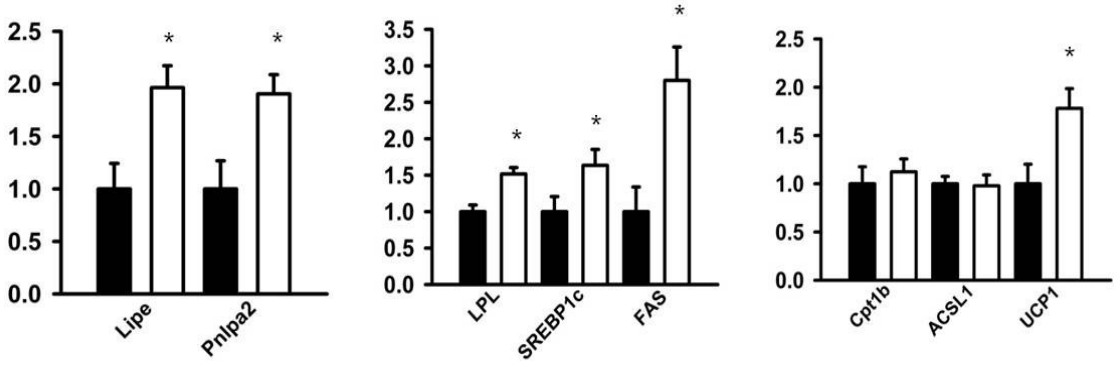
2.5
2.0
1.5
1.0
0.5
0.0
*
*
Lipe
Pnlpa2
3.5
3.0
2.5
2.0
1.5
1.0
0.5
0.0
*
*
*
LPL
SREBP1c
FAS
2.5
2.0
1.5
1.0
0.5
0.0
*
Cpt1b
ACSL1
UCP1

Figure 4-2. Increased gene expression of markers of lipolysis, fatty acid synthesis and energy uncoupling in FAT10 KO AT. *Left,* Gene expression of lipolytic markers. *Middle,* Gene expression of lipid uptake and synthetic genes. *Right,* Gene expression of β-oxidative markers. Data are expressed as mean ± SEM (n=8 mice/genotype). *, $P < 0.05$.

Figure 4-3

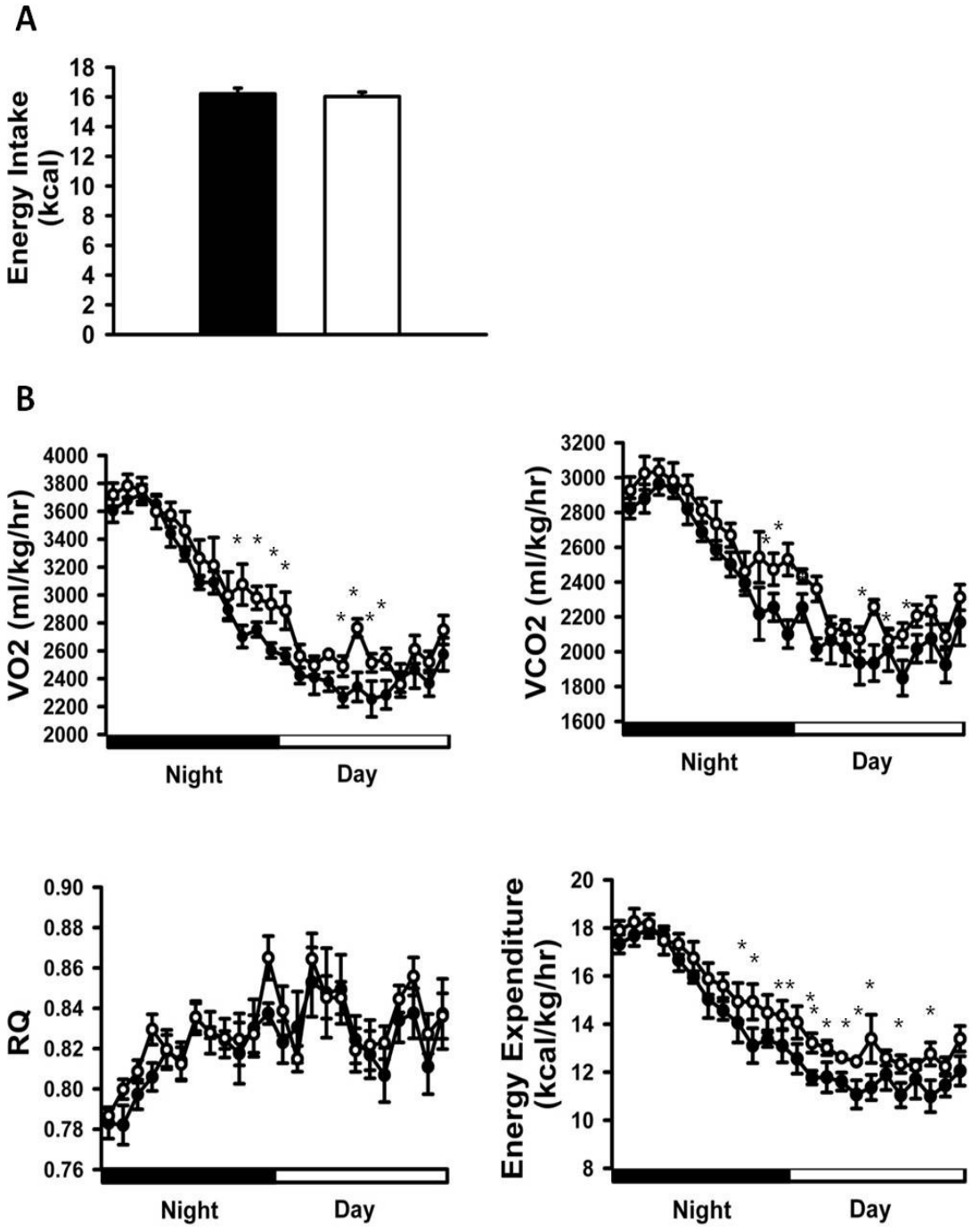
A
Energy Intake (kcal)
18
16
14
12
10
8
6
4
2
0
B
VO2 (ml/kg/hr)
4000
3800
3600
3400
3200
3000
2800
2600
2400
2200
2000
Night
Day
VCO2 (ml/kg/hr)
3200
3000
2800
2600
2400
2200
2000
1800
1600
Night
Day
RQ
0.90
0.88
0.86
0.84
0.82
0.80
0.78
0.76
Night
Day
Energy Expenditure (kcal/kg/hr)
20
18
16
14
12
10
8
Night
Day

Figure 4-3. HFD fed FAT10 KO mice have modest increases in energy expenditure. A) Total energy intake. B) Oxygen consumption (VO2), CO2 production (VCO2), Respiratory Quotient (RQ) and total Energy Expenditure were evaluated as described in *Materials and Methods*. Data are expressed as mean ± SEM (n=8 mice/genotype). *, $P < 0.05$.

Figure 4-4

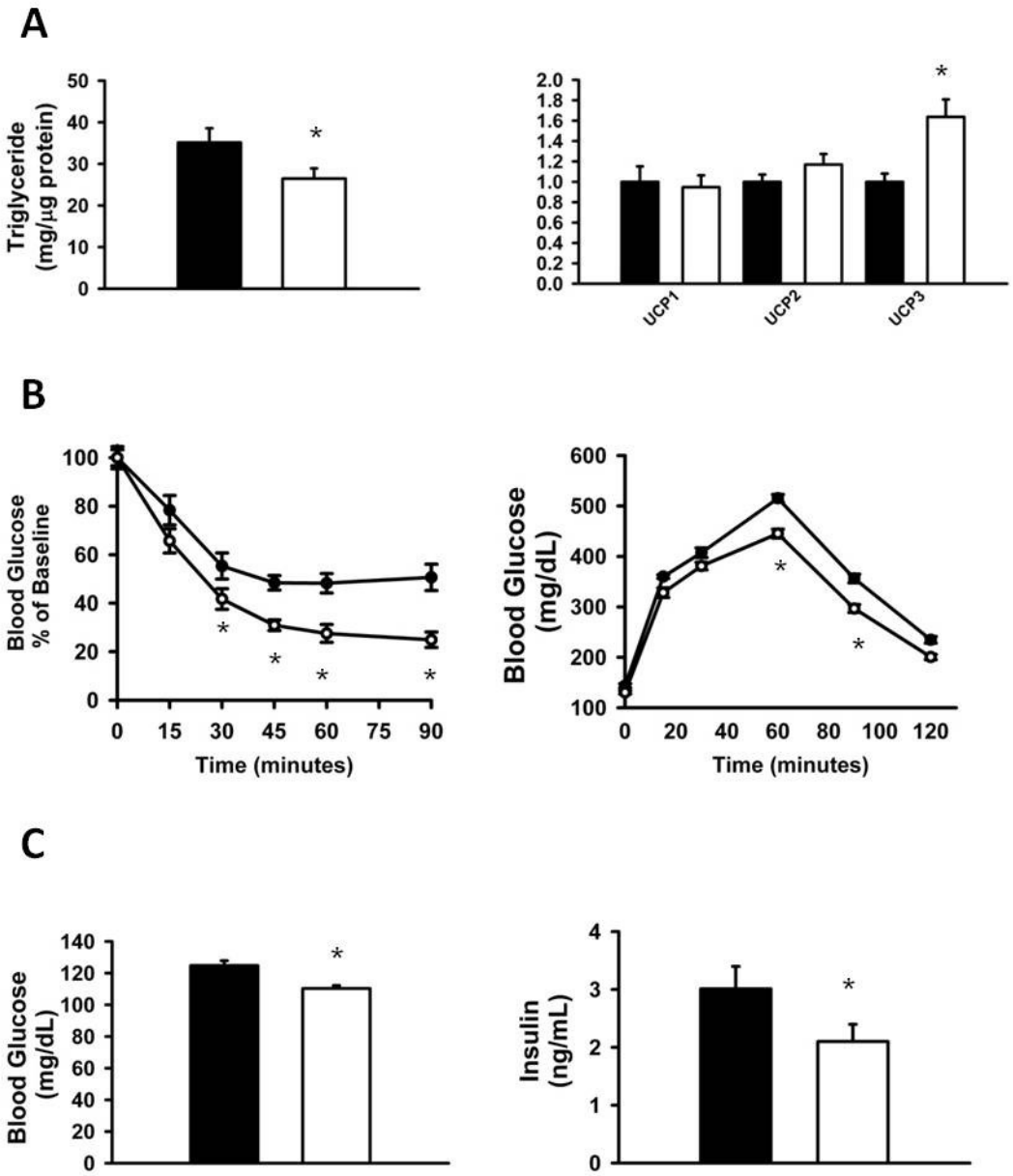
A
Triglyceride (mg/μg protein)
50
40
30
20
10
0
*
2.0
1.8
1.6
1.4
1.2
1.0
0.8
0.6
0.4
0.2
0.0
*
UCP1
UCP2
UCP3
B
Blood Glucose % of Baseline
100
80
60
40
20
0
0 15 30 45 60 75 90
Time (minutes)
* * * *
Blood Glucose (mg/dL)
600
500
400
300
200
100
0 20 40 60 80 100 120
Time (minutes)
* *
C
Blood Glucose (mg/dL)
140
120
100
80
60
40
20
0
*
Insulin (ng/mL)
4
3
2
1
0
*

Figure 4-4. FAT10 KO mice have decreased muscle triglyceride, increased uncoupling gene expression and increased insulin sensitivity. A) Triglyceride content from WT and FAT10 KO quadriceps. A) *Right,* UCP (1-3) gene expression from quadriceps. B) *Left,* Intraperitoneal insulin tolerance test and (*Right)* Intraperitoneal glucose tolerance test performed on FAT10 KO and WT mice after 10 weeks on HFD. C) *Left,* Fasting blood glucose and (*Right)* fasting insulin. Data are expressed as mean ± SEM (n=8 mice/genotype). *, $P < 0.05$.

CHAPTER IV

SUMMARY AND DISCUSSION

4.1. *Summary of the Lean FAT10 KO mice*

Regulation of insulin action by appropriate response to nutritional cues is important to maintain energy balance and a healthy body composition. Nutritional, pharmacological and genetic alterations that perturb the body's ability to sense nutrients and coordinate hormonal signals can alter energy stores. Decreasing the ability to store energy in fat can result from genetic lipodystrophies or by pharmacological HIV anti-viral treatment (123-127). In both cases FAs are re-distributed to peripheral metabolic tissues causing inflammation and insulin resistance. Conversely, excess energy storage results in obesity. Obesity is associated with expansion of adipose tissue, infiltration of inflammatory immune cells, increases in systemic circulating markers, insulin resistance and is a risk factor for cardiovascular complications and certain types of cancer (114). Therefore, understanding the contributing factors that influence energy storage may elucidate new therapeutics for battling pathologies of adipose tissue.

There has been no previous work examining a role for FAT10 in adipose tissue biology and energy metabolism. Prior work has revealed FAT10 expression in large gene array screens to be related to weight loss and lipodystrophy; however, the role for FAT10 in these processes was not investigated. In this study, we demonstrate that FAT10 gene expression increases with normal adipose tissue growth. AT is known to be composed of a highly heterogeneous population of cells that include adipocytes and SVCs. Because the expression of FAT10 was originally described in hematopoietic immune cells (81, 108), the increase in AT FAT10 expression could be due in part to increased expression

in immune cells. Interestingly, FAT10 gene expression was ~3-fold higher in adipocytes compared to the SVCs suggesting that the increase in FAT10 expression is contributed by the adipocytes rather than immune cells. These findings prompted our group to investigate the potential role FAT10 plays in AT tissue growth and metabolism as well as body composition by metabolically phenotyping FAT10 KO mice.

Work first describing the FAT10 KO phenotype did not evaluate body composition or energy metabolism (80). This current study demonstrates that in the absence of FAT10, mice on a normal diet exhibit changes in body composition, whole body energy expenditure and adipose tissue metabolism. At 12 weeks of age, KO mice had ~50% decreased adipose tissue mass compared to WT mice and this difference was due in part to a smaller proportion of adipocytes. Several knockout mouse models that exhibit decreased adiposity also had substantial increases in energy expenditure and food intake (95, 109-111). The reduced fat mass in FAT10 KO mice were associated with increases in energy expenditure; however, food intake adjusted for body weight showed a modest 10% increase. Furthermore, KO mice did not exhibit increased locomotor activity indicating that enhanced energy expenditure is due to an intrinsic mechanism of substrate utilization.

These data suggest that if there were a mutation in the FAT10 gene the result may be increased metabolism and decreased adipose mass. It would be interesting to determine whether single nucleotide polymorphisms (SNPs) in the human FAT10 gene are related to insulin homeostasis and adiposity. There are current rodent gene-wide association studies (GWAS) that indicate FAT10 is associated with increased risk for Type I diabetes . The decreased insulin secretion and islet area data from this study

suggest that FAT10 KO mice may later in life develop Type I diabetes. Longevity studies are needed to evaluate the role of FAT10 ablation in the possible development of Type I diabetes.

FAT10 KO mice appear to deal with perturbations in adipose tissue's response to low insulin by increasing substrate utilization. These data are evident when examining when FAT10 KO mice have significantly lower RQ values indicating a preference for metabolizing fatty acids. This can be achieved by increasing adipocyte lipolysis and burning fatty acids within the adipose tissue or in peripheral metabolic tissues such as muscle and liver (102). Both basal and stimulated lipolysis was increased in KO mice suggesting enhanced lipid flux. Additionally, fasting circulating NEFA concentrations were slightly elevated supporting a role for increased lipid release from adipocytes.

Adipocytes from KO mice up-regulated genes involved in β-oxidation and had an increased proportion of phosphorylated ACC1 suggesting a proportion of the lipid released from lipolysis was being oxidized within adipocytes. With reduced adipose tissue, FA can be shunted to peripheral metabolic tissues and stored as ectopic lipid interfering with insulin sensitivity (112). Inspection of skeletal muscle and liver triglyceride reveal no signs of ectopic lipid deposition and moreover suggest that muscle may also be involved in fatty acid utilization in this model.

In respect to insulin sensitivity, KO mice exhibited enhanced insulin sensitivity. Glucose tolerance was improved in KO mice. Paradoxically, insulin concentrations during the first and second phase insulin release during the GTT indicate that KO mice clear glucose with significantly lower insulin. To test insulin release under physiological conditions, mice were re-fed for 4 hours and circulating insulin concentrations were

measured. Re-fed KO mice exhibited lower insulin concentrations as well as decreased blood glucose. These data suggest that KO mice maintain glycaemia with reduced insulin. The GLUT4 transgenic (113) mice both exhibit improved glycemic control, decreased insulin concentrations and increased lipolysis resulting in high circulating fatty acids during fasting. Therefore, other KO models provide evidence where low insulin concentrations result in increased lipolysis.

Due to constitutively low insulin levels, we investigated whether Islets from KO mice were altered. We began by measuring total pancreatic insulin concentrations demonstrating that KO pancreata had slight but significant decreases in insulin. . We next examined pancreatic Islet area and discovered that KO mice have 27% reduced total islet area. Islet number between genotypes was not different.

As FAT10 is an ubiquitin-like molecule, it is of great importance to determine substrates that FAT10 covalently modifies. Recent work has demonstrated FAT10 modifies p53 and increases its transcriptional activity (83). P53 is known to affect energy sensing and cell growth pathways and is a viable target to investigate the biochemical function of FAT10. Additional work has demonstrated FAT10 is involved upstream of NFκB activation; however, no substrates were identified in this study (88). NFκB has been demonstrated to be necessary for glucose-stimulated insulin secretion from β-cells. Therefore, the primary site of FAT10 activity in normal, physiological processes may facilitate normal β-cell insulin release via promoting activation of the NFκB pathway.

FAT10 was demonstrated to be induced by double-stranded DNA, lipopolysaccharide as well as poly I:C, all known components of either viruses or bacteria (108). These findings suggest that FAT10 plays a role in pathogen sensing in the immune

system. Work in the obesity field has shown that adipocytes utilize 'infection' sensing pathways as a response to sterile inflammation (128) that occurs in obesity. Furthermore, infection results in systemic alterations such as fever and inflammation that promotes the use of energy storage in demand of high immune cell proliferation to ward off the infectious agent. In the absence of infection and inflammation, FAT10 may be playing a role in homeostatic nutrient flux. When challenged an infectious agent that promotes inflammation, FAT10 may be limiting the nutrient flux from adipose tissue to peripheral cells in the body that require increased substrate needs as FAT10 null animals have increased lipid release from adipocytes.

4.2. *Summary of the High Fat Diet Fed FAT10 KO mice*

Work first describing the FAT10 KO phenotype did not evaluate body composition or energy metabolism (80). Previous work from our lab investigating the lean phenotype of the FAT10 KO mice indicated that FAT10 KO mice are hyper-metabolic with alterations in both adipose tissue and muscle metabolism. This current study demonstrates that in the absence of FAT10, mice on a high fat diet are not completely resistant to obesity; however, mice are metabolically protected against insulin resistance.

As immune cell infiltrate increased, increased pro-inflammatory cytokine production and adipocyte death are associated with the onset of insulin resistance (49, 121). We investigated these criteria by histological analysis and gene expression. Both genotypes exhibited similar frequency of cell death and pro-inflammatory cytokine gene expression. However, to determine if there was similar expression of anti-inflammatory gene markers, FAT10 KO mice were revealed to have increased expression of IL4 and

IL3. These cytokines have been demonstrated to be protected against metabolic perturbations associated with obesity. It is interesting to speculate that FAT10 may influence not the production of pro-inflammatory cytokines but the response to balance the pro-inflammatory response in obesity. As FAT10 has been shown to be involved in B cell, dendritic cell and T cell activation (81, 108), FAT10 may be a candidate gene for modulating the inflammatory response in obese adipose tissue.

After 12 weeks on a high fat diet, FAT10 KO mice had ~16% decreased total adiposity compared to WT mice. This observation is in stark contrast to the 50% difference in adiposity observed in lean FAT10 KO mice. Several knockout mouse models that exhibit decreased adiposity also had substantial increases in energy expenditure and food intake (95, 109-111). The marginally reduced fat mass in FAT10 KO mice from the current study was associated with small but significant increases in energy expenditure. Furthermore, KO mice did not exhibit increased locomotor activity (data not shown) indicating that enhanced energy expenditure is due to an intrinsic mechanism of substrate utilization. Compared to the lean FAT10 KO mouse, the high fat diet fed KO mouse did not retain all the metabolic benefits the lean mouse exhibited.

Most interestingly, the FAT10 KO mouse retained complete insulin sensitivity on a high fat diet. Recently, FAT10 has been shown to interact with p53, enhancing p53's transcriptional activity (83). It is also well known that p53 heterozygous mice fed a high fat diet become obese but remain insulin sensitive (122). Therefore, it is tempting to suggest that FAT10 may exert its affects on insulin sensitivity in the obese state through modulation of p53 activity. However, this was not assessed in this study. Additionally, FAT10 has been shown to be involved in activation of NFκB (88). However, there were

no differences in pro-inflammatory gene expression of NFκB dependent genes analyzed in this study. On the other hand, STAT6 dependent genes IL4 and IL13 were significantly up-regulated in obese adipose tissue from FAT10 KO mice. Therefore, FAT10 may exert its influence in a tissue specific and cell signaling specific manner through modulation of anti-inflammatory mediators.

This work opens up many questions for the biological relevance of FAT10. It will be necessary to test whether FAT10 is mediating its affects primarily through p53, NFκB or an as-of-yet identified target protein. Additionally, tissue specific KO models of FAT10 are needed to determine the specific site of biological actions on insulin sensitivity in the high fat fed model.

4.3. Study Limitations

There are several limitations concerning the current study. The most obvious limitation was the lack of an antibody to detect FAT10 protein. Several human antibodies exist that are able to detect FAT10 in human cells; however, no suitable mouse antibody exists. In order to visualize changes in FAT10 protein levels a mouse antibody needs to be generated. The current targets for FAT10 conjugation have yet to be identified. P53 was recently shown to be covalently modified by FAT10. Investigation of the role of p53 and FAT10 in basal metabolic conditions is necessary to see if FAT10 modulates p53's role in metabolism. The role of p53 in insulin resistance related to diet induced obesity has been established (122); however, there are is no current data for the role of p53 in maintaining insulin sensitivity in a lean phenotype.

Another limitation of the study was the central nervous system and the brain was not evaluated. FAT10 may be regulating body temperature where elevated core

temperature induces a hyper-metabolic phenotype mimicking a fever. This would account for the increases in energy metabolism observed in these mice. Isolating the hypothalamus in WT and FAT10 KO mice will be important to determine a role for FAT10 in central regulation of energy metabolism.

4.4. Conclusions

In conclusion, genetic deletion of the FAT10 gene results in mice that have reduced adiposity and enhanced energy expenditure. Adipocytes from KO mice exhibit increased lipolysis, prefer FAs during the day as a metabolic substrate, up-regulate genes involved in β-oxidation and have increased phospho-ACC1 protein in AT. Taken together these data suggest that FAs released from lipolysis are oxidized within AT and possibly skeletal muscle. Decreased Islet area in KO mice in conjunction with slightly reduced total pancreatic insulin may result in constitutively low circulating insulin concentrations. This low circulating insulin may be the primary cause of enhanced lipolysis while peripheral metabolic tissues adapt by increases substrate utilization. When subjected to high fat diet feeding FAT10 KO mice exhibited small but statistically significant increases in energy expenditure during the day without changes in food intake. Therefore, in both normal and high fat diet feeding there appears to be a metabolic switch that increases energy metabolism when caloric intake is reduced as occurs with mice during the day. Additionally, modulation of dietary lipid from predominately polyunsaturated fatty acids (normal diet) to a predominately saturated fat diet (high fat diet) alters the magnitude of energy expenditure in the FAT10 KO mice.

This thesis work indicates that FAT10 is a novel gene involved in the regulation of systemic energy metabolism that may be dependent on the fatty acid composition of

the diet. Because the FAT10 gene was absent from all tissues, it is not possible to identify the tissue influencing the increased energy metabolism. This point warrants further dissection by tissue specific ablation of the FAT10 gene to identify how FAT10 affects systemic energy metabolism. Additionally, since FAT10 is associated with increased risk for chronic disease (diabetes, cancer, HIV associated nephropathy) and is interactive with key cellular regulators (p53 and NFκB), this research opens new avenues for further investigation of the tissue-specific biological function of FAT10.

4.5. *Future Directions*

Many questions remained concerning the role of FAT10 and controlling energy metabolism. The main site of FAT10's effects on metabolism was not specifically identified. This will require tissue specific dissection of energy metabolism in the absence and presence of the FAT10 gene. Also, in vitro knock down and rescue models in different cell lines will help elucidate the functional role of FAT10 in cell specific energy metabolism.

Because the FAT10 gene is interactive with important regulators of cellular survival and metabolism (p53, NFκB), this model may serve to understand the etiology of diet and cancer interactions. Additionally, FAT10 may bridge the gap between poor or over-nutrition and the susceptibility of certain forms of cancer. In order to understand the function of FAT10, the post-translational targets must be accurately identified. Additionally, FAT10's interactions with p53 and NFκB may mediate very specific effects in those signaling pathways and therefore future work needs to be aware that canonical, well established signaling mechanisms may not be the primary target for the FAT10's effect on these signaling cascades.

APPENDICES

Additional Studies Not Included in Main Body of Thesis

Appendix A

Dietary Blueberry Attenuates Whole Body Insulin Resistance in High Fat-Fed Mice by Reducing Adipocyte Death and Its Inflammatory Sequelae[1,2,3]

Published in the Journal of Nutrition

J Nutr. 2009 Aug;139(8):1510-6. Epub 2009 Jun 10.

Jason DeFuria, Grace Bennett, Katherine J. Strissel, James W. Perfield II[4], Paul E. Milbury*, Andrew S. Greenberg[§] and Martin S. Obin[§]

Obesity and Metabolism Laboratory and *Antioxidants Research Laboratory

JMUSDA-Human Nutrition Research Center on Aging at Tufts University

WORD COUNT: 6,509

NUMBER OF FIGURES: 3

NUMBER OF TABLES: 4

SUPPLEMENTARY MATERIAL: Online Supporting Materials: Supplemental Methods

Running title: Blueberry, adipocyte death and insulin resistance

Footnotes

[1] Supported by the United States Highbush Blueberry Council (MSO), the American Diabetes Association (MSO), USDA contract 5819507707 (ASG), NIH T32DK062032 (JD) and NIH TH32HL69772 (GB)

[2] Author disclosures: J. DeFuria, G. Bennett, K.J. Strissel, J.W. Perfield, A.S. Greenberg, and M.S.

Obin, no conflicts of interest. P.E. Milbury currently holds research funds from USHBC.

[3]Supplemental Methods are available as Online Supporting Material with the online posting of this paper at http://jn.nutrition.org.

[4]Current address: Depts of Nutrition & Exercise Physiology and Food Science, University

of Missouri, Columbia MO 65211

[5]Abbreviations Used: AT, adipose tissue; ATMΦ, adipose tissue macrophage, BB, blueberry; CHOP/GADD153, C/EBP-homologous protein/growth arrest/DNA-damage-inducible 153; GPx3, glutathione peroxidase 3; GRP78, glucose-regulated protein, 78kDa; HFD, high-fat diet; HFD+B, high-fat diet plus blueberry; IL-6, interleukin 6; IL-10, interleukin 10; iNOS, inducible nitric oxide synthase; ITT, insulin tolerance test; IR, insulin resistance; LFD, low-fat diet; MAPK, mitogen-activated protein kinase; MGL1, macrophage galactose N-acetyl-galactosamine specific lectin 1; MCP-1, monocyte chemoattractant protein 1; NFκB, nuclear factor κB; TNFα, tumor necrosis factor α.

[§] Correspondence: martin.obin@tufts.edu or andrew.greenberg@tufts.edu. JMUSDA HNRCA 711

Washington St, Boston, MA 02111. Tel (617) 556-3079 Fax (617) 556-3224.

Key words: blueberry, obesity, adipocyte, inflammation, insulin resistance

Abstract

Adipose tissue (AT) inflammation promotes insulin resistance (IR) and other obesity complications. AT inflammation and IR are associated with oxidative stress, adipocyte death, and the scavenging of dead adipocytes by pro-inflammatory CD11c+ AT macrophages (ATMΦ). We tested the hypothesis that supplementation of an obesitogenic (high fat) diet with whole blueberry (BB) powder protects against AT inflammation and IR. Male C57Bl/6j mice were maintained for 8 wk on one of three diets: low (10% of energy) fat diet (LFD), high (60% of energy) fat diet (HFD) or HFD containing 4% (w:w) whole BB powder (1:1 *V. ashei* and *V. corymbosum*) (HFD+B). BB supplementation (2.7% of total energy) had no effect on HFD-associated alterations in energy intake, metabolic rate, body weight or adiposity. We observed an emerging pattern of gene expression in AT of HFD mice indicating a shift towards global up-regulation of inflammatory genes (tumor necrosis factor α, interleukin-6, monocyte chemoattractant protein 1, inducible nitiric oxide synthase), increased M1-polarized ATMΦ (CD11c+) and increased oxidative stress (reduced glutathione peroxidase 3). This shift was attenuated or non-existent in HFD+B- fed mice. Furthermore, mice fed HFD+B were protected from IR and hyperglycemia coincident with reductions in adipocyte death. Salutary effects of BB on adipocyte physiology and ATMΦ gene expression may reflect the ability of BB anthocyanins to alter mitogen-activated protein kinase and nuclear factor κB stress signaling pathways, which regulate cell fate and inflammatory genes. These results suggest that cytoprotective and anti-inflammatory actions of dietary BB can provide metabolic benefits to combat obesity-associated pathology.

Introduction

The accumulation of bone marrow-derived inflammatory macrophages (MΦ) in adipose tissue (AT) is causally implicated in the pathogenesis of insulin resistance (IR) and other obesity complications (129, 130). In obese mice these recruited ATMΦ can be distinguished from resident ATMΦ by the absence of the cell surface marker macrophage galactose N-acetyl-galactosamine specific lectin 1 (MGL1), up-regulation of the dendritic cell marker CD11c, and polarization toward a classical pro-inflammatory (M1) phenotype (131-133). This phenotype is characterized by up-regulated expression of tumor necrosis factor α (TNFα), inducible nitric oxide synthase (iNOS) and other pro-inflammatory mediators that promote IR (130). Notably, ablation of CD11c+ cells or genetic abrogation of MΦ inflammatory signaling protects obese mice from IR (61, 134). Macrophage infiltration and resulting AT inflammation are mechanistically linked to adipocyte death, which increases in obese mice and humans (132, 133, 135, 136). Dead adipocytes are foci of CD11c+ ATMΦ recruitment, aggregation in crown-like structures, scavenging activity and pro-inflammatory gene expression (132, 133, 135). Obesity-associated adipocyte death is believed to reflect one or more cytotoxic stresses that are elevated in the AT of obese mice and humans, in particular oxidative and endoplasmic reticulum (ER) stress (137, 138) .

Dietary strategies for alleviating the metabolic complications of obesity are being pursued as alternatives to pharmaceutical interventions (e.g., (139)). The association of obesity with AT stress, adipocyte death, MΦ recruitment and inflammatory gene expression suggested that edible berries might provide an effective alternative or supplementary intervention to attenuate obesity- associated inflammation and IR. Berries such as blueberry (BB) (*Vaccinium sp*) are enriched in anthocyanins, polyphenolics

recognized for their ability to provide and activate cellular antioxidant protection, inhibit inflammatory gene expression and to consequently protect against oxidant-induced and inflammatory cell damage and cytotoxicity (140-142). BB-supplemented diets and preparations are also reported to inhibit MΦ infiltration (143) and to attenuate bacterial translocation to extra-intestinal sites (144), a phenomenon implicated in the inflammatory and metabolic pathology associated with diets high in fat (145). Considered together, these observations suggested that BB could attenuate or delay the adipocyte death, ATMΦ recruitment and pro-inflammatory gene expression that promote obesity-associated IR.

In the present study, mice fed HFD or HFD+B for 8 wk gained identical amounts of weight and were comparably obese. However, mice fed HFD+B were protected from adipocyte death, AT inflammatory gene expression and whole body IR. These observations suggest that the cytoprotective and anti-inflammatory actions of 'whole' BB can provide metabolic benefits to combat obesity-associated pathology.

Experimental Procedures

Animals and diets. Male C57BL/6 mice were obtained from Jackson Labs at 5 wk of age and housed individually at the JMUSDA-HNRCA as previously described (133). Ethical treatment of animals was assured by the Tufts University Institutional Animal Care and Use Committee. After several days of acclimation, mice were assigned to cohorts (n = 8 mice per cohort) that received one of three pelleted diets for 8 wk (Research Diets, Inc., New Brunswick, NJ). These were a low fat (LFD) diet containing 10% of energy from fat (# D12450B), a high fat diet (HFD) containing 60% of energy from fat (# D12492) and a

modified HFD supplemented with 4% (w:w) freeze-dried whole blueberry powder (HFD+B) (Table 1). The powder was provided in aluminum cans under nitrogen by the U.S. Highbush Blueberry Council and consisted of a 1:1 blend of *Vaccinium ashei* (Tifblue) and *Vaccinium corymbosum* (Rubel). Energy from sucrose and total carbohydrates were adjusted in the HFD to be equivalent to energy from sucrose and total carbohydrates in the HFD+B. BB powder (14,537 kJ/kg) constituted 2.7% of total energy in the HFD+B diet. Diets were irradiated, packed under inert gas in individual 2.5 kg foil bags and maintained at -20°C until use. Fresh diet was provided at least twice per wk to minimize oxidization of the fats and deterioration of the anthocyanins.

Anthocyanin analysis of blueberry powder. BB powder was dissolved in 5% acetonitrile in water containing 1% formic acid to produce a 100 mg/L extract. Anthocyanin content of the extract (Table 2) was determined by LC-MS/MS using a modification of the method of Kalt *et a*l (146).[1]

Metabolic variables. Energy intake and indirect calorimetry were obtained for subsets of mice (n = 5-8 per group) between study days 45 and 52 using metabolic chambers (TSE Calorimetry Systems). The TSE system simultaneously and continuously monitors food intake, oxygen consumption and CO_2 production. Data were collected for 72 h during which time mice had free access to food and water. The first 24 h were considered an acclimation period and excluded from analyses.

Insulin resistance. Intraperitoneal insulin tolerance tests (ITT) were performed on food-deprived (6 h), non-anesthetized mice. Glucose measures were obtained from whole tail vein blood using an automated glucometer at baseline and at 30, 45, 60 and 90 min following intraperitoneal (IP) injection of human insulin (0.75 mU/kg). Glucose values following insulin injection were calculated as a proportion of the value at baseline. Glucose area under the curve (AUC) was calculated using these values and analyzed by ANOVA. Plasma insulin concentrations of food-deprived were measured using ELISA (133).

Histology and immunohistochemistry. Mice were euthanized by cervical dislocation following CO_2 narcosis. Epididymal AT (eAT) and inguinal subcutaneous AT (scAT) were dissected, fixed, embedded in paraffin and sectioned (135). Digital images were acquired with an Olympus DX51 light microscope. For each mouse, morphometric data were obtained from digitized tracings of ≥ 500 adipocytes from 3 or more sections cut at least 50 μm apart. Adipocyte size was calculated as described (133).

Adipocyte death. To quantify the frequency of dead adipocytes in individual mice, high resolution images of at least two histological sections of epididymal adipose tissue (eAT) at least 50 μm apart were scored for crown-like structures (CLS) (133). A minimum of 600 adipocytes were counted for each mouse. Each tissue section was scored for CLS by three observers who were unaware of the study objectives or dietary treatments. Percent CLS ([number dead adipocytes/number total adipocytes] x 100) for each mouse was calculated as the average of the three values.

Quantitative-PCR. Adipose tissues were dissected, snap frozen in liquid nitrogen and stored at -80 °C. Total RNA was extracted, quantified and analyzed by SYBR® Green real-time PCR on an Applied Biosystems 7300 Real-time PCR System (133). Fold expression relative to an endogenous control gene (cyclophilin B) was calculated as $2^{-\Delta\Delta Ct}$ using using mice fed the LFD as the "comparer." Primers used were: *F4/80* (5'-CTTTGGCTATGGGCTTCCAGTC-3', 5'-GCAAGGAGGACAGAGTTTATCGTG-3'), *CD11c* (5'-CTGGATAGCCTTTCTTCTGCTG-3', 5'-GCACACTGTGTCCGAACTC-3'), *Galectin-3* (5'-CAACAGGAGAGTCATTGTGTGTAAC-3', 5'-TTCAACCAGGACTTGTATTTTGAAT-3'), *MGL1* (5'-TCTCTGAAAGTGGATGTGGAGG-3', 5'-CACTACCCAGGTCAAACACAATCC-3'), *IL-6* (5-CCAGTTGCCTTCTTGGGACT-3', 5'-GGTCTGTTGGGAGTGGTATCC-3'), *iNOS* (5'-CAGAGGACCCAGAGACAAGC-3', 5'-TGCTGAAACATTTCCTGTGC-3'), *IL-10* (5'-CCAGGGAGATCCTTTGATGA-3', 5'-CATTCCCAGAGGAATTGCAT-3'), *TNFα* (5'-AATGGAAGGTTGGACGAAAA-3', 5'-GAGGCAACCTGACCACTCTC-3'), *MCP-1* (5'-ACTGAAGCCAGCTCTCTCTTCCTC-3,' 5'-TTCCTTCTTGGGGTCAGCACAGAC-3'), *GRP78* (5'-GGCCAAATTTGAAGAGCTGA-3', 5'-GCTCCTTGCCATTGAAGAAC-3'), *CHOP/GADD153* (5'-TCTTGACCCTGCGTCCCTAG-3', 5'-TGGGCACTGACCACTCTGTTT-3'), *Glutathione Peroxidase 3* (5'-ATGGTACCACTCATACCGCC-3', 5'-CATCCTGCCTTCTGTCCCT-3'), *Adiponectin* (5'-GAATCATTATGACGGCAGCA-3', 5'-TCATGTACACCGTGATGTGGTA-3'), *Leptin* (5'-

TTCACACACGCAGTCGGTAT-3', 5'- TGGTCCATCTTGGACAAACTC-3'), *Arginase* (5'-AGGAACTGGCTGAAGTGGTTA-3', 5'-GATGAGAAAGGAAAGTGGCTG-3'), *Ym1* (5'-AGAAGGGAGTTTCAAACCTGG-3', 5'-GTCTTGCTCATGTGTGTAAGT-3'), *Cyclophilin B* (5'-ATGTGGTTTTCGGCAAAGTT-3', 5'-TGACATCCTTCAGTGGCTTG-3').

Statistics. Data are expressed as mean ± SEM. Data were analyzed using SYSTAT v10. ANOVA or GLM procedures were used in conjunction with protected post-hoc tests (Tukey's HSD). Association between two variables is reported as the Pearson correlation coefficient. Frequency data of adipocyte death were transformed as $arcsin\sqrt{x}$ prior to statistical analysis. An attained significance level of $\alpha = 0.05$ was deemed significant.

Results

Effects of BB on HFD-induced weight gain, adiposity and metabolic parameters. As expected, mice fed the HFD for 8 wk gained significantly more weight (~3 g) than mice fed the LFD ($p < 0.005$; Fig. 1). However, the addition of BB to the HF diet did not protect against HFD-induced weight gain, as the mean body weights of mice fed the HFD (31.2 g ± 0.8 g) or HFD+B (31.1 g ± 0.8 g) did not differ (Fig. 1). Similar to changes in body weight, eAT mass of mice fed HFD or HFD+B was significantly greater than eAT mass of mice fed LFD ($p = 0.03$), but did not differ between HFD and HFD+B-fed mice (Table 3). In addition, mean adipocyte size in eAT of HFD- and HFD+B-fed mice was significantly greater than in LFD-fed mice ($p < 0.001$), but did not differ between HFD and HFD+B cohorts (Table 3). Similarly, scAT depots in HFD- and HFD+B-fed mice

tended to be heavier than scAT of mice fed the LFD ($p = 0.06$ and 0.07, respectively), but did not differ from each other (Table 3). Collectively, these results indicate that addition of BB to HFD did not have protective effects on body weight, adiposity or adipocyte hypertrophy. Consistent with these data, HFD and HFD+B similarly altered gene expression of adiponectin, which was lower in these groups than in the LFD-fed mice ($p = .02$, data not shown) and of leptin which was higher than in the LFD group ($p = .04$, data not shown).

As expected, energy intakes in mice fed the HFD or HFD+B were significantly greater than in LFD-fed mice ($p = 0.02$, Table 3). Moreover, as compared with LFD mice, HFD and HFD+B mice exhibited significantly lower respiratory exchange ratios (RER) ($p < 0.001$), oxygen consumption ($p = 0.03$) and heat production ($p = 0.01$) (Table 3). Importantly, we detected no significant differences between HFD and HFD+B cohorts in any of these measures (Table 3). These data indicate that greater energy intake, altered substrate utilization favoring fat over carbohydrate and lower metabolic rate contribute to increased body weight and adiposity in mice fed HFD and HFD+B as compared with LFD. Together, these results suggest that BB supplementation did not significantly alter HFD-associated changes in energy intake or metabolic rate, consistent with observed increases in body weight and adiposity (Fig. 1 and Table 3).

BB protects against HFD-induced insulin resistance. ITT were performed after 8 wk of dietary treatment to assess the effects of BB on HFD-induced peripheral IR (assessed as $ITT_{[AUC]}$). IR was greater in mice fed the HFD (AUC = 5,292.6 ± 1,105.6) as compared with those fed LFD (AUC = 2,489.5 ± 612.3, $p = 0.005$, Fig. 2), consistent with prior

studies from our laboratory (133). Notably, mice fed the HFD+B were significantly less insulin resistant than mice fed the HFD (AUC = 2,545.7 ± 627.1, $p = 0.03$, Fig. 2). In fact, $ITT_{[AUC]}$ was not significantly different between the LFD and HFD+B cohorts (Fig. 2). Consistent with the observed improvement in insulin sensitivity, fasting blood glucose levels tended ($p = 0.07$) to be lower in food-deprived HFD+B mice (7.34 ± 0.58 mmol/L) when compared to HFD mice (8.57 ± 0.51 mmol/L) but not to LFD mice (5.80 ± 0.35 mmol/L). Together, these results demonstrate that mice fed the HFD+B for 8 wk were less insulin resistant and had a mild improvement in glucose homeostasis as compared with mice fed the HFD. However, fasting insulin levels in mice fed HFD (148.01 ± 37.01 pmol/L) or HFD+B (148.07 ± 45.02 pmol/L) tended to be approximately one-fold greater than fasting insulin levels in LFD-fed mice (70.59 ± 13.67 pmol/L). Thus, HFD+B did not ameliorate the modest hyperinsulinemia observed in mice fed the HFD.

BB protects against HFD-induced adipocyte death. The frequency of dead adipocytes was 5- fold greater in mice fed the HFD (0.64% ± 0.08) as compared with mice fed the LFD (0.10% ± 0.05) ($p < 0.001$; Fig. 3A,B). Supplementation of the HFD with BB was associated with a ~50% lower frequency of dead adipocytes (0.33% ± 0.03) as compared with the HFD ($p = 0.02$, Fig. 3B,C), coincident with significantly lower IR (Fig. 2). The frequency of dead adipocytes was correlated with IR ($ITT_{[AUC]}$) when data from mice fed all three diets were included ($r = 0.46$, $p = 0.06$). Together these results confirm the positive association of obesity-induced IR and adipocyte death (133) and demonstrate that the beneficial effects of BB on whole body IR are coincident with BB-mediated attenuation of adipocyte death.

BB attenuates the HFD-associated change in gene hallmarks of recruited (M1) vs. resident (M2) ATMΦ. CD11c and macrophage galactose N-acetyl-galactosamine specific lectin 1 (MGL1) gene expression provide useful measures of the numbers of recruited (M1-polarized) ATMΦ (CD11c+/MGL1-) and resident (M2-polarized) ATMΦ (CD11c-/MGL1+) (131, 147). Employing real-time PCR, we determined gene expression levels of markers of total eAT monocytes/ MΦ (galectin-3), differentiated MΦ (F4/80), recruited ATMΦ (CD11c) and resident ATMΦ (MGL1), respectively. The HFD was associated with significantly greater galectin-3 ($p = 0.04$) and CD11c gene expression ($p = 0.02$; Table 4). These results are consistent with HFD-induced recruitment of monocytes (galectin-3+) into eAT and their subsequent maturation into M1-polarized (CD11c+) ATMΦ (F4/80+). As CD11c+ ATMΦ preferentially localize to dead adipocytes (132), these results are also in agreement with the greater frequency of dead adipocytes in eAT of HFD-fed mice (Fig. 3) (133, 135).

In contrast, expression of MGL1 and Ym1, hallmarks of resident (M2-polarized) ATMΦ (131, 148) were not significantly altered in response to HFD (Table 4). Thus the ratio of CD11c gene expression to MGL1 gene expression was significantly greater in mice fed HFD as compared with those fed LFD ($p = 0.02$; Table 4). Remarkably, this index of the relative numbers of M1 and M2 ATMΦ was significantly reduced in mice fed HFD+B as compared with mice fed HFD ($p = 0.05$) and did not differ from mice fed LFD (Table 4). Similar results were obtained when gene expression of Ym1 was considered (data not shown). Together these results suggest that BB selectively effects the recruitment and/or maturation of M1-polarized (CD11c+ / MGL1-) ATMΦ in mice made obese by HFD.

BB protects against HFD-induced ATMΦ inflammatory gene expression in eAT. TNFα and iNOS, which are produced predominantly by M1-polarized ATMΦ, and IL-6 and MCP-1 which are produced by ATMΦ and other AT cells, have each been implicated as disrupters of insulin signaling and/or promoters of obesity-associated IR *in vivo* (130). Consistent with the role of CD11c+ ATMΦ in obesity-associated AT inflammation, CD11c gene expression was significantly correlated with gene expression of TNFα ($r = 0.73$, $p < 0.001$), iNOS ($r = 0.54$, $p = 0.009$), interleukin 6 (IL-6, $r = 0.53$, $p = 0.02$), and MCP-1 (monocyte chemoattractant protein 1, $r = 0.49$, $p = 0.04$; Table 4). Feeding the HFD resulted in significantly greater expression of TNFα ($p = 0.005$) and MCP-1 ($p = 0.05$; Table 4). Notably, supplementing the HFD with BB was associated with significantly reduced expression of TNFα ($p = 0.01$; Table 4). Considered together, these results indicate that BB can reduce mRNA levels of ATMΦ-derived pro-inflammatory genes that promote obesity-associated IR.

Interleukin 10 (IL-10) is an immunosuppressive cytokine that limits the inflammatory response to pathogens and injury, thereby preventing or minimizing tissue damage. IL-10 is up-regulated by resident M2-polarized ATMΦ during the course of HF diet-induced AT inflammation, ostensibly as a counter-regulatory mechanism (131, 133, 148). In the present study, IL-10 gene expression in eAT was significantly greater in mice fed HFD compared to those fed LFD ($p = 0.003$; Table 4). Surprisingly, BB supplementation of the HFD was associated with a 50% lower IL-10 gene expression as compared with HFD alone ($p = 0.02$; Table 4) coincident with attenuated ATMΦ expression of pro-inflammatory genes (Table 4). These results suggest that the biological

action(s) of BB result in down-regulation of HFD-induced inflammatory gene expression in both M1-polarized and M2-polarized ATMΦ.

Effects of Blueberry on HFD-induced oxidative stress in eAT. Obesity promotes oxidative and ER stress in adipose tissue, and these stresses are mechanistically linked to adipose tissue inflammation and the metabolic complications of obesity (137, 138, 149). To assess the effect of BB supplementation on oxidative stress in AT, we quantified gene expression of glutathione peroxidase 3 (GPx3), a sensitive index of oxidative stress in AT (149). GPx3 gene expression was significantly greater in mice fed HFD+B as compared with mice fed HFD ($p = 0.05$) and tended ($p = 0.11$) to be greater than in mice fed LFD (Table 4). These data suggest that protection from HFD-induced adipocyte death (Fig. 3) and AT inflammation (Table 4) is coincident with attenuated oxidative stress in AT of mice fed the HFD+B diet. Surprisingly, neither HFD nor HFD+B had any effect on adipose ER stress, assessed as gene expression of glucose regulated protein 78 (GRP78) and C/EBP-homologous protein (CHOP/GADD153) ((150); data not shown). These results suggest that oxidative stress precedes ER stress during the development of obesity and AT inflammation in this model.

Discussion

The genus *Vaccinium* (e.g., blueberry, bilberry, cranberry) has been used traditionally as a source of folk remedies for established diabetic symptoms, primarily as leaf or stem infusions or decoctions (151). Here we demonstrate that supplementing a HFD with *Vaccinium* berry powder inhibits the early inflammatory events in AT that promote obesity-associated IR. Consistent with these observations, mice fed the HFD+B

diet for 8 wk were substantially protected from IR based on significant improvements in the ITT $_{[AUC]}$ compared to those fed HFD. The ITT measures whole body glucose disposal in response to an insulin bolus and reflects both increased skeletal muscle glucose uptake and decreased liver glucose production. BB also improved HFD-induced fasting hyperglycemia, although this improvement was modest and was not coincident with attenuated fasting hyperinsulinemia. As fasting glucose levels largely reflect hepatic glucose output (which is normally suppressed by insulin), these observations suggest that supplementing the HFD with BB did not significantly reverse HFD-induced hepatic IR. Hyperinsulinemic-euglycemic 'clamp' studies will be required to verify this conclusion. Overall, however, these results demonstrate for the first time that dietary BB can protect against whole body IR and can improve glycemia in a model of obesity-induced IR.

A prior study of BB effects on diet-induced obesity and obesity complications reported no protection from IR in mice fed a BB-supplemented high fat diet (HFD) for 12 wk (152). However, these results were confounded by significantly greater food intake and adiposity in mice fed the BB-supplemented HFD. Similarly in our studies, mice fed HFD+B for 12 wk were (~3 g) heavier and (30%) more obese than HFD mice ($p = 0.03$, data not shown), reflecting higher energy intake and somewhat reduced energy expenditure after wk 8 (data not shown). Intriguingly however, despite the significantly greater adiposity of HFD+B mice, $ITT_{[AUC]}$ values were essentially identical between HFD and HFD+B mice ($p = 0.92$, data not shown), suggesting that BB supplementation may have continued to provide metabolic benefit after wk eight.

Peripheral insulin resistance is thought to be caused by increased circulating

levels of free fatty acids and lipids (7, 130). One mechanism contributing to elevated circulating free fatty acids in obesity is adipocyte lipolysis (7, 138). Inflammatory mediators up-regulated in AT in obesity (e.g., TNFα, iNOS, IL-6) exacerbate lipolysis by antagonizing the anti-lipolytic effects of insulin on adipocytes and/or by directly stimulating lipolysis (7, 138). Accordingly, the insulin-sensitizing effects of BB in the present study were associated with attenuated AT inflammation, manifest as 1) lower frequency of dead adipocytes and 2) lower gene expression indices of ATMΦ infiltration and inflammatory activation. Studies from our laboratory and others indicate that adipocyte death and ATMΦ infiltration are mechanistically intertwined in the pathogenesis of AT inflammation. Specifically, the infiltration, accumulation and pro-inflammatory activation of M1-polarized ATMΦ in obesity are functionally linked to the selective recruitment of CD11c+ ATMΦ to scavenge dead adipocytes and their remnant lipid (132, 133, 135). Thus, a decrease in the proportion of ATMΦ expressing CD11c+ and coincident reductions in inflammatory cytokines in eAT of mice fed the HFD+B diet is consistent with the lower frequency of dead adipocytes in these mice.

It is noteworthy that whereas HFD+B was associated with frequencies of adipocyte death and levels of CD11c gene expression intermediate between those of mice fed LFD and HFD, AT gene expression of TNFα did not differ between mice fed HFD+B as compared with those fed LFD. This observation suggests that, in addition to reducing adipocyte death and ATMΦ infiltration, BB blocks HFD-induced AT inflammation by inhibiting inflammatory gene expression in ATMΦ (and presumably other AT cells). Prior studies of BB protective actions in contexts other than obesity (142, 143, 153) suggest that one potential mechanism of this inflammatory gene down-

regulation is through inhibition of stress-induced mitogen-activated protein kinase (MAPK) and nuclear factor κB (NFκB) signaling pathways, which modulate inflammatory gene expression in MΦ (154). Future studies employing alternative sampling methods (e.g., flow cytometry) will be required to determine the extent to which the salutary effect of BB on HFD-induced ATMΦ inflammation reflects reduced ATMΦ infiltration or alternatively, reduced ATMΦ inflammatory gene expression. In addition, our data do not exclude the possibility that the anti-inflammatory effects of the HFD+B diet also reflect the previously-reported actions of BB to inhibit bacterial translocation to extra-intestinal sites (144). Extra-intestinal bacterial translocation and resulting low grade endotoxemia are associated with chronic HFD regimes and are implicated in the development of AT inflammation and IR (145). Irrespective of the mechanism(s) of action we suggest that the ability of BB to inhibit inflammatory gene expression in AT plays a critical role in preventing obesity-associated IR in the present study. However, a limitation of our study is the absence of ELISA data confirming that BB-associated patterns of gene expression are manifest as functionally-significant alterations in expressed inflammatory proteins.

Increased adipocyte death in obesity is suggested (135) to reflect the elevated levels of cytotoxic stressors reported for obese AT (137, 138, 149). In the present study, higher frequencies of dead adipocytes in mice fed HFD were coincident with lower gene expression of GPx3, an oxidative stress-sensitive gene in AT (155). Notably, feeding the HFD+B diet was not associated with lower GPx3 gene expression coincident with lower frequency of dead adipocytes. Together these observations provide an empirical association between AT oxidative stress and obesity-associated adipocyte death. As with

the inflammation-suppressive effects of BB on ATMΦ the cytoprotective effects of BB on adipocytes are in theory consistent with the demonstrated ability of BB to modulate MAPK and NFκB signaling pathways (143, 153, 156), as these two pathways coordinately regulate cell fate (157). BB-enhanced adipocyte survival may also indirectly reflect the effects of BB on ATMΦ, specifically the attenuation of ATMΦ TNFα, as this inflammatory mediator promotes oxidative stress and apoptosis (158, 159). Consistent with the notion that the actions of BB to prevent adipocyte apoptosis reflect the salutary effects of BB on ATMΦ are recent observations (134, 160) suggesting that inflammatory CD11c+ ATMΦ participate in adipocyte execution as well as clearance (see also (135)).

Our data demonstrating comparable weight and adiposity in mice fed either HFD or HFD+B distinguish the protective effects of whole BB extract on AT inflammation and IR in the present study from the actions of flavonoids and other polyphenolics that achieve similar protection by blocking adiposity *per se* (152, 161). In particular, despite its presence in the we observed none of the reported actions (161, 162) of the anthocyanin cyanidin-3 glucoside (C3G) to block HFD-induced obesity or to promote insulin sensitivity by altering retinol binding protein-4 (RBP-4) and glucose transporter 4 (GLUT-4) gene expression (data not shown). The study of Prior and colleagues (152) similarly failed to detect anti-obesity effects of a BB extract containing ≥2-fold higher concentrations of C3G than that (0.2% of diet) reported to robustly inhibit HF diet-induced obesity (161). However, Prior et al reported that a purified preparation of BB anthocyanins partially inhibited HF diet-induced increases in adiposity (152), suggesting that the 'whole' BB matrix may restrict the bioavailability or bioactivity of C3G and potentially other BB polyphenolics.

We find it additionally encouraging that in humans, 2.7% of total energy from BB (as in the present study) could be achieved with 20 g of BB powder or 140 g of whole BB per day (based on a daily energy intake of 14,500 kJ). Thus, the metabolic benefits of BB are in theory attainable with feasible levels of dietary intervention. These benefits are likely to reflect, at least in part, the biological activities of BB anthocyanins. Although anthocyanin bioavailability is generally considered to be low (163), recent *in vivo* studies suggest that even low levels of anthocyanins can be highly bioavailable and well-retained in tissues (146). Although our data strongly suggest that adipose tissue is an important site of BB actions to ameliorate obesity complications, it is plausible that the protective effects of BB in the present study reflect retention and direct action of BB components in non-adipose tissues, including skeletal muscle, liver, pancreas and circulating immune cells. Studies elucidating the tissue distribution of BB anthocyanins and anthocyanin metabolites in mice fed HFD+B will help clarify the cell targets and molecular mechanism(s) by which dietary BB protects against obesity-induced AT inflammation and IR.

[1] Detailed methods for the LC-MS/MS analysis of blueberry anthocyanins are available as Online Supporting Material.

TABLE 1 Composition of low fat, high fat, and high fat plus blueberry diets

Ingredient	LFD		HFD		HFD+B	
	g/kg	*kJ/kg*	*g/kg*	*kJ/kg*	*g/kg*	*kJ/kg*
Casein	**189.6**	**3174.7**	**258.4**	**4328.2**	**255.7**	**4282.9**
L-cystine	**2.8**	**47.6**	**3.9**	**64.9**	**3.8**	**64.2**
Cornstarch	**545.0**	**9127.2**	**0.0**	**0.0**	**0.0**	**0.0**
Malt	**1**	**19**	**1**	**27**	**1**	**2**

odextrin 10	**18.5**	**84.2**	**61.5**	**05.2**	**59.8**	**676.8**
Sucrose	**0.0**	**0.0**	**88.9**	**1488.9**	**63.9**	**1070.07**
Cellulose	**47.4**	**0.0**	**64.6**	**0.0**	**57.5**	**0.0**
Lard	**19.0**	**714.3**	**316.6**	**11929.8**	**313.3**	**1180.47**
Soyb	**2**	**89**	**3**	**12**	**3**	**1**

ean oil	**3.7**	**2.9**	**2.3**	**17.3**	**2.0**	**20.4.6**
Mineral Mix[1]	**9.5**	**63.5**	**12.9**	**86.2**	**12.8**	**85.6**
DiCalcium phosphate	**12.3**	**0.0**	**16.8**	**0.0**	**16.6**	**0.0**
Calcium carbonate	**5.2**	**0.0**	**7.1**	**0.0**	**7.0**	**0.0**
Potassium citrate·1$H_2$0	**15.6**	**0.0**	**21.3**	**0.0**	**21.1**	**0.0**

Vitamin mixture[2]	**9.5**	**155.7**	**12.9**	**211.4**	**12.8**	**209.7**
Choline bitartrate	**1.9**	**0.0**	**2.6**	**0.0**	**2.6**	**0.0**
Blueberry powder	**0.0**	**0.0**	**0.0**	**0.0**	**40.9**	**40.9**
FD&C blue dye #1	**0.024**	**0.0**	**0.00**	**0.0**	**0.047**	**0.0**
FD&C red dye	**0.024**	**0.0**	**0.00**	**0.0**	**0.00**	**0.0**

#40						
FD&C yellow dye #5	**0.00**	**0.0**	**0.00**	**0.0**	**0.00**	**0.0**
Total	**1000**	**1616**	**1000**	**2203**	**1000**	**2144.02**

[1]Containing the following (g/kg mineral mix): sodium chloride, 259; magnesium oxide, 41.9; magnesium sulfate.7H_2O, 257.6; chromium KSO_4.12H_2O, 1.925; cupric carbonate, 1.05; sodium fluoride, 0.2; potassium iodate, 0.035; ferric citrate, 21.0; manganous carbonate, 12.25; ammonium molybdate.4H_2O, 0.3; sodium selenite, 0.035; zinc carbonate, 5.6; sucrose, 399.105. Sucrose in the mineral mix provided 63.5 kJ energy/kg diet.

[2]Containing the following (g/kg vitamin mix): all-trans retinol acetate, 0.8; Cholecalciferol, 1.0; dl-α-tocopheryl acetate, 10.0; menadione sodium bisulfate, 0.08; biotin (1.0%), 2.0; cyanocobalamin (0.1%), 1.0; folic acid, 0.2; nicotinic acid, 3.0;

calcium pantothenate, 1.6; pyridoxine-HCl, 0.7; riboflavin, 0.6; thiamin-HCl, 0.6; sucrose, 978.42. Sucrose in the vitamin mix provided 163.9 kJ energy/kg diet.

TABLE 2 Relative anthocyanin composition in freeze-dried blueberry (BB) powder incorporated into the high fat diet as determined by LC-MS/MS[1]

	g/kg dry weight
delphinidin-3-galactoside	1.383
delphinidin-3-glucoside	0.467
cyanidin-3-galactoside	0.493
cyanidin-3-glucoside	0.333
cyanidin-3-arabinoside	0.673
peonidin-3-galactoside	0.538
peonidin-3-glucoside	13.915
peonidin-3-arabinoside	4.378
malvidin-3-galactoside	0.156
malvidin-3-arabinoside	9.104
Total	31.44

[1] Detailed methods for the LC-MS/MS analysis of blueberry anthocyanins are available as Online Supporting Material.

TABLE 3 Adiposity, energy intake, substrate utilization and indices of metabolic rate in mice fed the LFD, HFD or HFD+B for 8 wk[1]

	LFD	HFD	HFD+B
Adiposity			
eAT Weight *(g)*	0.80 ± 0.06[a]	1.49 ± 0.22[b]	1.35 ± 0.12[b]
scat Weight *(g)*	0.54 ± 0.03[a]	0.86 ± 0.13[b]	0.84 ± 0.09[b]
Adipocyte Size *(μm^2)*	2,210 ± 90.00[a]	5,150 ± 320.00[b]	5,090 ± 670.00[b]
Metabolic Variables			
Energy Intake *($kJ \cdot d^{-1}$)*	50.55 ± 4.30[a]	55.99 ± 2.64[b]	56.06 ± 5.65[b]
RER *(arbitrary units)*	0.83 ± 0.02[b]	0.72 ± 0.01[a]	0.73 ± 0.01[a]
VO_2 *($mg \cdot kg^{-1} \cdot h^{-1}$)*	1458.71 ± 41.58[b]	1288.37 ± 29.02[a]	1333.73 ± 53.42[a]
Heat *($kJ \cdot h^{-1} \cdot kg^{-1}$)*	29.74 ± 0.95[b]	25.57 ± 0.60[a]	26.53 ± 1.07[a]

[1]Values are means ± SEM, *n*=5-8. Means in a row with superscripts without a common letter differ, $p < 0.05$.

Table 4 Gene expression (real-time PCR) in whole eAT for gene markers of ATMΦ and ATMΦ polarization, inflammatory mediators and oxidative stress in mice fed the LFD, HFD or HFD+B for 8 wk[1]

	LFD	HFD	HFD+B
ATMΦ markers			
Galectin 3	1.00 ± 0.10[a]	1.78 ± 0.28[b]	1.52 ± 0.24[b]
F4/80	1.00 ± 0.17	1.34 ± 0.19	1.13 ± 0.13
CD11c	1.00 ± 0.26[a]	3.66 ± 1.10[b]	2.55 ± 0.66[b]
MGL1	1.00 ± 0.12	0.91 ± 0.08	1.15 ± 0.09
Ym1	1.00 ± 0.16	1.21 ± 0.28	1.42 ± 0.23
CD11c / MGL1	1.00 ± 0.17[a]	6.17 ± 1.50[b]	1.42 ± 0.47[a]
Inflammatory mediators			

TNFα	1.00 ± 0.14[a]	2.60 ± 0.41[b]	1.19 ± 0.24[a]
MCP-1	1.00 ± 0.26[a]	4.32 ± 1.06[b]	2.95 ± 0.88[b]
IL-6	1.00 ± 0.12	1.35 ± 0.19	1.11 ± 0.14
iNOS	1.00 ± 0.17	1.55 ± 0.24	1.03 ± 0.17
IL-10	1.00 ± 0.21[a]	2.29 ± 0.40[b]	1.46 ± 0.29[a]
Oxidative stress			
GPx3	1.00 ± 0.42[a,b]	0.62 ± 0.16[a]	1.24 ± 0.31[b]

[1]Values are mean ± SEM, n=8. Means at wk 8 without a common letter differ, $p < 0.05$.

Literature Cited

FIGURE LEGENDS

FIGURE 1 Body weight of mice fed the LFD, HFD or HFD+B for 8 wk. Values are means ±

SEM, n=8. Means at wk 8 without a common letter differ ($p < 0.05$).

FIGURE 2 Insulin tolerance tests in mice fed the LFD, HFD or HFD+B for 8 wk. Data represent the clearance of blood glucose in response to an insulin bolus in food-deprived mice. Glucose values at 30, 45, 60 and 90 minutes after IP insulin injection were expressed for each mouse as a proportion of the value at baseline (100%). Values are means ± SEM, n=8. $ITT_{[AUC]}$ for lines identified by different letters are significantly different ($p < 0.05$).

FIGURE 3 The frequency of dead adipocytes in mice fed the LFD, HFD or HFD+B for 8 wk.

Representative H & E-stained histological sections of eAT from mice (n = 8) maintained on (A) LFD, (B) HFD, and (C) HFD+B. Dead adipocytes are indicated by crown-like structures of ATMΦ surrounding remnant lipid droplets (arrows). Scale Bar = 200 μm.

Online Supporting Material - DeFuria et al.

DeFuria et al., Supplemental Methods

Analysis of Blueberry Anthocyanins by LC / MS

Sample Preparation.

A freeze dried blueberry powder was obtained from the U.S. High bush Blueberry Council (USHBC) which was comprised of a 50/50 blend of the blueberry varieties *Vaccinium ashei* (Tifblue) and *Vaccinium corymbosum* (Rubel) designated 10506. Dried powder was stored at -80 °C until analysis.

Powder was dissolved to a concentration of 1 g dry powder/L of either 5% acetonitrile (Fisher Co., Fair Lawn, NJ) in water containing 1% formic acid (HFO) (Sigma Chemical Co., St. Louis, MO) or in methanol containing 1% formic acid. This solution was diluted in 5% acetonitrile in water containing 1% formic acid to produce a 0.1 g/L berry extract for injection on HPLC-MS/MS with a diode array detector (DAD) in line.

LC-MS Analysis.

LC/MS analysis was accomplished by modification of a previously reported method (146). Chromatographic separation of extracted anthocyanins was conducted using an Agilent 1100 HPLC system (Agilent Technologies, Palo Alto, CA) fitted with a Phenomenex Synergy Max-RP C18 analytical columns, 250 x 4.6 mm, 4 μm particle size. The columns were protected with a Phenomenex Max-RP cartridge. Anthocyanin separation was achieved using a gradient between 4.5% HFO in water (mobile phase A) to 4.5% HFO in 100% acetonitrile (mobile phase B) over an 80 min analytical run at a flow rate of 0.0003 L/min. The gradient profile was as follows: mobile phase B, 5% at 0 min, 12% at 12 min, 24% at 40 min, 40% between 45 and 50 min, 100% from 55 to 70 min, and then 5% from 75 to 80 min. Using a six-port valve, the eluent flowing from the analytical column was directed to waste until just before anthocyanins began to elute at 18 min. The flow was then redirected to an Agilent UV G1315A DAD, where absorbance was monitored between 250 and 700 nm. Once through the DAD, the eluent was directed to a Bruker Esquire ion trap MS/MS (Bruker Daltonics Inc., Billerica, MA). This MS unit was fitted with an electrospray interface and was operated in the positive ion mode with alternating MS and MS/MS scans from *m/z* 150 to1000.

MS/MS scans of anthocyanins were compared with authentic anthocyanin standards that were obtained from either Polyphenols AS (Sandnes, Norway) or Extrasynthase (Genay, France). Eight pure anthocyanins standards were used including cyanidin 3-glucoside (Cyn glu), cyanidin 3-galactoside (Cyn gal), cyanidin 3-arabinoside (Cyn ara), delphinidin 3-glucoside (Del glu), peonidin 3-glucoside (Peo glu), peonidin 3-galactoside (Peo gal), peonidin 3-arabinoside (Peo ara), and malvidin 3-glucoside (Mal

glu). MS data were handled using Bruker Daltronics Esquire LC 4.5 software for collection (Build 21)and analysis (Build 49). Compounds were identified by matching their HPLC retention time, UV absorption profile, *m*/*z* of their molecular ions, and their MS/MS fragmentation pattern with standards. Area counts of the intensity scans for the individual anthocyanin aglycone fragment obtained by MS/MS were collected for anthocyanins in the blueberry powder and standards. An equation for the standard curves was calculated by fitting a linear line using the least squares method. The resulting equation was used to calculate the value of anthocyanins in the blueberry powder.

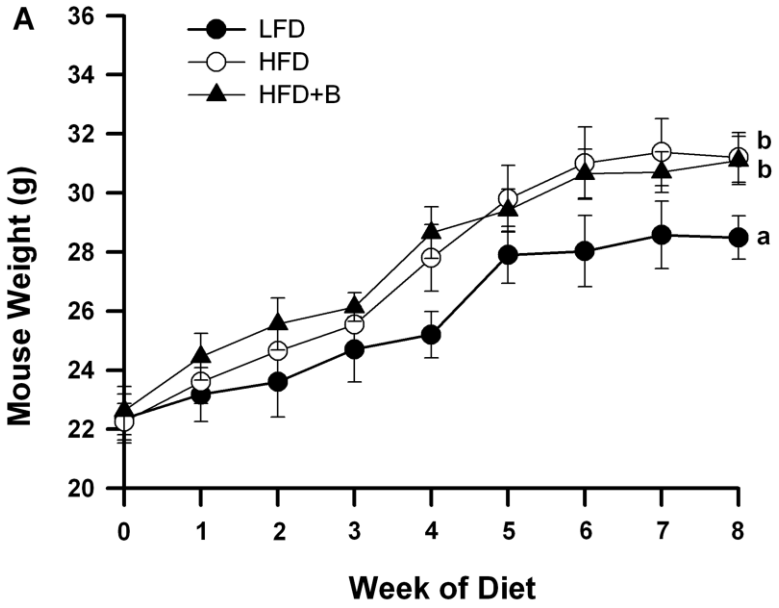

Figure 1

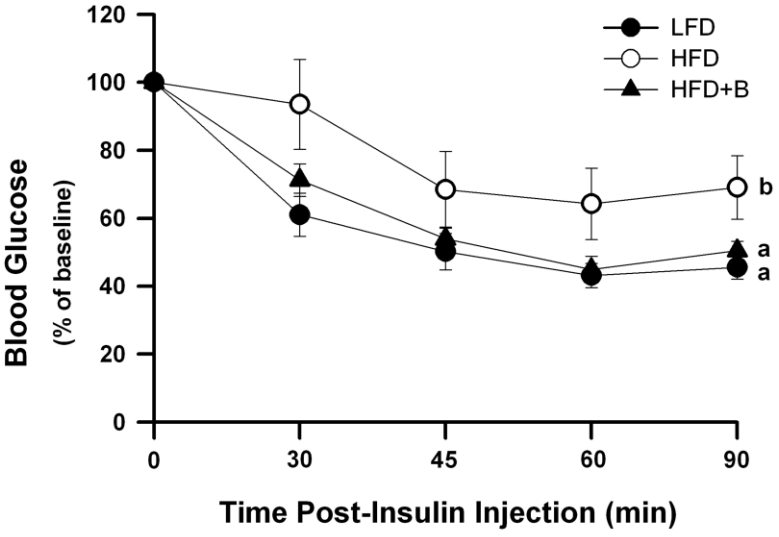

Figure 2

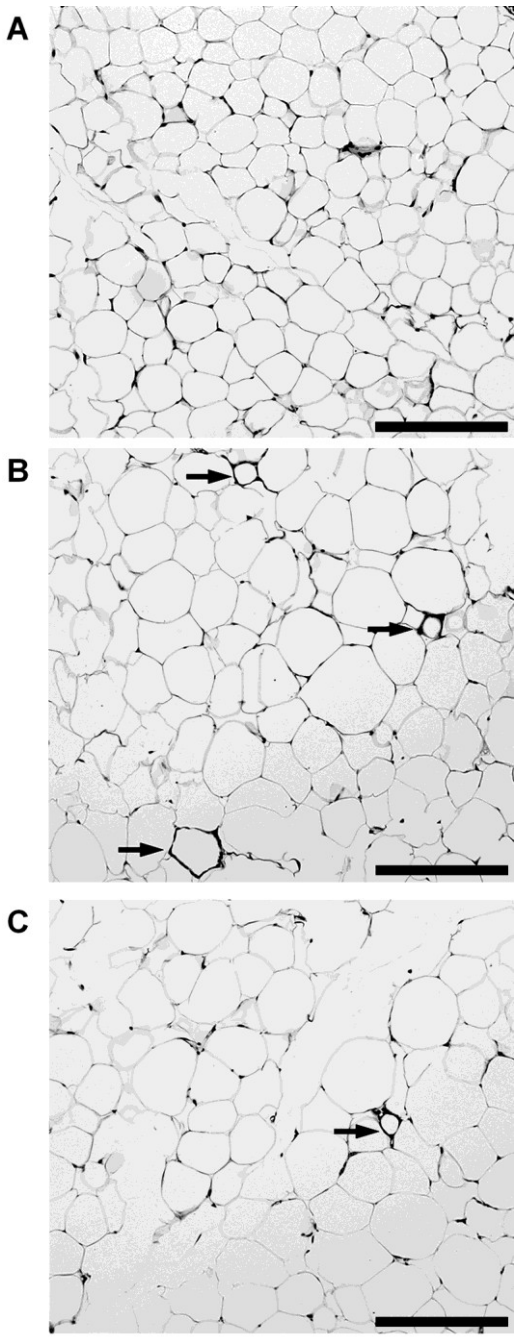

Figure 3

T Cell Recruitment and Th1 Polarization in Adipose Tissue During Diet-Induced Obesity in C57BL/6 mice

Katherine J Strissel, **Jason DeFuria**, Merav Esther Shaul, Grace Bennett

Andrew S Greenberg & Martin S Obin

Published in Obesity

Obesity (Silver Spring). 2010 Oct;18(10):1918-25. Epub 2010 Jan 28

Obesity & Metabolism Laboratory, JM-USDA Human Nutrition Research Center on Aging at Tufts University, Boston, MA 02111

Corresponding author: MS Obin (martin.obin @tufts.edu) or KJ Strissel (katherine.strissel@tufts.edu)

Short title: *T cell recruitment and polarization in obesity*

Key words: T cell, adipose tissue, obesity, inflammation, insulin resistance

Word count: 4491

Number of Tables: 0

Number of Figures: 4

Supplementary Material: 1 Table, 2 Figures

Nonstandard abbreviations: epididymal adipose tissue (eAT); adipose tissue macrophage (ATMΦ); stromal vascular cells (SVCs); crown-like structure (CLS).

Funding sources: Su*pported by NIH DK074979, the American Diabetes Association, BONRC NIDDK 5P30DK46200-14, and USDA-ARS.*

ABSTRACT

The role of adaptive immunity in obesity-associated adipose tissue (AT) inflammation and insulin resistance (IR) is controversial. We employed flow cytometry and quantitative PCR to assess T-cell recruitment and activation in epididymal AT (eAT) of C57BL/6 mice during 4-22 weeks of a high (60% energy) fat diet (HFD). By week 6, eAT mass and stromal vascular cell (SVC) number increased 3-fold in mice fed HFD, coincident with onset of IR. We observed no increase in the proportion of CD3+ SVCs or in gene expression of CD3, IFNγ, or regulated upon activation, normal T-cell expressed and secreted (RANTES) during the first 16 weeks of HFD. In contrast, CD11c+ macrophages (MΦ) were enriched 6-fold by week 8 ($p < 0.01$). SVC enrichment for T cells (predominantly CD4+ and CD8+) and elevated IFNγ and RANTES gene expression were detected by 20-22 weeks of HFD ($p < 0.01$), coincident with the resolution of eAT remodeling. HFD-induced T cell priming earlier in the obesity time course is suggested by (1) elevated (5-fold) IL-12p40 gene expression in eAT by week 12 ($p \leq 0.01$) and (2) greater IFNγ secretion from PMA/ionophore-stimulated eAT explants at week 6 (1 fold, $p = 0.08$) and week 12 (5 fold, $p < 0.001$). In summary, T cell enrichment and IFNγ gene induction occur subsequent to ATMΦ recruitment, onset of IR and resolution of eAT remodeling. However, enhanced priming for IFNγ production suggests the contribution of CD4+ and/or CD8+ effectors to cell-mediated immune responses promoting HFD-induced AT inflammation and IR.

INTRODUCTION

Visceral obesity is characterized by a state of low-grade chronic inflammation, which is now recognized as an important contributor to the pathogenesis of obesity complications, in particular insulin resistance (IR) (164, 165). A significant advance in our understanding of obesity-associated adipose tissue (AT) inflammation has been the recognition of the important role of innate immunity, specifically the recruitment, localization and functional heterogeneity of AT macrophages (MΦ) during the development of obesity (129). Initial studies documenting robust ATMΦ recruitment in obese mice noted few if any coincident changes in numbers of other immune cells, including lymphocytes (166, 167). However, T cell and NK cell-derived cytokines are important modulators of MΦ response patterns and functions within tissues, in particular as regards the M1/M2 polarization paradigm (168, 169). In this paradigm pro-inflammatory MΦ activation directed against intracellular pathogens (M1) is driven by the canonical T helper cell type-1 (Th-1) cytokine interferon-gamma (IFNγ) (170). A variety of 'alternative' (M2) MΦ activation states driven by T helper cell type-2 (Th2) cytokines IL-4 and IL-13 and functionally modulated by IL-10 (171) mediate anti-parasite defense, wound healing, tissue remodeling and the resolution of acute inflammation. AT expansion involves extensive tissue remodeling (172) and thus the regulated actions of M2-polarized ATMΦs. However, in mice, chronic obesity is associated with the accumulation of M1-polarized, CD11c+ ATMΦs in intra-abdominal fat (132, {Strissel, 2007 #83, 133, 173). This "phenotype switch" (173) in ATMΦ polarization from M2 to M1 made it plausible that T cells and Th1/2 cytokines act as orchestrators

of ATMΦ responses during the development of obesity-associated AT inflammation and IR.

Flow cytometry studies by Penicaud and colleagues (174, 175) initially characterized lymphocyte cell populations in mouse AT, reporting depot-specific profiles and positive associations of obesity and/or mass of epididymal AT (eAT) with the percentage of lymphocytes that were T cells. Subsequent studies have reported obesity-associated increases in AT T cells in mice and extended these observations to obese humans (176-179). In obese humans, visceral fat is distinguished by greater numbers of T and NK cells and elevated gene expression of both IFNγ and the Th1 chemokine, regulated upon activation, normal T-cell expressed and secreted [RANTES] as compared with subcutaneous fat (176, 180). Notably, obese IFNγ null mice fed high fat/high cholesterol, choline-deficient diet exhibited reduced accumulation of ATMΦ as well as attenuated pro-inflammatory cytokine expression in epididymal AT (eAT), coincident with improved glucose tolerance relative to wild-type mice (177). These results provide empirical support for the hypothesis that T cells accumulate in AT in obesity and that Th1-polarized T cells regulate AT inflammation and impact systemic glucose homeostasis.

Expanding this notion, Kintscher and coworkers (179) proposed that T cell recruitment was a primary event in the development of AT inflammation and IR. They reported that mRNA of the pan-T cell marker CD3 was significantly elevated in eAT during the initial stages of high fat diet (HFD)-induced obesity (week 5), coincident with IR, yet weeks before increased mRNA levels of the MΦ marker

F4/80. Additional evidence supporting a role for activated T cells in ATMΦ recruitment and AT inflammation comes from studies in lean, atherosclerotic CD4dnTGFbR mice (181). T cells in these mice are constitutively activated due to reduced TGF-β signaling. This constitutive T cell activation was associated with increased recruitment of CD4+ T cells and ATMΦ as well as elevated MCP-1, TNF-α and IFNγ gene expression in AT (181). However, as these mice remained insulin sensitive, the role of activated T cells and IFNγ in the development of IR was questioned (181). An additional challenge to the notion that activated T cells are an underlying cause of AT inflammation and IR comes from data (182) suggesting that T cells are selectively *depleted* from eAT to facilitate ATMΦ recruitment and AT expansion while dampening inflammation. Consistent with this idea, the absence of T cells in RAG2-/- mice was associated with larger AT depots and more ATMΦ in response to a HFD (182).

In the present study we investigate T cell recruitment and activation within eAT of C57BL/6 mice during a 22 week time course of HFD-induced obesity. Previously-established metabolic hallmarks of this obesity time course include the development of glucose intolerance by week 1, doubling of eAT weight and hyperinsulinemia by week 4, and IR (assessed by intraperitoneal insulin tolerance tests) by week 6, progressively increasing to maximal levels by week 16 (133). Accompanying these metabolic changes are progressive increases in CD11c+ ATMΦ recruitment and inflammatory gene expression, adipocyte death, and tissue remodeling, with eAT mass reduced by ~50% at week 16 and then partially restored (regrowth) by new adipogenesis by week 20 (133). Our objective was to determine

the temporal pattern and magnitude of T cell responses during the progression of these hallmark events.

METHODS and PROCEDURES

Animals, Diets. Studies were approved and monitored by the Institutional Animal Care & Use Committee of the JMUSDA-HNRCA at Tufts University. All studies used male C57BL/6 mice (Jackson Labs, Bar Harbor, Maine) that were fed *ad libitum*. Three sets of mouse studies were completed: (1) Gene expression studies of T cell markers and T cell-associated cytokines were conducted with archived frozen epididymal adipose tissue (eAT) from male mice that were divided into two weight-matched groups and fed either a low fat diet (LFD, 10% energy from fat, Research Diets #D12450Bi), or a high fat diet (HFD, 60% energy from fat, Research Diets #D12492i) for 1, 4, 8, 12, 16, or 20 weeks beginning at 5 weeks of age. Morphometric, metabolic and macrophage-mediated inflammatory profiles of eAT from these mice have been previously reported (133); (2) For flow cytometry and associated gene expression studies 5 week-old male mice were fed either the LFD or HFD for 6, 8, 12, 16 and 22 weeks while housed at the Jackson Laboratory. Mice were shipped to the HNRCA where they were maintained on the same diet for 2-3 d before use. (3) Gene expression studies of short-term HFD-induced T cell and macrophage recruitment mice were conducted with fourteen week-old mice that were divided into two weight-matched groups and fed either a LFD or HFD for 5 weeks.

Metabolic measures. Glucose measurements were obtained from whole tail vein blood of fasted (6 h), non-anesthetized mice using an automated glucometer. Fasting

(overnight) serum insulin was measured by ELISA using mouse insulin as a standard (Crystal Chem., Downers Grove, IL).

Quantitative PCR. Procedures for epididymal adipose tissue RNA extraction, first strand cDNA synthesis and SYBR® Green real-time PCR reactions were as previously described (133). RNA from sorted ATMΦs was amplified using the WT-Ovation amplification system (NuGEN, San Carlos, CA). Determination of relative gene expression levels was based on the comparative critical threshold (Ct) method. Target gene expression was normalized to the average expression of an endogenous control gene (cyclophilin A), and fold difference was calculated by $2^{-\Delta\Delta Ct}$ (corrected for primer efficiency [E]). Primer sequences are provided in online Supplementary Material.

Stromal Vascular Cell isolation, cell labeling. Stromal vascular cells (SVCs) were isolated from eAT using Liberase Blenzyme 3 for cell sorting experiments (Roche, Indianapolis, IN) or collagenase (for FACS) and centrifugation as previously described (33) with minor modifications. The samples were incubated at 37 °C with shaking until digestion was complete (30-40 min). The digested tissue was passed through a 100 micron mesh filter and the flow through centrifuged to obtain the final SVC pellet. The SVC pellet was re-suspended with 1 ml red blood cell lysis buffer (Sigma, St. Louis, MO), followed by the addition of chilled FACS labeling buffer (1xPBS with 1% fatty acid-free BSA, 1mM EDTA, 25mM HEPES). For ATMΦ sorting, FACS buffer contained RNAse inhibitor. SVC numbers were determined and the cells re-suspended in fresh FACS labeling buffer (~$1x10^6$ cells/100□l). Prior to

labeling, cells were incubated in Fc block for 10 min, washed with FACS buffer and re-pelleted. Cells ($5x10^5$ cells/100□l) were labeled in FACS buffer for 40 min on ice with desired primary fluorophore-conjugated antibodies or appropriate isotype controls. Labeled cells were then washed and re-suspended three times before flow cytometric analysis.

The following antibodies were used to label SVCs: anti-CD3e-488, (#53-0031), anti-CD8b-PE-Cy5, (#53-0083), anti-CD25-488 (#53-0251), anti-F4/80-PE-Cy5 (#15-4801) and anti-CD69-FITC (#11-0691) from eBiosciences (San Diego, CA); anti-NK1.1-RPE (#MCA1266PE) from Serotec (Raleigh, NC); anti-CD44-FITC (#553133), anti-CD4-PE, (#553730), anti-CD8a-PE-Cy5 (#553034), anti-CD11c-PE (#557401) and Fc-block (#553142) from BD Pharmingen (San Jose, CA); goat anti-mouse MGL1/2 (#AF4292), R&D Systems (Minneapolis, MN); and anti-goat-A488 (#705-486-147), Jackson ImmunoResearch (West Grove, PA).

Flow Cytometry. Labeled cells were quantified by fluorescence activated cell sorting (FACS) using the FACSCalibur 2 laser 4 color analytical flow cytometer (Becton Dickinson, San Jose, CA) with CellQuest software for data capture at the Tufts Laser Cytometry Core facility. Collected data were analyzed using Summit software (Beckman Coulter, Fullerton, CA). Autofluorescence was identified and excluded using Isotype controls. Lymphocytes were quantified in the R1 gate, defined by forward and side scatter properties and CD3 positive events. ATMΦs were sorted on a MoFlo Multi-laser system (MLS) sorter (Beckman Coulter) using Summit software.

Sorted cells were stored in sorting buffer at -80C until RNA extraction and real-time PCR (see above).

Adipose tissue explant culture, T cell priming assay. Explant cultures of eAT were established essentially as described by Thalmann (183). Briefly, eAT (100 mg/well) was dissected, weighed, minced and placed into 6 well tissue culture dishes with either T cell activation medium (DMEM Gibco #11995 containing 10% FBS, 1% penicillin/streptomycin, 5 ng/ml PMA and 1ng/ml ionomycin) or control medium (complete DMEM with vehicle). Conditioned medium was collected after 4 and 24 h and analyzed by IFNγ ELISA (BD Pharmingen).

Statistics. 2-way ANOVA or GLM procedures were used in conjunction with Tukey's 'Honestly Significant Difference' Test (SAS v9.1). Frequency data were transformed as $arcsin\sqrt{x}$ prior to statistical analysis. Significance was set at $P \leq 0.05$

RESULTS

Stromal Vascular Cell and Lymphocyte dynamics in eAT during the HFD Time course.

eAT was obtained for FACS analysis from mice fed either a LFD or HFD for 6, 8, 12, 16 or 22 weeks. By week 6, mice fed HFD were significantly heavier ($p < 0.01$; **Figure 1a**), had significantly heavier eAT ($p < 0.001$; **Figure 1b**), and were more insulin resistant ($p < 0.01$, **Figure 1c**) than mice fed the LFD. eAT weight declined between weeks 8 and 16 ($p < 0.01$) (Fig. 1B), reflecting increased adipocyte death during this period (133). eAT weight was partially re-established at week 22 (**Figure**

1b), reflecting new adipogenesis and reconstitution of the depot with small adipocytes (133). Overall, total SVCs per gram eAT were significantly greater in mice fed HFD as compared with LFD (p for diet < 0.001), although differences between diets at any one time point were statistically significant only at week 12 ($p = 0.03$) (**Figure 1d**).

T cells, T cell subsets and NK cells were identified and quantified by FACS using R1 gating and specific cell surface markers (see Supplementary Material, Figure S1). FACS analysis indicated that T (CD3+) cells comprise ~4-5% of the SVC fraction of eAT in mice fed the LFD (**Figure 2a**). As compared with mice fed LFD, the proportion of T cells in the SVC fraction was not significantly different in mice fed the HFD during the first 16 weeks of the time course ($p = 0.26$), although values for HFD-fed mice tended to be slightly (10%) greater through week 12 (**Figure 2a,b**). These results indicate that HFD-induced obesity was not associated with significant T cell enrichment in the SVC of eAT during the first 4 months of HFD feeding. However, because the number of SVCs per gram eAT is modestly elevated in mice fed HFD (**Figure 1d**) the number of T cells per gram eAT is consequently increased as well.

FACS analysis of T cell subsets indicated no significant HFD-associated change during the first 16 weeks of HFD in the proportion of CD3+ cells expressing either CD4 ($p = 0.26$, **Fig. 2b**), CD8 ($p = 0.75$, **Fig. 2c**) or NK1.1 ($p = 0.35$, data not shown). However, mice fed HFD had modestly (≤ 30%) greater SVC enrichment of CD4+ and CD8+ T cells and NK (CD3-/CD4+) cells at week 6, which were not observed by week 12 (**Figure 2b-d**). These results suggest that subtle increases in the

proportion of CD4+ and CD8+ T cells and NK cells may occur in eAT during the initial 8 weeks of HFD.

Significant increases in the proportion of T cells in the SVC fraction were observed at week 22 of HFD (**Fig. 2a,e**). At this time the percentage of CD3+ SVCs in eAT increased by 2-fold (to 11%) as compared with mice fed the LFD ($p = 0.02$) or as compared to mice fed the HFD for 6, 8, 12 or 16 weeks ($p < 0.01$) (**Figure 2a,e**). This increase reflected elevated (although nonsignificant) levels of CD4+ (**Figure 2b,e**), CD8+ (**Figure 2c,e**) cells and an additional T cell population presumably expressing the γδ T cell receptor (174) (**Figure 2e**). These results indicate that multiple T cell populations are enriched in eAT between weeks 16 and 22 of HFD.

FACS was next employed to quantify recruitment of CD11c+ ATMΦs to eAT using additional cohorts of mice fed either LFD or HFD for 8 and 12 weeks. By week 8, CD11c+ ATMΦs were enriched ~6-fold in the SVC fraction of mice fed HFD (8.7% ± 1.4% of ATMΦs, n = 6) as compared with mice fed LFD (1.3% ± 0.4% of ATMΦs, n = 6) ($p < 0.01$). By week 12 CD11c+ ATMΦs were enriched ~12-fold in eAT of mice fed HFD (13.9% ± 1.1% of ATMΦs, n = 10) as compared with mice fed LFD (1.1% ± 0.1% of ATMΦs, n = 6) ($p < 0.001$). These results indicate that, in contrast to T or NK cells, CD11c+ ATMΦs were significantly enriched in the SVC fraction of eAT by week 8 of HFD and continued to increase at least through week 12.

To confirm these observations obtained with mice fed HFD during the period of adipose tissue growth and maturation, we additionally assessed T cell and ATMΦ

recruitment to eAT of adult mice fed either the LFD or HFD for 5 weeks beginning at 14 weeks of age. Mice fed the HFD were heavier (40.03g ± 1.92g, n = 6) than mice fed the LFD (32.31g ± 0.97, n = 4) ($p = 0.02$) and were more insulin resistant (HOMA-IR: HFD = 5.82 ± 0.81 ng/ml; LFD = 2.10 ± 0.43 ng/ml, $p \leq 0.01$). Notably, 5 weeks of feeding the HFD resulted in no significant increase in CD3 mRNA (fold increase relative to LFD = 1.11 ± 0.15; $p = 0.60$). Similar results for CD3 gene expression were obtained when either cyclophilin A, GAPDH or 18s RNA were used as 'housekeeping' genes (data not shown). In contrast, CD11c mRNA levels were 5.98 ± 1.29-fold greater in mice fed HFD as compared with LFD ($p < 0.01$). These results confirm that CD11c+ ATMΦ recruitment and dysregulated glucose homeostasis occur in the absence of T cell enrichment in eAT.

Effect of HFD on Th1 and Th2 cytokines in eAT. We next investigated the effect of HFD on mRNA levels of Th1 and Th2 cytokines and other modulators of T cell-mediated inflammation using eAT from mice fed either the LFD or HFD for 4, 8, 12, 16 and 20 weeks (133). Maximal whole body IR and levels of CD11c+ and TNF-α mRNA were observed in these mice at week 16, and loss of eAT mass and subsequent regrowth were observed at weeks 16 and 20, respectively (133). Consistent with FACS data (**Figure 2a**) mRNA for the pan T cell marker CD3 was not elevated relative to levels in mice fed LFD through the first 16 weeks (**Figure 3a**). However, CD3 mRNA levels at week 20 were on average 5-6-fold greater in mice fed HFD ($p < 0.05$) (**Figure 3a**). Similarly, mRNA levels of IFNγ and the Th1 chemokine RANTES were not significantly elevated until week 20 of HFD ($p \leq 0.05$) although trends for increases were observed beginning at week 12 (**Figure 3b**). In

contrast to RANTES, gene expression of the CXC chemokines IFN-gamma-inducible protein 10 (IP-10) and monokine induced by IFN-gamma (Mig) declined significantly after week 4 (Supplementary Material, Figure 2Sa,b). These results in conjunction with FACS analysis (**Figure 2a,e**) implicate RANTES in the recruitment of Th1-polarized T cells to eAT at weeks 20-22 of HFD (184).

IL-18 and IL-12 are Th1 cytokines produced primarily by macrophages and dendritic cells that induce IFNγ production by T cells. IL-18 mRNA was elevated 1.5-fold at week 4 in eAT of mice fed HFD as compared with LFD-fed controls, but was subsequently down regulated ($p = 0.05$, Supplementary Material, Figure S2c). In contrast, mRNA for the p40 subunit of IL-12 (IL-12p40/p35) tended to be higher in mice fed HFD by week 6 (1.8-fold as compared with LFD) and increased at week 12 (6 fold, $p = 0.01$) and week 22 (15-fold, $p < 0.001$) (**Figure 3d**). Real-time PCR of ATMΦs sorted for both CD11c and the M2 marker MGL1 (132) indicate that 8 weeks of HFD feeding upregulated IL-12p40 gene expression 4-fold in resident (MGL1+CD11c-) ATMΦs and ~ 40-fold in recruited (MGL1-/CD11c+) ATMΦs (**Figure 3e**). Thus HFD-associated increase in IL-12p40 mRNA in eAT between weeks 6 and 12 reflect both ATMΦ recruitment and upregulated ATMΦ IL-12 p40 gene expression. Constitutive levels of mRNA coding for the IL-12p35 subunit were not significantly different between the two ATMΦ subtypes and did not change significantly in response to HFD (data not shown).

Coincident with the increase in IL-12p40 gene expression, gene expression of the canonical Th2 cytokine IL-4 was reduced ~4-fold between weeks 4 and 12 in eAT

of mice fed the HFD and remained attenuated through week 20 ($p = 0.02$) (**Figure 3f**). Similar (nonsignificant) reductions were also detected in IL-13 gene expression between weeks 8 and 12 of HFD (online Supplemental Material, Figure S2d). Overall, gene expression data for IL-12p40, IL-4 and IL-13 suggest the development of a more Th1-polarizing cytokine milieu in eAT between weeks 8 and 12 of HFD.

T cell priming in response to HFD. Elevated IFNγ synthesis in response to combined stimulation by PMA/ionophore provides an established measure of T cell priming by IL-12 and other Th1-polarizing stimuli (185, 186). To assess diet-associated differences in T cell priming eAT explants from mice fed LFD or HFD for 6, 12 and 20 weeks were challenged with a sub-maximal dose of PMA/ionophore for 4 and 24 h (**Figure 4**). In the absence of PMA/ionophore stimulation, IFNγ protein was undetectable in conditioned medium of eAT explants independent of diet (limit of detection = 5 pg/ml) (data not shown). Within 4 h of stimulation with PMA/ionophore, IFNγ mRNA levels in eAT explants increased up to 75-fold on average (data not shown) and explants from both LFD and HFD cohorts secreted measurable levels of IFNγ into the medium (**Figure 4**). Notably, levels of IFNγ produced by eAT of mice fed HFD were 2-fold greater after 6 weeks of HFD (trend, $p = 0.08$) and 5-fold greater after 12 weeks of HFD ($p < 0.001$) than levels secreted by explants from mice fed LFD (**Figure 4**). These observations suggest that there are more T cells primed for INF production per gram eAT in mice fed HFD as compared with mice fed LFD. This difference may reflect both a higher proportion of primed T cells in the SVC, as well as a higher proportion of SVCs per gram eAT in mice fed HFD **(Figure 1d**). Evidence for enhanced T cell priming in response to

HFD is consistent with gene expression data (**Figure 3d and Figure 4**) suggesting elevated IL-12 protein levels in eAT of mice fed HFD (**Figure 3d**).

DISCUSSION

Activation of innate immunity in AT is now recognized as a contributing factor in the development of obesity, obesity-associated inflammation and IR (129, 164-166, 187). Less is known concerning the role of adaptive immunity in these events. Recent reports (177, 179) have promoted the view that T cell recruitment and the actions of IFNγ in eAT are important to the development of AT inflammation and IR during diet-induced obesity. In contrast, other studies have questioned the importance of Th1 cytokines to the development of IR (181) and have suggested that the presence of T cells in AT in fact constrains AT expansion and ATMΦ accumulation induced by a HFD (182). In an effort to address this controversy the present study quantified T cells and Th1/Th2 cytokine mRNA expression in eAT of mice during 20-22 weeks of HFD-induced obesity. Our objective was to document the temporal pattern and magnitude of T cell responses during hallmark events in this model (133), in particular eAT expansion, CD11c+ ATMΦ infiltration and the onset of IR.

A key result of our study is that neither T cell recruitment (i.e., enrichment in the SVC) nor significant up-regulated IFNγ and RANTES gene expression were observed until 20 weeks of HFD- i.e., months after increases in eAT mass (**Figure 1b**), CD11c+ ATMΦ recruitment and onset of IR (**Figure 1c**), and one month after maximal IR is observed in this model (133). These results were confirmed by a 5 week HFD time course in adult mice, in which significant increases in CD11c+ gene

expression in eAT and IR were observed in mice fed the HFD in the absence of increased CD3 gene expression. Therefore, while our data support prior reports of T cell recruitment and up regulated RANTES gene expression in obese mice and humans (176-179), the timing of these increases in the present study calls into question the extent to which they contribute to the onset of AT inflammation and IR. In particular the present study fails to support the observation (179) of robust (3-fold) increases in CD3 mRNA in eAT after 5 weeks of feeding a 60% HFD or the conclusion based in large part on this observation that T cell recruitment is a primary event that precedes ATMΦ recruitment, AT inflammation and IR in response to HFD. Similarly, despite an overall attenuation of Th1 chemokine gene expression after week 6 (online supplemental material, Figure S2) our FACS data do not support the view (182).that total T cells in eAT are selectively 'depleted' from AT after the initial stages of HFD (6 weeks in the present study) in order to facilitate increases in ATMΦ

Although we found no evidence of enhanced T cell recruitment until weeks 20-22 of HFD, the number of SVCs (and thus T cells) per gram eAT increased ~40% in response to HFD as early as week 6 (**Figure 1d)**. We cannot rule out that this modest 'non-selective' increase in the density of T cells in eAT, contributes to early inflammatory and metabolic pathology in our model. Supporting this concept are our observations of IL-12p40 and IL-18 gene expression in eAT. These cytokines, in combination with antigen(s) or synergistically in an antigen-independent manner (188) promote CD4+ T cell differentiation along the Th1 pathway and induce IFNγ production (185). CD4+T cells 'primed' by IL-12 up regulate IFNγ synthesis independent of IL-12

stimulation upon re-encounter with antigen (189) or in response to exogenous stimulation with PMA and ionophore (186). Our data (**Figure 4**) suggest that T cells in eAT of mice fed the HFD are primed for IFNγ production in response to PMA/ionophore stimulation by week 6 of HFD. Moreover, the magnitude of IFNγ release increased between weeks 6 and 12, (**Figure 3d**) coincident with recruitment of CD11c+ ATMΦ robustly expressing IL-12p40 mRNA (**Figure 3e**). These M1-polarized ATMΦ localize to crown-like structures surrounding dead adipocytes (132, 133, 167), and it is therefore likely that T cells proximal to such structures will be preferentially primed by IL-12. Intriguingly, increases in IL-12p40 mRNA and Th1 priming are coincident with the reported progression of AT inflammation and IR in this model (133), suggesting a potential mechanistic association between lymphocyte activation and AT inflammation and IR. Overall, our results strongly suggest a biphasic adaptive immune response in eAT in which the first phase performs a priming function and the second stage (post week 16) is more grossly proinflammatory.

Despite this evidence for Th-1 priming, levels of IFNγ mRNA or protein were not significantly elevated during the first 16 weeks of HFD in the absence of exogenous stimulation (PMA/ionophore). This suggests either the absence of relevant antigenic re-stimulation and/or the inhibition of Th1 effector cell maturation and IFNγ production (185). A potential mediator of such inhibition is IL-10, an inflammation-suppressive cytokine that constrainsTh1 responses in lymphocytes (190). IL-10 mRNA levels increase in eAT during the HFD time course, becoming maximally (15-fold) elevated at week 16 (133). These increases are due at least in part to up-regulated IL-10 gene expression by M2-polarized resident (MGL1+ / CD11c-) ATMΦs in response to HFD

(our unpublished data). Importantly, IL-10 gene expression in eAT is subsequently down regulated by ~50% at week 20 of HFD (133), presumably reflecting the progression of the ATMΦ 'phenotype switch' from M2 to M1 polarization (132). This down regulation of IL-10 gene expression in combination with attenuation of IL-4 and IL-13 gene expression in eAT (**Figure 3f** and Supplementary Material, Figure S2d) coincides with T cell enrichment and up regulated expression of IFNγ and RANTES at weeks 20-22 (**Figure 3b, c**).

These observations suggest a shift in the cytokine/chemokine environment of eAT from one favoring Th2 responses toward one favoring Th1 responses, including IFNγ production. Additional factors may also promote the T cell enrichment and Th-1 cytokine/chemokine expression observed in eAT after week 16. One intriguing possibility is reductions or loss of the inhibitory actions of regulatory T cells (Tregs), which maintain immune homeostasis by secreting IL-10 and TGF-β (191). Whether this loss occurs and whether it is coincident with differentiation of proinflammatory Th17 cells (191) is currently unknown. Other factors that could promote Th1 responses in eAT include HFD-associated systemic endotoxemia (145) as well as endogenous signals released from dying adipocytes and surrounding matrix (damage-associated molecular patterns [DAMPS]) that can act as immune adjuvants and favor Th1 polarization (reviewed in (192)).

In conclusion, the development of obesity and the onset of obesity-associated AT inflammation and IR occurred in the absence of T cell enrichment or significant increases in IFNγ or RANTES gene expression in eAT. The absence of robust Th1

responses during the initial 16 weeks of HFD in the present study are consistent with the depot-wide tissue remodeling observed during this period (133). Tissue remodeling is integral to AT expansion and thus to energy metabolism homeostasis (133, 193, 194). It is therefore not unexpected that the cytokine/chemokine milieu of AT would favor repair and tolerance over inflammation and immunogenicity during the development of obesity. However, given that T cell priming for INFγ production was detected relatively early in the obesity-time course, it is reasonable to expect that Th1-polarized T cells present in eAT (and perhaps intra-abdominal fat in general) contribute to the progression of obesity-associated inflammation and IR. The challenge before us is to determine the pathophysiologic impact(s) of T cell-mediated inflammatory responses in AT of chronically obese mice and humans.

Supplement Summary

Primer sequences used for real time quantitative PCR are included within Table 1. Figure S1 specifies the gating procedures used for FACS analyses. Figure S2 presents quantitative PCR results consistent with generalized down-regulation of Th1-associated genes after 4 to 8 weeks of high fat diet.

ACKNOWLEDGEMENTS

This work was supported by NIH grants 1 RO1 DK074979-01A1 (M.S.O.) and 5P30DK46200-14 (Boston Obesity and Nutrition Research Center), American Diabetes Association Research Award 1-06-RA-96 (M.S.O) and USDA-ARS contract 58-1950-7-707. We thank the animal facility personnel for their expert assistance with animal

husbandry. We would also like to thank our colleagues, in particular Gerald Denis, for their valuable comments on the manuscript.

DISCLOSURES

none

FIGURE LEGENDS

Figure 1. Weight, adiposity, stromal vascular cells and HOMA-IR in mice fed HFD or LFD for up to 22 weeks starting at 6 weeks of age. (**a**) body weight (**b**) epididymal adipose tissue (eAT) weight (n = 5-12 mice for wk 6, 8 and 12; n = 4-7 for wk 16; n=3 for wk 22). (**c**) HOMA-IR determined at week 6 (n = 4-5). (**d**) number of stromal vascular cells per gram eAT (n = 4-8, for wk 6, 8, 12 and 16; n = 3 for wk 22). *, $P \leq 0.05$ for comparison between diets at the indicated time point. #, significantly different from HFD wk 8 ($P \leq 0.05$). Bars designated by different letters are significantly different ($P \leq 0.05$).

Figure 2. T cells, T cell subsets and NK cells in eAT of mice fed HFD or LFD. Stromal vascular cell fractions of eAT were isolated and analyzed by FACS. (**a**) numbers of CD3+ cells, (**b**) CD4+ cells, (**c**) CD8+ cells and (**d**) NK (CD3-NK1.1+) cells within the lymphocyte gate per 10,000 total cells (n = 4-12 for 6 to 16 wks; n = 3 for 22 wks) (**e**) representative FACS histograms showing SVC enrichment for CD3+CD4+ and CD3+CD8+ cells at 22 weeks of HFD as compared with LFD . *, $P \leq 0.05$ for comparison between diets at the indicated time point; $^{\#}$, $P \leq 0.01$ for effect of HFD over the time course.

Figure 3. T cell (CD3+) and Th1/2-associated gene expression in eAT during 20 weeks of HFD or LFD. Shown are mRNA levels of (**a**) CD3 (**b**) IFNγ, (**c**) RANTES, (**d**) IL-12p40, and (**f**) IL-4 in eAT of HFD-fed mice relative to LFD controls. (**e**) mRNA levels of IL-12p40 in resident (MGL1+/CD11c-) ATMΦs and recruited (MGL1-/CD11c+) ATMΦs from mice fed HFD for 8 weeks. Data are expressed as fold-difference relative to LFD controls (designated as "1" and indicated by the horizontal line) (n = 4-6 at each time point) *, $P \leq 0.05$ for comparison between diets at the indicated time point; $^{\#}$, $P \leq 0.01$ for effect of HFD over the time course.

Figure 4. Effects of HFD on T cell priming for IFNγ production. Whole eAT explant cultures from mice fed LFD or HFD for 6, 12 or 22 weeks were stimulated with a submaximal dose of PMA/ionophore for 24 hours. IFNγ secreted into the medium was quantified by ELISA (n= 2-3 for LFD and 3-4 for HFD). *, $P \leq 0.05$ for comparison between diets at the indicated time point. Bars designated by different letters are significantly different ($P \leq 0.05$).

Table 1. Primer sequences used for real time PCR (3' to 5')

Gene target	**Forward**	**Reverse**
Cyclophilin A	GTGGTCTTTGGGAAGGTGAA	TTACAGGACATTGCGAGCAG
Cd11c	CTGGATAGCCTTTCTTCTGCTG	GCACACTGTGTCCGAACTC
IL-12p40	GGAGACACCAGCAAAACGAT	GATTCAGACTCCAGGGGACA
IFN-□	TCTGGAGGAACTGGCAAAAG	TTCAAGACTTCAAAGAGTCTGA

		GG
IL-4	TCAACCCCCAGCTAGTTGTC	TGTTCTTCGTTGCTGTGAGG
IL-18	CAGTGAACCCCAGACCAGAC	GGCAAGCAAGAAAGTGTCCT
IL-13	CCAGGTCCACACTCCATACC	TGCCAAGATCTGTGTCTCTCC
RANTES	CAGGAGCAAGTGCTCCAATCTT	TTCTTGAACCCACTTCTTCTCTGG
CD3	AGGCACTGTAGCCCAGACAAATA	AGCCACTTGATAGTCTTGTCAGTCA
IP-10/CXCL10	GCTGCCGTCATTTTCTGC	TCTCACTGGCCCGTCATC
MIG/CXCL9	CTTTTCCTTTTGGGCATCAT	CGATCGTGCATTCCTTATCA
I-A	GTGGTGCTGATGGTGCTG	CCATGAACTGGTACACGAAATG

Supplement Figure Legends.

Figure S1. Gating procedures used for FACS analyses. (**a**) Ungated and uncompensated plots showing forward and side scatter properties and (**b**) positive CD3-staining were used to define the lymphocyte (R1) gate for each SVC sample. For each experiment, matched isotype-conjugated controls were used to define non-specific background fluorescence events, which were excluded (not shown). (**c**) Colored gating [red for anti-CD4-PE(FL2), and blue for anti-CD8-PECy5(FL3)] indicates the positive events counted within the SVC population of the lymphocyte gate for cell surface markers of interest.

Dot plots showing how single fluorescence channels were used to quantify positive events of double-and triple-stained samples. (**d**) CD4, (**e**) CD8, and (**f**) CD3-positive events.

Figure S2. Temporal dynamics of mRNA levels of Th1-associated genes and IL-13 in whole eAT through 20 weeks of high fat diet (HFD). (**a**) IP-10, (**b**) Mig, (**c**) IL-18, and (**d**) IL-13. Data are expressed as fold change (mean ± sem) relative to low fat diet (LFD). Bars identified by different letters are significantly different ($P \leq 0.05$). $^{\#}$, $P \leq 0.05$ for effect of time; *, $P \leq 0.05$ for comparison between diets at the indicated time point.

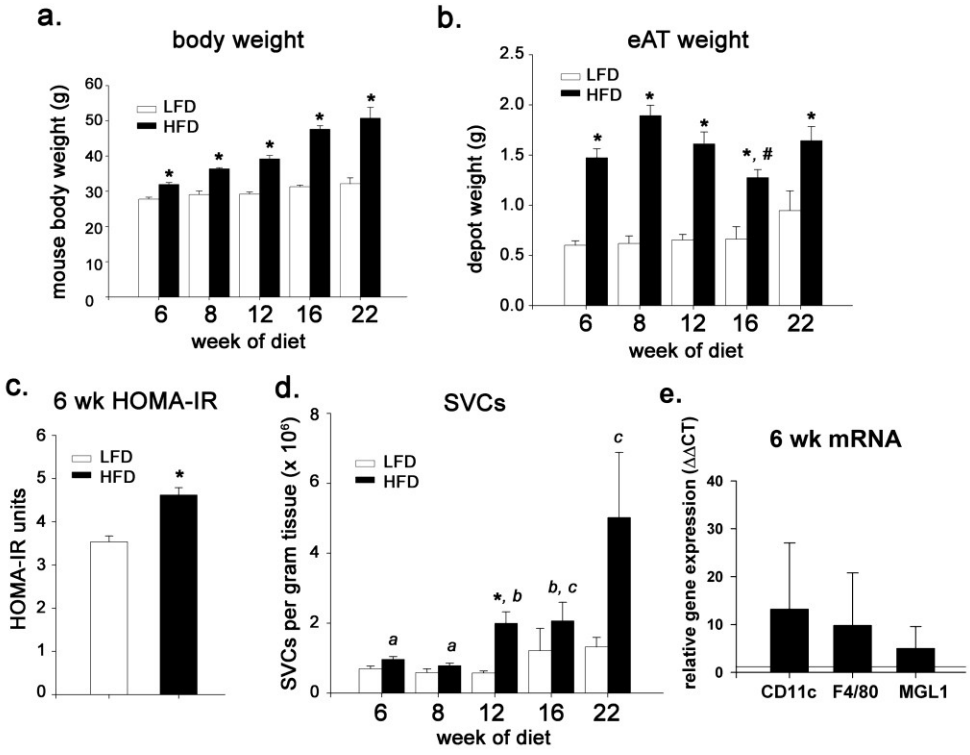

Figure 1.

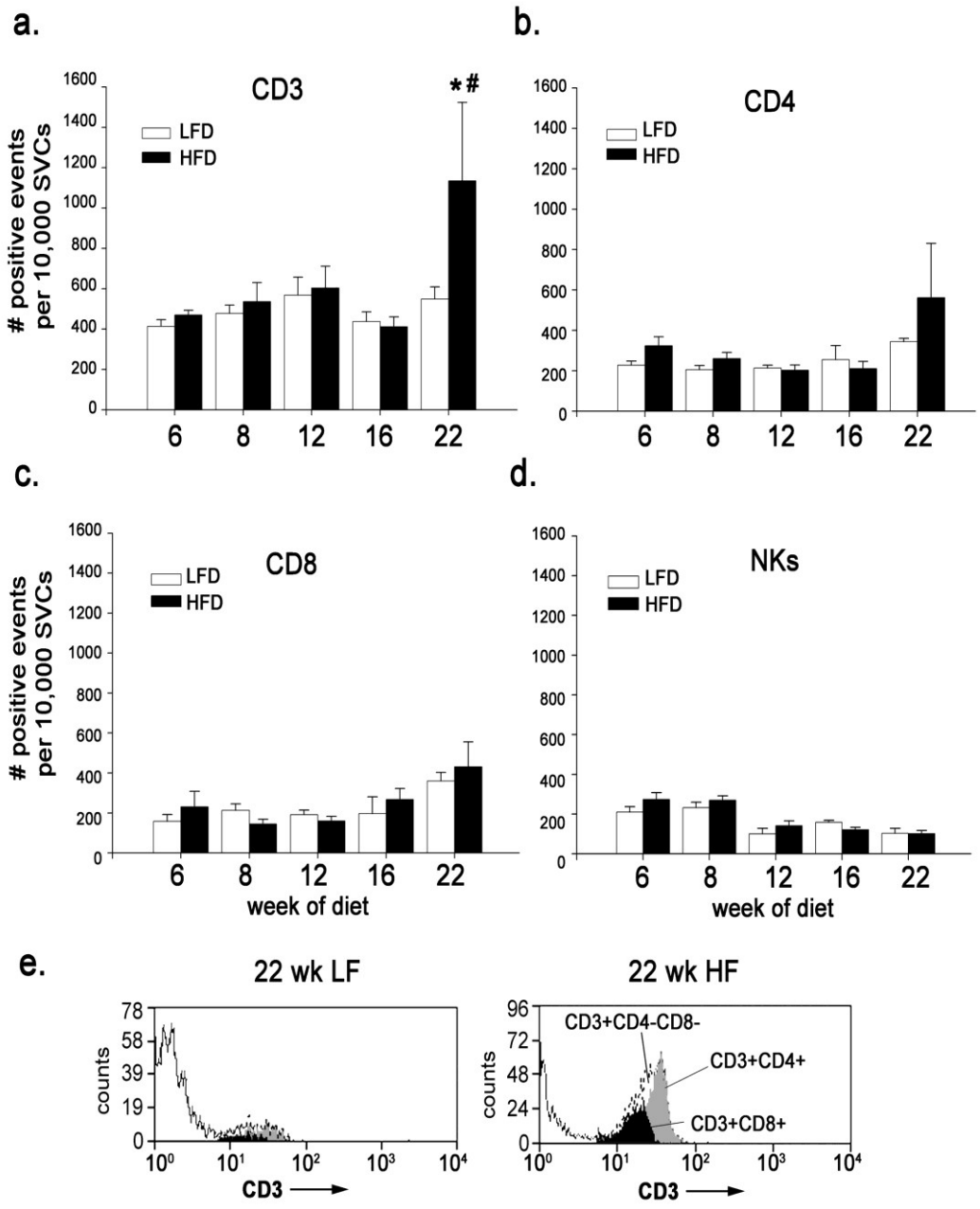
a.
CD3
*#
LFD
HFD
positive events per 10,000 SVCs
b.
CD4
c.
CD8
d.
NKs
week of diet
e.
22 wk LF
22 wk HF
counts
CD3+CD4-CD8-
CD3+CD4+
CD3+CD8+
CD3

Figure 2

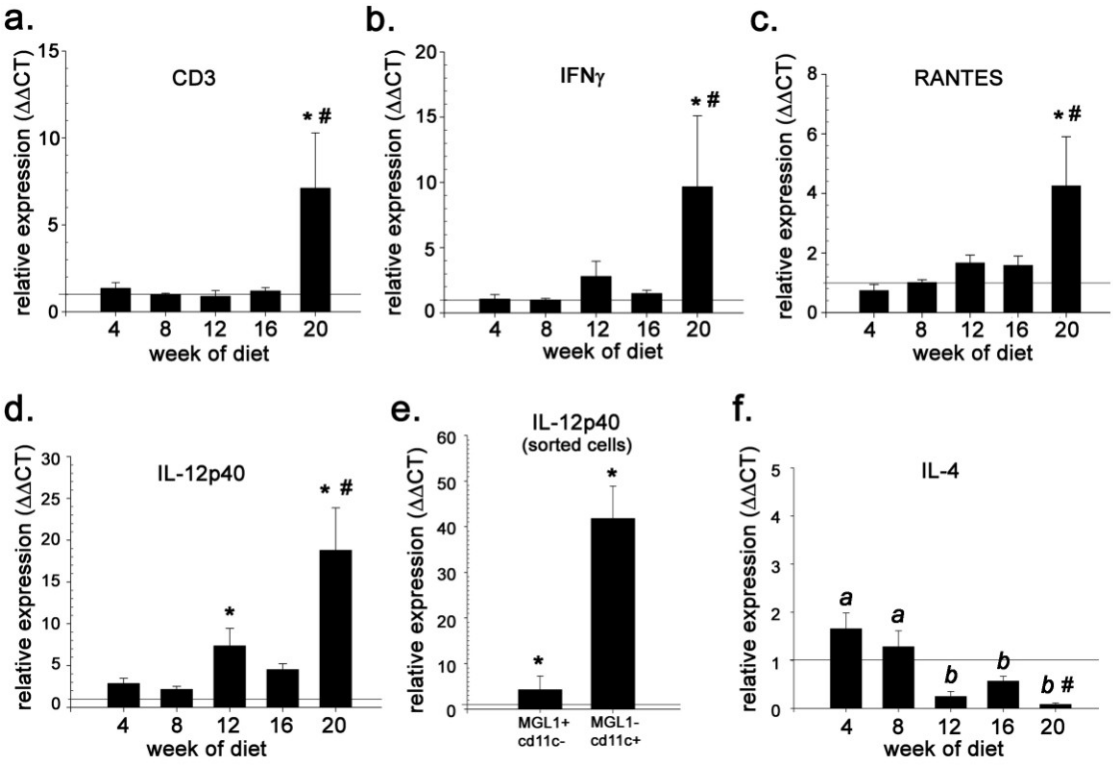
a.
CD3
relative expression (ΔΔCT)
week of diet
b.
IFNγ
relative expression (ΔΔCT)
week of diet
c.
RANTES
relative expression (ΔΔCT)
week of diet
d.
IL-12p40
relative expression (ΔΔCT)
week of diet
e.
IL-12p40
(sorted cells)
relative expression (ΔΔCT)
MGL1+ cd11c-
MGL1- cd11c+
f.
IL-4
relative expression (ΔΔCT)
week of diet

Figure 3

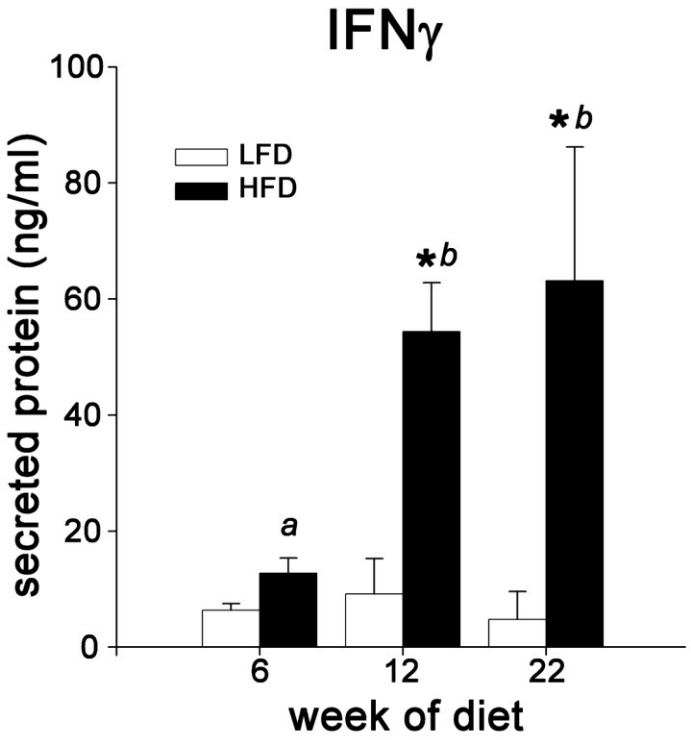
IFNγ
100
80
60
40
20
0
secreted protein (ng/ml)
LFD
HFD
a
*b
*b
6
12
22
week of diet

Figure 4

BIBLIOGRAPHY

1. **Marshall S** 2006 Role of insulin, adipocyte hormones, and nutrient-sensing pathways in regulating fuel metabolism and energy homeostasis: a nutritional perspective of diabetes, obesity, and cancer. Sci STKE 2006:re7
2. **Thorens B** 2008 Glucose sensing and the pathogenesis of obesity and type 2 diabetes. Int J Obes (Lond) 32 Suppl 6:S62-71
3. **Greenberg AS, Egan JJ, Wek SA, Garty NB, Blanchette-Mackie EJ, Londos C** 1991 Perilipin, a major hormonally regulated adipocyte-specific phosphoprotein associated with the periphery of lipid storage droplets. J Biol Chem 266:11341-11346
4. **Zhang H, Souza S, Muliro K, Kraemer F, Obin M, Greenberg AS** 2003 Lipase-selective functional domains of perililpin A differentially regulate constitutive and protein kinase A-stimulated lipolysis. J Biol Chem 278(51):51535-42. Epub 2003 Oct 2.
5. **Nonogaki K** 2000 New insights into sympathetic regulation of glucose and fat metabolism. Diabetologia 43:533-549
6. **Ahmadian M, Wang Y, Sul H-S** 2009 Lipolysis in adipocytes. The International Journal of Biochemistry and Cell Biology In press
7. **Wang S, Soni KG, Semache M, Casavant S, Fortier M, Pan L, Mitchell GA** 2008 Lipolysis and the integrated physiology of lipid energy metabolism. Mol Genet Metab 95:117-126
8. **Nye C, Kim J, Kalhan SC, Hanson RW** 2008 Reassessing triglyceride synthesis in adipose tissue. Trends Endocrinol Metab 19:356-361
9. **Narasimhan SD, Yen K, Tissenbaum HA** 2009 Converging pathways in lifespan regulation. Curr Biol 19:R657-666
10. **Hietakangas V, Cohen SM** 2009 Regulation of tissue growth through nutrient sensing. Annu Rev Genet 43:389-410
11. **Madsen L, Kristiansen K** The importance of dietary modulation of cAMP and insulin signaling in adipose tissue and the development of obesity. Ann N Y Acad Sci 1190:1-14
12. **Burgering BM, Coffer PJ** 1995 Protein kinase B (c-Akt) in phosphatidylinositol-3-OH kinase signal transduction. Nature 376:599-602
13. **Gredinger E, Gerbe A, Tamir Y, Tapscott S, Bengal E** 1998 Mitogen-activated protein kinase pathway is involved in the differentiation of muscle cells. J Biol Chem 273:10436-10444
14. **Summers SA, Whiteman EL, Birnbaum MJ** 2000 Insulin signaling in the adipocyte. Int J Obes Relat Metab Disord 24 Suppl 4:S67-70
15. **Greenberg AS, Coleman RA, Kraemer FB, McManaman JL, Obin MS, Puri V, Yan QW, Miyoshi H, Mashek DG** The role of lipid droplets in metabolic disease in rodents and humans. J Clin Invest 121:2102-2110

16. **Markan KR, Jurczak MJ, Brady MJ** Stranger in a strange land: roles of glycogen turnover in adipose tissue metabolism. Mol Cell Endocrinol 318:54-60
17. **Anthony F, Acar J, Franklin A, Gupta R, Nicholls T, Tamura Y, Thompson S, Threlfall EJ, Vose D, van Vuuren M, White DG** 2001 Antimicrobial resistance: responsible and prudent use of antimicrobial agents in veterinary medicine. Rev Sci Tech 20:829-839
18. **Furuhashi M, Hotamisligil GS** 2008 Fatty acid-binding proteins: role in metabolic diseases and potential as drug targets. Nat Rev Drug Discov 7:489-503
19. **Sano H, Hsu D, Apgar J, Yu L, Sharma B, Kuwabara I, Izui S, Liu F-T** 2003 Critical role of galectin-3 in phagocytosis by macrophages. j Clin Invest 112:389-397
20. **Hashiramoto M, James DE** 2000 Characterization of insulin-responsive GLUT4 storage vesicles isolated from 3T3-L1 adipocytes. Mol Cell Biol 20:416-427
21. **Karylowski O, Zeigerer A, Cohen A, McGraw TE** 2004 GLUT4 is retained by an intracellular cycle of vesicle formation and fusion with endosomes. Mol Biol Cell 15:870-882
22. **Waters SB, D'Auria M, Martin SS, Nguyen C, Kozma LM, Luskey KL** 1997 The amino terminus of insulin-responsive aminopeptidase causes Glut4 translocation in 3T3-L1 adipocytes. J Biol Chem 272:23323-23327
23. **Tozzo E, Shepherd PR, Gnudi L, Kahn BB** 1995 Transgenic GLUT-4 overexpression in fat enhances glucose metabolism: preferential effect on fatty acid synthesis. Am J Physiol 268:E956-964
24. **Shepherd PR, Gnudi L, Tozzo E, Yang H, Leach F, Kahn BB** 1993 Adipose cell hyperplasia and enhanced glucose disposal in transgenic mice overexpressing Glut 4 selectively in adipose tissue. J Biol Chem 268:22243-22246
25. **Arner P** 1996 Regulation of Adipocyte Lipolysis. Diabetes Reviews 4:450-463
26. **Achyuthan KE, Slaughter TF, Santiago MA, Enghild JJ, Greenberg CS** 1993 Factor XIIIa-derived peptides inhibit transglutaminase activity. Localization of substrate recognition sites. J Biol Chem 268:21284-21292
27. **Zechner R, Strauss J, Haemmerle G, Lass A, Zimmermann R** 2005 Lipolysis: pathway under construction.
. Current Opinion in Lipidology 16:333-340
28. **Zimmermann R, Strauss JG, Haemmerle G, Schoiswohl G, Birner-Gruenberger R, Riederer M, Lass A, Neuberger G, Eisenhaber F, Hermetter A, Zechner R** 2004 Fat mobilization in adipose tissue is promoted by adipose triglyceride lipase. Science 306:1383-1386
29. **Zimmerman R, Lass A, Haemmerle G, Riederer M, Schoiswohl G, Schweiger M, Strauss J, Gorkiewicz G, Zechner R** 2006 Triglyceride accumulation in Chanarin-Dorfman Syndrome is caused by defective activation of adipose triglyceride lipase by CGI-58. In: Keystone Symposia: Adipogenesis, Obesity and Inflammation. Vancouver, BC
30. **Tzivion G, Dobson M, Ramakrishnan G** FoxO transcription factors; Regulation by AKT and 14-3-3 proteins. Biochim Biophys Acta

31. **Chakrabarti P, Kandror KV** 2009 FoxO1 controls insulin-dependent adipose triglyceride lipase (ATGL) expression and lipolysis in adipocytes. J Biol Chem 284:13296-13300
32. **Carey AL, Lamont B, Andrikopoulos S, Koukoulas I, Proietto J, Febbraio MA** 2003 Interleukin-6 gene expression is increased in insulin-resistant rat skeletal muscle following insulin stimulation. Biochem Biophys Res Commun 302:837-840
33. **Deng C, Capecchi MR** 1992 Rexamination of gene targeting frequency as a function of the extent of homology between the targeting vector and the target locus. Mol Cell Biol 12:3365-3371
34. **Maury E, Brichard SM** Adipokine dysregulation, adipose tissue inflammation and metabolic syndrome. Mol Cell Endocrinol 314:1-16
35. **Ouchi N, Parker JL, Lugus JJ, Walsh K** Adipokines in inflammation and metabolic disease. Nat Rev Immunol 11:85-97
36. **Szendroedi J, Roden M** 2009 Ectopic lipids and organ function. Curr Opin Lipidol 20:50-56
37. **Atshaves B, Storey S, McIntosh A, Petrescu A, Lyuksyutova O, Greenberg A, Schroeder F** 2001 Sterol carrier protein-2 expression modulates protein and lipid composition. J Biol Chem 276(27):25324-25335
38. **Fruebis J, Tsao TS, Javorschi S, Ebbets-Reed D, Erickson MR, Yen FT, Bihain BE, Lodish HF** 2001 Proteolytic cleavage product of 30-kDa adipocyte complement-related protein increases fatty acid oxidation in muscle and causes weight loss in mice. Proc Natl Acad Sci U S A 98:2005-2010
39. **Maeda N, Shimomura I, Kishida K, Nishizawa H, Matsuda M, Nagaretani H, Furuyama N, Kondo H, Takashia M, Arita Y, Komuro R, N O, Kihara S, Tochino Y, Okutomi K, Horie M, Takeda S, Aoyama T, Funahashi T, Matsuzawa Y** 2002 Diet-induced insulin resistance in mice lacking adiponectin/acrp 30. Nature Medicine 8:731-737
40. **Yamauchi T, Kamon J, Minokoshi Y, Ito Y, Waki H, Uchida S, Yamashita S, Noda M, Kita S, Ueki K, Eto K, Akanuma Y, Froguel P, Foufelle F, Ferre P, Carling D, Kimura S, Nagai R, Kahn BB, Kadowaki T** 2002 Adiponectin stimulates glucose utilization and fatty-acid oxidation by activating AMP-activated protein kinase. Nat Med 8:1288-1295
41. **Yamauchi T, Kamon J, Waki H, Terauchi Y, Kubota N, Hara K, Mori Y, Ide T, Murakami K, Tsuboyama-Kasaoka N, Ezaki O, Akanuma Y, Gavrilova O, Vinson C, Reitman M, Kagechika H, Shudo K, Yoda M, Nakano Y, Tobe K, Nagai R, Kimura S, Tomita M, Froguel P, Kadowaki T** 2001 The fat-derived hormone adiponectin reverses insulin resistance associated with lipoatrophy and obesity. Nature Medicine 7:941-=946
42. **Herrero L, Shapiro H, Nayer A, Lee J, Shoelson SE** Inflammation and adipose tissue macrophages in lipodystrophic mice. Proc Natl Acad Sci U S A 107:240-245
43. **Doerrler W, Feingold KR, Grunfeld C** 1994 Cytokines induce catabolic effects in cultured adipocytes by multiple mechanisms. Cytokine 6:478-484

44. **Feingold KR, Doerrler W, Dinarello CA, Fiers W, Grunfeld C** 1992 Stimulation of lipolysis in cultured fat cells by tumor necrosis factor, interleukin-1, and the interferons is blocked by inhibition of prostaglandin synthesis. Endocrinology 130:10-16
45. **Feingold KR, Grunfeld C** 1992 Role of cytokines in inducing hyperlipidemia. Diabetes 41 Suppl 2:97-101
46. **Grunfeld C, Feingold K** 1991 The metabolic effects of tumor necrosis factor and other cytokines. Biotherapy 3:143-158
47. **Grunfeld C, Feingold K** 1992 Tumor necrosis factor, interleukin, and interferon induced changes in lipid metabolism as part of host defense. Proc Soc Exp Biol Med 200:224-227
48. **Baron A, Brechtel G, Wallace P, Edelman S** 1988 Rates and tissue sites of non-insulin and insulin mediated glucose uptake in man. Am J Physiol 255:E769-774
49. **Donath MY, Shoelson SE** Type 2 diabetes as an inflammatory disease. Nat Rev Immunol 11:98-107
50. **Hardie DG** Sensing of energy and nutrients by AMP-activated protein kinase. Am J Clin Nutr 93:891S-896
51. **Hawley SA, Davison M, Woods A, Davies SP, Beri RK, Carling D, Hardie DG** 1996 Characterization of the AMP-activated protein kinase kinase from rat liver and identification of threonine 172 as the major site at which it phosphorylates AMP-activated protein kinase. J Biol Chem 271:27879-27887
52. **Pyper SR, Viswakarma N, Yu S, Reddy JK** PPARalpha: energy combustion, hypolipidemia, inflammation and cancer. Nucl Recept Signal 8:e002
53. **Baar K** 2004 Involvement of PPAR gamma co-activator-1, nuclear respiratory factors 1 and 2, and PPAR alpha in the adaptive response to endurance exercise. Proc Nutr Soc 63:269-273
54. **Park H, Kaushik VK, Constant S, Prentki M, Przybytkowski E, Ruderman NB, Saha AK** 2002 Coordinate regulation of malonyl-CoA decarboxylase, sn-glycerol-3-phosphate acyltransferase, and acetyl-CoA carboxylase by AMP-activated protein kinase in rat tissues in response to exercise. J Biol Chem 277:32571-32577
55. **McGarry JD** 2001 Travels with carnitine palmitoyltransferase I: from liver to germ cell with stops in between. Biochem Soc Trans 29:241-245
56. **Cheng Z, White MF** Targeting Forkhead box O1 from the concept to metabolic diseases: lessons from mouse models. Antioxid Redox Signal 14:649-661
57. **Chen XZ, Jiang K, Hu JK, Zhang B, Gou HF, Yang K, Chen ZX, Chen JP** 2008 Cost-effectiveness analysis of chemotherapy for advanced gastric cancer in China. World J Gastroenterol 14:2715-2722
58. **Furuyama T, Kitayama K, Yamashita H, Mori N** 2003 Forkhead transcription factor FOXO1 (FKHR)-dependent induction of PDK4 gene expression in skeletal muscle during energy deprivation. Biochem J 375:365-371
59. **Piva R, Belardo G, Santoro MG** 2006 NF-kappaB: a stress-regulated switch for cell survival. Antioxid Redox Signal 8:478-486
60. **Solt LA, May MJ** 2008 The IkappaB kinase complex: master regulator of NF-kappaB signaling. Immunol Res 42:3-18

61. **Arkan MC, Hevener AL, Greten FR, Maeda S, Li ZW, Long JM, Wynshaw-Boris A, Poli G, Olefsky J, Karin M** 2005 IKK-beta links inflammation to obesity-induced insulin resistance. Nat Med 11:191-198
62. **Bashan N, Dorfman K, Tarnovscki T, Harman-Boehm I, Liberty IF, Bluher M, Ovadia S, Maymon-Zilberstein T, Potashnik R, Stumvoll M, Avinoach E, Rudich A** 2007 MAP kinases, IKK and insulin signaling in human omental versus subcutaneous adipose tissue in obesity. Endocrinology 148:2955-2962
63. **Chiang SH, Bazuine M, Lumeng CN, Geletka LM, Mowers J, White NM, Ma JT, Zhou J, Qi N, Westcott D, Delproposto JB, Blackwell TS, Yull FE, Saltiel AR** 2009 The protein kinase IKKepsilon regulates energy balance in obese mice. Cell 138:961-975
64. **Scheja L, Heese**
B, Seedorf K Beneficial effects of IKKepsilon-deficiency on body weight and insulin sensitivity are lost in high fat diet-induced obesity in mice. Biochem Biophys Res Commun 407:288-294
65. **Yuan M, Konstantopoulos N, Lee J, Hansen L, Li Z, Karin M, Shoelson S** 2001 Reversal of obesity- and diet-induced insulin resistance with salicylates or targeted discruption of Ikk-beta. Science 293:1673-1877
66. **Newsholme P, Gaudel C, McClenaghan NH** Nutrient regulation of insulin secretion and beta-cell functional integrity. Adv Exp Med Biol 654:91-114
67. **Straub SG, Sharp GW** 2002 Glucose-stimulated signaling pathways in biphasic insulin secretion. Diabetes Metab Res Rev 18:451-463
68. **Norlin S, Ahlgren U, Edlund H** 2005 Nuclear factor-{kappa}B activity in {beta}-cells is required for glucose-stimulated insulin secretion. Diabetes 54:125-132
69. **Bedford L, Lowe J, Dick LR, Mayer RJ, Brownell JE** Ubiquitin-like protein conjugation and the ubiquitin-proteasome system as drug targets. Nat Rev Drug Discov 10:29-46
70. **Hochstrasser M** 2009 Origin and function of ubiquitin-like proteins. Nature 458:422-429
71. **Rome S, Meugnier E, Vidal H** 2004 The ubiquitin-proteasome pathway is a new partner for the control of insulin signaling. Curr Opin Clin Nutr Metab Care 7:249-254
72. **Ahmed Z, Smith BJ, Pillay TS** 2000 The APS adapter protein couples the insulin receptor to the phosphorylation of c-Cbl and facilitates ligand-stimulated ubiquitination of the insulin receptor. FEBS Lett 475:31-34
73. **Kamura T, Sato S, Haque D, Liu L, Kaelin WG, Jr., Conaway RC, Conaway JW** 1998 The Elongin BC complex interacts with the conserved SOCS-box motif present in members of the SOCS, ras, WD-40 repeat, and ankyrin repeat families. Genes Dev 12:3872-3881
74. **Rui L, Yuan M, Frantz D, Shoelson S, White MF** 2002 SOCS-1 and SOCS-3 block insulin signaling by ubiquitin-mediated degradation of IRS1 and IRS2. J Biol Chem 277:42394-42398

75. **Matsuzaki H, Daitoku H, Hatta M, Tanaka K, Fukamizu A** 2003 Insulin-induced phosphorylation of FKHR (Foxo1) targets to proteasomal degradation. Proc Natl Acad Sci U S A 100:11285-11290
76. **Liu LB, Omata W, Kojima I, Shibata H** 2007 The SUMO conjugating enzyme Ubc9 is a regulator of GLUT4 turnover and targeting to the insulin-responsive storage compartment in 3T3-L1 adipocytes. Diabetes 56:1977-1985
77. **Dai XQ, Plummer G, Casimir M, Kang Y, Hajmrle C, Gaisano HY, Manning Fox JE, MacDonald PE** SUMOylation regulates insulin exocytosis downstream of secretory granule docking in rodents and humans. Diabetes 60:838-847
78. **Liu S, Chen ZJ** Expanding role of ubiquitination in NF-kappaB signaling. Cell Res 21:6-21
79. **Fan W, Cai W, Parimoo S, Schwarz DC, Lennon GG, Weissman SM** 1996 Identification of seven new human MHC class I region genes around the HLA-F locus. Immunogenetics 44:97-103
80. **Canaan A, Yu X, Booth CJ, Lian J, Lazar I, Gamfi SL, Castille K, Kohya N, Nakayama Y, Liu YC, Eynon E, Flavell R, Weissman SM** 2006 FAT10/diubiquitin-like protein-deficient mice exhibit minimal phenotypic differences. Mol Cell Biol 26:5180-5189
81. **Bates EE, Ravel O, Dieu MC, Ho S, Guret C, Bridon JM, Ait-Yahia S, Briere F, Caux C, Banchereau J, Lebecque S** 1997 Identification and analysis of a novel member of the ubiquitin family expressed in dendritic cells and mature B cells. Eur J Immunol 27:2471-2477
82. **Raasi S, Schmidtke G, de Giuli R, Groettrup M** 1999 A ubiquitin-like protein which is synergistically inducible by interferon-gamma and tumor necrosis factor-alpha. Eur J Immunol 29:4030-4036
83. **Li T, Santockyte R, Yu S, Shen RF, Tekle E, Lee CG, Yang DC, Chock PB** FAT10 modifies p53 and upregulates its transcriptional activity. Arch Biochem Biophys 509:164-169
84. **Lim CB, Zhang D, Lee CG** 2006 FAT10, a gene up-regulated in various cancers, is cell-cycle regulated. Cell Div 1:20
85. **Zhang DW, Jeang KT, Lee CG** 2006 p53 negatively regulates the expression of FAT10, a gene upregulated in various cancers. Oncogene 25:2318-2327
86. **Hipp MS, Kalveram B, Raasi S, Groettrup M, Schmidtke G** 2005 FAT10, a ubiquitin-independent signal for proteasomal degradation. Mol Cell Biol 25:3483-3491
87. **Liu YC, Pan J, Zhang C, Fan W, Collinge M, Bender JR, Weissman SM** 1999 A MHC-encoded ubiquitin-like protein (FAT10) binds noncovalently to the spindle assembly checkpoint protein MAD2. Proc Natl Acad Sci U S A 96:4313-4318
88. **Gong P, Canaan A, Wang B, Leventhal J, Snyder A, Nair V, Cohen CD, Kretzler M, D'Agati V, Weissman S, Ross MJ** 2009 The Ubiquitin-Like Protein FAT10 Mediates NF-{kappa}B Activation. J Am Soc Nephrol
89. **Hotamisligil GS, Shargill NS, Spiegelman BM** 1993 Adipose Expression of Tumor Necrosis Factor-alpha: Direct role in obesity-linked insulin resistance. Science 259:87-91

90. **Franckhauser S, Elias I, Rotter Sopasakis V, Ferre T, Nagaev I, Andersson CX, Agudo J, Ruberte J, Bosch F, Smith U** 2008 Overexpression of Il6 leads to hyperinsulinaemia, liver inflammation and reduced body weight in mice. Diabetologia 51:1306-1316
91. **Jager J, Gremeaux T, Cormont M, Le Marchand-Brustel Y, Tanti JF** 2007 Interleukin-1beta-induced insulin resistance in adipocytes through down-regulation of insulin receptor substrate-1 expression. Endocrinology 148:241-251
92. **Kim S, Huang LW, Snow KJ, Ablamunits V, Hasham MG, Young TH, Paulk AC, Richardson JE, Affourtit JP, Shalom-Barak T, Bult CJ, Barak Y** 2007 A mouse model of conditional lipodystrophy. Proc Natl Acad Sci U S A 104:16627-16632
93. **Hirosumi J, Tuncman G, Chang L, Gorgun C, Uysal K, Maeda K, Karin M, Hotamisligil G** 2002 A central role for JNK in obesity and insulin resistance Nature 420:333-336
94. **Wallenius V, Wallenius K, Ahren B, Rudling M, Carlsten H, Dickson SL, Ohlsson C, Jansson JO** 2002 Interleukin-6-deficient mice develop mature-onset obesity. Nat Med 8:75-79
95. **Somm E, Henrichot E, Pernin A, Juge-Aubry CE, Muzzin P, Dayer JM, Nicklin MJ, Meier CA** 2005 Decreased fat mass in interleukin-1 receptor antagonist-deficient mice: impact on adipogenesis, food intake, and energy expenditure. Diabetes 54:3503-3509
96. **Aguirre V, Uchida T, Yenush L, Davis R, White M** 2000 The c-jun NH2-terminal kinase promotes insulin resistance during association with insulin receptor substrate-1 and phosphorylation of ser307. J Biol Chem 275:9047-9054
97. **Lukasiak S, Schiller C, Oehlschlaeger P, Schmidtke G, Krause P, Legler DF, Autschbach F, Schirmacher P, Breuhahn K, Groettrup M** 2008 Proinflammatory cytokines cause FAT10 upregulation in cancers of liver and colon. Oncogene 27:6068-6074
98. **Wheatley KE, Nogueira LM, Perkins SN, Hursting SD** Differential effects of calorie restriction and exercise on the adipose transcriptome in diet-induced obese mice. J Obes 2011:265417
99. **DeFuria J, Bennett G, Strissel KJ, Perfield JW, 2nd, Milbury PE, Greenberg AS, Obin MS** 2009 Dietary blueberry attenuates whole-body insulin resistance in high fat-fed mice by reducing adipocyte death and its inflammatory sequelae. J Nutr 139:1510-1516
100. **Perfield JW, 2nd, Lee Y, Shulman GI, Samuel VT, Jurczak MJ, Chang E, Xie C, Tsichlis PN, Obin MS, Greenberg AS** Tumor progression locus 2 (TPL2) regulates obesity-associated inflammation and insulin resistance. Diabetes 60:1168-1176
101. **Miyoshi H, Perfield JW, 2nd, Souza SC, Shen WJ, Zhang HH, Stancheva ZS, Kraemer FB, Obin MS, Greenberg AS** 2007 Control of adipose triglyceride lipase action by serine 517 of perilipin A globally regulates protein kinase A-stimulated lipolysis in adipocytes. J Biol Chem 282:996-1002
102. **Ahmadian M, Duncan RE, Varady KA, Frasson D, Hellerstein MK, Birkenfeld AL, Samuel VT, Shulman GI, Wang Y, Kang C, Sul HS** 2009

Adipose overexpression of desnutrin promotes fatty acid use and attenuates diet-induced obesity. Diabetes 58:855-866

103. **Jensen MD, Ekberg K, Landau BR** 2001 Lipid metabolism during fasting. Am J Physiol Endocrinol Metab 281:E789-793
104. **Lo CM, Obici S, Dong HH, Haas M, Lou D, Kim DH, Liu M, D'Alessio D, Woods SC, Tso P** Impaired Insulin Secretion and Enhanced Insulin Sensitivity in Cholecystokinin-Deficient Mice. Diabetes
105. **MacDonald PE, Joseph JW, Yau D, Diao J, Asghar Z, Dai F, Oudit GY, Patel MM, Backx PH, Wheeler MB** 2004 Impaired glucose-stimulated insulin secretion, enhanced intraperitoneal insulin tolerance, and increased beta-cell mass in mice lacking the p110gamma isoform of phosphoinositide 3-kinase. Endocrinology 145:4078-4083
106. **Sorensen H, Wendell MS, Brand CL, Fosgerau K, Gelling RW, Nishimura E, Ahren B** 2006 Glucagon receptor knockout mice display increased insulin sensitivity and impaired beta-cell function. Diabetes 55:3463-3469
107. **Tomimoto S, Ojika T, Shintani N, Hashimoto H, Hamagami K, Ikeda K, Nakata M, Yada T, Sakurai Y, Shimada T, Morita Y, Ishida C, Baba A** 2008 Markedly reduced white adipose tissue and increased insulin sensitivity in adcyap1-deficient mice. J Pharmacol Sci 107:41-48
108. **Ebstein F, Lange N, Urban S, Seifert U, Kruger E, Kloetzel PM** 2009 Maturation of human dendritic cells is accompanied by functional remodelling of the ubiquitin-proteasome system. Int J Biochem Cell Biol 41:1205-1215
109. **Zong H, Wang CC, Vaitheesvaran B, Kurland IJ, Hong W, Pessin JE** Enhanced energy expenditure, glucose utilization, and insulin sensitivity in VAMP8 null mice. Diabetes 60:30-38
110. **Chadt A, Leicht K, Deshmukh A, Jiang LQ, Scherneck S, Bernhardt U, Dreja T, Vogel H, Schmolz K, Kluge R, Zierath JR, Hultschig C, Hoeben RC, Schurmann A, Joost HG, Al-Hasani H** 2008 Tbc1d1 mutation in lean mouse strain confers leanness and protects from diet-induced obesity. Nat Genet 40:1354-1359
111. **Jayasooriya AP, Mathai ML, Walker LL, Begg DP, Denton DA, Cameron-Smith D, Egan GF, McKinley MJ, Rodger PD, Sinclair AJ, Wark JD, Weisinger HS, Jois M, Weisinger RS** 2008 Mice lacking angiotensin-converting enzyme have increased energy expenditure, with reduced fat mass and improved glucose clearance. Proc Natl Acad Sci U S A 105:6531-6536
112. **Zhai W, Xu C, Ling Y, Liu S, Deng J, Qi Y, Londos C, Xu G** Increased lipolysis in adipose tissues is associated with elevation of systemic free fatty acids and insulin resistance in perilipin null mice. Horm Metab Res 42:247-253
113. **Treadway JL, Hargrove DM, Nardone NA, McPherson RK, Russo JF, Milici AJ, Stukenbrok HA, Gibbs EM, Stevenson RW, Pessin JE** 1994 Enhanced peripheral glucose utilization in transgenic mice expressing the human GLUT4 gene. J Biol Chem 269:29956-29961
114. **Calle EE, Rodriguez C, Walker-Thurmond K, Thun MJ** 2003 Overweight, obesity, and mortality from cancer in a prospectively studied cohort of U.S. adults. N Engl J Med 348:1625-1638

115. **Muzumdar R, Allison DB, Huffman DM, Ma X, Atzmon G, Einstein FH, Fishman S, Poduval AD, McVei T, Keith SW, Barzilai N** 2008 Visceral adipose tissue modulates mammalian longevity. Aging Cell 7:438-440
116. **Lee CG, Ren J, Cheong IS, Ban KH, Ooi LL, Yong Tan S, Kan A, Nuchprayoon I, Jin R, Lee KH, Choti M, Lee LA** 2003 Expression of the FAT10 gene is highly upregulated in hepatocellular carcinoma and other gastrointestinal and gynecological cancers. Oncogene 22:2592-2603
117. **Bardag-Gorce F, Oliva J, Li J, French BA, French SW** SAMe prevents the induction of the immunoproteasome and preserves the 26S proteasome in the DDC-induced MDB mouse model. Exp Mol Pathol 88:353-362
118. **Dev S, Mizuguchi H, Das AK, Baba Y, Fukui H** Transcriptional microarray analysis reveals suppression of histamine signaling by Kujin alleviates allergic symptoms through down-regulation of FAT10 expression. Int Immunopharmacol
119. **Oliva J, Bardag-Gorce F, French BA, Li J, McPhaul L, Amidi F, Dedes J, Habibi A, Nguyen S, French SW** 2008 Fat10 is an epigenetic marker for liver preneoplasia in a drug-primed mouse model of tumorigenesis. Experimental and Molecular Pathology 84:102-112
120. **Snyder A, Alsauskas Z, Gong P, Rosenstiel PE, Klotman ME, Klotman PE, Ross MJ** 2009 FAT10: a novel mediator of Vpr-induced apoptosis in human immunodeficiency virus-associated nephropathy. J Virol 83:11983-11988
121. **Shoelson SE, Lee J, Goldfine AB** 2006 Inflammation and insulin resistance. J Clin Invest 116:1793-1801
122. **Minamino T, Orimo M, Shimizu I, Kunieda T, Yokoyama M, Ito T, Nojima A, Nabetani A, Oike Y, Matsubara H, Ishikawa F, Komuro I** 2009 A crucial role for adipose tissue p53 in the regulation of insulin resistance. Nat Med 15:1082-1087
123. **Carr A, Samaras K, Burton S, Law M, Freund J, Chisholm D, Cooper D** 1998 A syndrome of peripheral lipodystrophy, hyperlipidemia, and insulin resistance in patients receiving HIV protease inhibitors. AIDS 12:F51-58
124. **Carr A, Samaras K, Thorisdottir A, Kaufmann G, Chisholm D, Cooper D** 1999 Diagnosis, prediction and natural course of HIV-1 protease inhibitor-associated lipodystrophy, hyperlipidaemia, and diabetes mellitus, a cohort study. Lancet 353:2093-2099
125. **Grigem S, Fischer-Posovszky P, Debatin K, Loizon E, Vidal H, Wabitsch M** 2005 The effect of the HIV protease inhibitor ritonavir on proliferation, differentiation, lipogenesis, gene expression and apoptosis of human preadipocytes and adipocytes.

. Horm Metab Res 37:602-609
126. **Grunfeld C** 2002 HIV protease inhibitors and glucose metabolism. JAIDS 16:925-926
127. **Jain R, Lenhard J** 2002 Select HIV Protease Inhibitors Alter Bone and Fat Metabolism ex-Vivo. J Biol Chem 277:19247-19250
128. **Arita Y, Kihara S, Ouchi N, Takahashi T, Maeda K, Miyagawa J, Hotta K, Shimomura I, Nakamura T, Miyaoka K, Kuryiyama H, Nishida M,**

Yamashihta S, Okubo K, Matsubara K, Muraguchi M, Ohmoto Y, Funahashi T, Matsuzawa Y 1999 Paradoxical decrease of an adipose-specific protein, adiponectin, in obesity. Bioc Biophys Res Commun 2:79-83

129. **Surmi BK, Hasty AH** 2008 Macrophage infiltration into adipose tissue: initiation, propagation and remodeling. Future Lipidology 3:545-556
130. **Shoelson S, Herreroa L, Naaza A** 2007 Obesity, inflammation, and insulin resistance. Gastroenterology 1323:2169-2180
131. **Lumeng CN, Bodzin JL, Saltiel AR** 2007 Obesity induces a phenotypic switch in adipose tissue macrophage polarization. J Clin Invest 117:175-184
132. **Lumeng CN, DelProposto JB, Westcott DJ, Saltiel AR** 2008 Phenotypic switching of adipose tissue macrophages with obesity is generated by spatiotemporal differences in macrophage subtypes. Diabetes 57:3239-3246
133. **Strissel KJ, Stancheva Z, Miyoshi H, Perfield JW, II, DeFuria J, Jick Z, Greenberg AS, Obin MS** 2007 Adipocyte death, adipose tissue remodeling, and obesity complications. Diabetes 56:2910-2918
134. **Solinas G, Vilcu C, Neels J, Bandyopadhyay G, Luo J-L, Naugler W, Grivennikov S, Wynshaw-Boris A, Scadeng M, Olefsky J, Karin M** 2007 JNK1 in hematopoietically derived cells contributes to diet-induced inflammation and insulin resistance without affecting obesity. Cell Metab 6:386-397
135. **Cinti S MG, Barbatelli G, Murano I, Ceresi E, Faloia E, Wang S, Fortier M, Greenberg AS, Obin MS** 2005 Adipocyte death defines macrophage localization and function in adipose tissue of obese mice and humans. J Lipid Res 46:2347-2355
136. **Murano I, Barbatelli G, Parisani V, Latini C, Muzzonigro G, Castellucci M, Cinti S** 2008 Dead adipocytes, detected as crown-like structures, are prevalent in visceral fat depots of genetically obese mice. J Lipid Res 49:1562-1568
137. **Houstis N, Rosen ED, Lander ES** 2006 Reactive oxygen species have a causal role in multiple forms of insulin resistance. Nature 440:944-948
138. **Lionetti L, Mollica MP, Lombardi A, Cavaliere G, Gifuni G, Barletta A** 2009 From chronic overnutrition to insulin resistance: the role of fat-storing capacity and inflammation. Nutr Metab Cardiovasc Dis 19:146-152
139. **Cefalu WT, Ye J, Zuberi A, Ribnicky DM, Raskin I, Liu Z, Wang ZQ, Brantley PJ, Howard L, Lefevre M** 2008 Botanicals and the metabolic syndrome. Am J Clin Nutr 87:S481-487
140. **Williams RJ, Spencer JP, Rice-Evans C** 2004 Flavonoids: antioxidants or signalling molecules? Free Radic Biol Med 36:838-849
141. **Zafra-Stone S, Yasmin T, Bagchi M, Chatterjee A, Vinson JA, Bagchi D** 2007 Berry anthocyanins as novel antioxidants in human health and disease prevention. Mol Nutr Food Res 51:675-683
142. **Lau FC, Bielinski DF, Joseph JA** 2007 Inhibitory effects of blueberry extract on the production of inflammatory mediators in lipopolysaccharide-activated BV2 microglia. J Neurosci Res 85:1010-1017
143. **Atalay Mustafa, Gordillo Gayle, Roy Sashwati, Rovin Brad, Bagchi Debasis, Bagchi Manashi, K. SC** 2003 Anti-angiogenic property of edible berry in a model of hemangioma. FEBS Letters 544:252-257

144. **Osman N, Adawi D, Ahrné S, Jeppsson B, Molin G** 2007 Endotoxin- and d-galactosamine-induced liver injury improved by the administration of Lactobacillus, Bifidobacterium and blueberry. Dig Liver Dis 39:849-856
145. **Cani PD, Bibiloni R, Knauf C, Waget A, Neyrinck AM, Delzenne NM, Burcelin R** 2008 Changes in gut microbiota control metabolic endotoxemia-induced inflammation in high-fat diet-induced obesity and diabetes in mice. Diabetes 57:1470-1481
146. **Kalt W, Blumberg JB, McDonald JE, Vinqvist-Tymchuk MR, Fillmore SAE, Graf BA, Leary JM, Milbury P** 2008 Identification of anthocyanins in the liver, eye, and brain of blueberry-fed pigs. J Agric Food Chem 56:705-712
147. **Ito A, Suganami T, Yamauchi A, Degawa-Yamauchi M, Tanaka M, Kouyama R, Kobayashi Y, Nitta N, Yasuda K, Hirata Y, Kuziel WA, Takeya M, Kanegasaki S, Kamei Y, Ogawa Y** 2008 Role of CC chemokine receptor 2 in bone marrow cells in the recruitment of macrophages into obese adipose tissue. J Biol Chem 283:35715-35723
148. **Lumeng C, Deyoung S, Bodzin J, Saltiel A** 2007 Increased inflammatory properties of adipose tissue macrophages recruited during diet-induced obesity. Diabetes 56:16-23
149. **Ahn J, Lee H, Kim S, Park J, Ha T** 2008 The anti-obesity effect of quercetin is mediated by the AMPK and MAPK signaling pathways. Biochemical and Biophysical Research Communications 373:545-549
150. **Cheng J** 2008 Dissection of endoplasmic reticulum stress signaling in alcoholic and non-alcoholic liver injury. J Gastroenterol Hepatol 23:S16-S24
151. **Martineau LC, Couture A, Spoor D, Benhaddou-Andaloussi A, Harris C, Meddah B, Leduc C, Burt A, Vuong T, Mai Le P** 2006 Anti-diabetic properties of the Canadian lowbush blueberry Vaccinium angustifolium Ait. Phytomedicine 13:612-623
152. **Prior RL, Wu X, Gu L, Hager TJ, Hager A, Howard LR** 2008 Whole berries versus berry anthocyanins: Interactions with dietary fat levels in the C57BL/6J mouse model of obesity. J Agric Food Chem 56:647-653
153. **Williams CM, El Mohsen MA, Vauzour D, Rendeiro C, Butler LT, Ellis JA, Whiteman M, Spencer JPE** 2008 Blueberry-induced changes in spatial working memory correlate with changes in hippocampal CREB phosphorylation and brain-derived neurotrophic factor (BDNF) levels. Free Radic Biol Med 45:295-305
154. **Suganami T, Tanimoto-Koyama K, Nishida J, Itoh M, Yuan X, Mizuarai S, Kotani H, Yamaoka S, Miyake K, Aoe S, Kamei Y, Ogawa Y** 2007 Role of the Toll-like receptor 4/NF-{kappa}B pathway in saturated fatty acid-induced inflammatory changes in the interaction between adipocytes and macrophages. Arterioscler Thromb Vasc Biol 27:84-91
155. **Lee YS, Kim AY, Choi JW, Kim M, Yasue S, Son HJ, Masuzaki H, Park KS, Kim JB** 2008 Dysregulation of adipose glutathione peroxidase 3 in obesity contributes to local and systemic oxidative stress. Mol Endocrinol 22:2176-2189
156. **Joseph JA, Carey A, Brewer GJ, Lau FC, Fisher DR** 2007 Dopamine and Abeta-induced stress signaling and decrements in Ca2+ buffering in primary

neonatal hippocampal cells are antagonized by blueberry extract. J Alzheimers Dis 11:433-446

157. **Herr I, Debatin K-M** 2001 Cellular stress response and apoptosis in cancer therapy. Blood 98:2603-2614
158. **Domingo P, Vidal F, Domingo JC, Veloso S, Sambeat MA, Torres F, Sirvent JJ, Vendrell J, Matias-Guiu X, Richart C** 2005 Tumour necrosis factor alpha in fat redistribution syndromes associated with combination antiretroviral therapy in HIV-1-infected patients: potential role in subcutaneous adipocyte apoptosis. Eur J Clin Invest 35:771-780
159. **Mori M** 2007 Regulation of nitric oxide synthesis and apoptosis by arginase and arginine recycling. J Nutr 137:S1616-1620
160. **Patsouris D, Li P-P, Thapar D, Chapman J, Olefsky JM, Neels JG** 2008 Ablation of CD11c-positive cells normalizes insulin sensitivity in obese insulin resistant animals. Cell Metab 8:301-309
161. **Tsuda T, Horio F, Uchida K, Aoki H, Osawa T** 2003 Dietary cyanidin 3-O-{beta}-D-glucoside-rich purple corn color prevents obesity and ameliorates hyperglycemia in mice. J Nutr 133:2125-2130
162. **Sasaki R, Nishimura N, Hoshino H, Isa Y, Kadowaki M, Ichi T, Tanaka A, Nishiumi S, Fukuda I, Ashida H, Horio F, Tsuda T** 2007 Cyanidin 3-glucoside ameliorates hyperglycemia and insulin sensitivity due to downregulation of retinol binding protein 4 expression in diabetic mice. Biochem Pharmacol 74:1619-1627
163. **McGhie TK, Walton MC** 2007 The bioavailability and absorption of anthocyanins: Towards a better understanding. Mol Nutr Food Res 51:702-713
164. **Nayer A, Shoelson S** 2007 Differential distribution of adipositis induced by high-fat diet in abdominal fat depots.
165. **Zeyda M, Stulnig TM** 2009 Obesity, inflammation, and insulin resistance--a mini-review. Gerontology 55:379-386
166. **Su CL, Sztalryd C, Contreras JA, Holm C, Kimmel AR, Londos C** 2003 Mutational analysis of the hormone-sensitive lipase translocation reaction in adipocytes. J Biol Chem 278:43615-43619
167. **Cancello R, Henegar C, Viguerie N, Taleb S, Poitou C, Rouault C, Coupaye M, Pelloux V, Hugol D, Bouillot JL, Bouloumie A, Barbatelli G, Cinti S, Svensson PA, Barsh GS, Zucker JD, Basdevant A, Langin D, Clement K** 2005 Reduction of macrophage infiltration and chemoattractant gene expression changes in white adipose tissue of morbidly obese subjects after surgery-induced weight loss. Diabetes 54:2277-2286
168. **Mariotti S, Sargentini V, Marcantonio C, Todero E, Teloni R, Gagliardi MC, Ciccaglione AR, Nisini R** 2008 T-cell-mediated and antigen-dependent differentiation of human monocyte into different dendritic cell subsets: a feedback control of Th1/Th2 responses. FASEB J 22:3370-3379
169. **Martinez FO, Helming L, Gordon S** 2009 Alternative activation of macrophages: an immunologic functional perspective. Annu Rev Immunol 27:451-483

170. **Dalton DK, Pitts-Meek S, Keshav S, Figari IS, Bradley A, Stewart TA** 1993 Multiple defects of immune cell function in mice with disrupted interferon-gamma genes. Science 259:1739-1742
171. **Martinez FO, Sica A, Mantovani A, M. L** 2008 Macrophage activation and polarization. Front Biosci 13:453-461
172. **Ledoux S, Queguiner I, Msika S, Calderari S, Rufat P, Gasc JM, Corvol P, Larger E** 2008 Angiogenesis associated with visceral and subcutaneous adipose tissue in severe human obesity. Diabetes 57:3247-3257
173. **Lesniewski L, Hosch S, Neels J, de Luca C, Pashmforoush M, Lumeng C, Chiang S-H, Scadeng M, Saltiel A, Olefsky J** 2007 Bone marrow–specific Cap gene deletion protects against high-fat diet–induced insulin resistance. Nat Med 13:455-462
174. **Caspar-Bauguil S, Cousin B, Galinier A, Segafredo C, Nibbelink M, Andre M, Casteilla L, Penicaud L** 2005 Adipose tissues as an ancestral immune organ: site-specific change in obesity. FEBS Lett Jul 4;579(17):3487-92 579:3487-3492
175. **Caspar-Bauguil S CB, Andre M, Nibbelink M, Galinier A, Periquet B, Casteilla L, Penicaud L. , Related Articles L, leptin. AW-dcoisiatio, 2. ECRJ-EM**
176. **Eguchi J, Yan QW, Schones DE, Kamal M, Hsu CH, Zhang MQ, Crawford GE, Rosen ED** 2008 Interferon regulatory factors are transcriptional regulators of adipogenesis. Cell Metab 7:86-94
177. **Rocha VZ, Folco EJ, Sukhova G, Shimizu K, Gotsman I, Vernon AH, Libby P** 2008 Interferon-gamma, a Th1 cytokine, regulates fat inflammation: a role for adaptive immunity in obesity. Circ Res 103:467-476
178. **Rausch ME, Weisberg S, Vardhana P, Tortoriello DV** 2008 Obesity in C57BL/6J mice is characterized by adipose tissue hypoxia and cytotoxic T-cell infiltration. Int J Obes (Lond) 32:451-463
179. **Kintscher U, Hartge M, Hess K, Foryst-Ludwig A, Clemenz M, Wabitsch M, Fischer-Posovszky P, Barth TF, Dragun D, Skurk T, Hauner H, Bluher M, Unger T, Wolf AM, Knippschild U, Hombach V, Marx N** 2008 T-lymphocyte infiltration in visceral adipose tissue: a primary event in adipose tissue inflammation and the development of obesity-mediated insulin resistance. Arterioscler Thromb Vasc Biol 28:1304-1310
180. **O'Rourke RW, Metcalf MD, White AE, Madala A, Winters BR, Maizlin II, Jobe BA, Roberts CT, Jr., Slifka MK, Marks DL** 2009 Depot-specific differences in inflammatory mediators and a role for NK cells and IFN-[gamma] in inflammation in human adipose tissue. Int J Obes
181. **Holtrop JS, Dosh SA, Torres T, Arnold AK, Baumann J, White LL, Pathak PK** 2009 Nurse consultation support to primary care practices to increase delivery of health behavior services. Appl Nurs Res 22:243-249
182. **Duffaut C, Galitzky J, Lafontan M, Bouloumie A** 2009 Unexpected trafficking of immune cells within the adipose tissue during the onset of obesity. Biochem Biophys Res Commun
183. **Thalmann S, Juge-Aubry C, Meier C** 2008 Explant cultures of white adipose tissue. . 2 ed. Totowa, New Jersey: Humana Press

184. **Makino Y, Cook DN, Smithies O, Hwang OY, Neilson EG, Turka LA, Sato H, Wells AD, Danoff TM** 2002 Impaired T Cell Function in RANTES-Deficient Mice. Clinical Immunology 102:302-309
185. **Schulz EG, Mariani L, Radbruch A, Höfer T** 2009 Sequential Polarization and Imprinting of Type 1 T Helper Lymphocytes by Interferon-[gamma] and Interleukin-12. Immunity 30:673-683
186. **Heckford S, Gelmann E, Agnor C, Jacobson S, Zinn S, Matis L** 1986 Distinct signals are required for proliferation and lymphokine gene expression in murine T cell clones. J Immunol 137:3652-3663
187. **Patsouris D, Li PP, Thapar D, Chapman J, Olefsky JM, Neels JG** 2008 Ablation of CD11c-positive cells normalizes insulin sensitivity in obese insulin resistant animals. Cell Metab 8:301-309
188. **Nembrini C, Abel B, Kopf M, Marsland BJ** 2006 Strong TCR signaling, TLR ligands, and cytokine redundancies ensure robust development of type 1 effector T cells. J Immunol 176:7180-7188
189. **Feng XZ, He XS, Zhuang YZ, Luo Q, Jiang JH, Yang S, Tang XF, Liu JL, Chen T** 2008 Investigation of transcriptional gene silencing and mechanism induced by shRNAs targeted to RUNX3 in vitro. World J Gastroenterol 14:3006-3014
190. **Couper KN, Blount DG, Riley EM** 2008 IL-10: the master regulator of immunity to infection. J Immunol 180:5771-5777
191. **Zhu J, Paul WE** 2008 CD4 T cells: fates, functions, and faults. Blood 112:1557-1569
192. **Manfredi AA, Capobianco A, Bianchi ME, P. R-Q** 2009 Regulation of dendritic- and T-cell fate by injury-associated endogenous signals. Crit Rev Immunol 29:69-86
193. **Huber J, Loffler M, Bilban M, Reimers M, Kadl A, Todoric J, Zeyda M, Geyeregger R, Schreiner M, Weichhart T, Leitinger N, Waldhausl W, Stulnig TM** 2006 Prevention of high-fat diet-induced adipose tissue remodeling in obese diabetic mice by n-3 polyunsaturated fatty acids. Int J Obes 31:1004-1013
194. **Chun T-H, Hotary KB, Sabeh F, Saltiel AR, Allen ED, Weiss SJ** 2006 A Pericellular Collagenase Directs the 3-Dimensional Development of White Adipose Tissue. Cell 125:577-591